AN ELECTROCHEMICAL STUDY OF AZO DYES

By

NDISHAVHELAFHI AMOS MPHEPHU

B.Sc. (Hons) Rhodes University

Submitted in partial fulfilment of
the requirements for the degree of
Master of Science in the
Department of Chemistry
University of Natal

Durban 1996

The fear of the Lord is the beginning of knowledge, but fools despise wisdom and instruction.

Proverbs 1: 7

PREFACE

The experimental work described in this thesis was carried out in the Department of Chemistry, University of Natal, Durban, under the supervision of Prof. H. C. Brookes.

These studies represent original work by the author and have not been submitted in any form to another University. Where use was made of work of others, it has been duly acknowledged in the text.

DECLARATION

I hereby certify that this research is the result of my own investigation, which has not already been accepted in any substance for any degree, and is not being concurrently submitted in candidature for any other degree.

Signed.....

N. A. Mphephu

B.Sc. (Hons) Rhodes

I hereby certify that the above statement is correct.

Signed.....

Professor H. C. Brookes

Ph.D. (Cape Town)

Professor of Inorganic Chemistry

University of Natal

Durban

Department of Chemistry

University of Natal

Durban

1996

ACKNOWLEDGEMENT

My sincere appreciation is due to:

Prof. H. C. Brookes for all his assistance throughout the project

Dr F. Graham and Mr C.H.L Tonkinson for their advice

Dr Dulcie Mulholland for her assistance in interpreting the NMR spectra

The Water Pollution Research Group (PRG) (University of Natal, Durban (UND)) for their assistance and Prof. C. Buckley the Leader of PRG for useful discussions

Mr Dave Balson for his assistance with the maintenance of the electrical equipment.

Mr Jodi Couling for machining the Teflon and graphite

Mr Dillip Jagivan for running NMR spectra

FRD for funding the research and for their postgraduate bursary.

University of Natal research fund for funding the project

W.R.C. for their partial financial support via PRG (UND)

I would especially like to thank my parents for their support and patience during my studies. I would also like to thank Transnet for granting me an unpaid study leave.

Finally I thank God, the Creator of Heaven and Earth for the gift of life.

ABSTRACT

Electrochemical and spectroscopic techniques have been used to investigate the behaviour of azo dyes, particularly the reactive azo dyes. The azo dyes studied were Methyl Orange (4-[4-(dimethylamino)phenylazo]benzenesulphonic acid), Orange II (4-(2-hydroxy-1-naphthylazo)benzenesulphonic acid) and Procion Red MX 5B, (Reactive Red 2) viz.5-[4,6-dichloro triazin-2-yl amino)-4-hydroxy-3-phenylazo, 2,7-naphthalene disulphonic acid. Reactive azo dyes are coloured organic compounds that contain one or two cyanuric chloride groups that can form a covalent bond between a dye molecule and a cellulosic fibre. These dyes are known pollutants in textile waste water and their colour persists notwithstanding conventional waste-water treatment. The polluted water then enters local water bodies. Procion Red MX 5B in particular is one of the more intensely coloured water soluble reactive dyes used in the textile industry.

Azo dyes can undergo two electron reduction giving a hydrazo derivative, or they could undergo 4e -reduction to give the corresponding aromatic amines, thereby decolourising the dye. The aim of the study was to electrochemically decolourize the reactive azo dyes in solution, and to this end the electrochemical reduction of Procion Red MX 5B dye was studied.

Cyclic voltammetry (CYV) is one of the techniques used in this investigation of the electrochemical reduction of Procion Red MX 5B. A three electrode system was used to study the electrochemistry of Procion Red MX 5B in the aqueous solution buffered with phosphate buffers of pH range 3-11. The working electrode was a glassy carbon disc, saturated calomel was the reference electrode and the counter electrode was either a spiral platinum wire or graphite rod electrode. The effect of pH on the reduction peak of the dye was studied and it was found that the reduction peak potential of the dye shifts to negative potentials as the pH increases. The effect of a second voltammetric cycle, and the scan rate, on the first reduction peak that appeared was studied. The interdependence of the peaks was studied by varying the potential window and changing the direction of the sweep. This was done in acidic media (pH 3 and 6), basic media (pH 8) and neutral media (pH 7).

Results obtained suggested that the dye was undergoing electroreduction into corresponding amines.

Bulk electrolysis on the dye at a potential indicated by the CYV studies at pH 7.06 yielded one of the aromatic amines expected from the electrodegradation of Reactive Red 2 which proved unequivocally that the electrochemical reduction of Reactive Red 2 leads to corresponding aromatic amines. The working electrode used for bulk electrolysis was a graphite rod. The degradation of the dye was monitored by UV-vis spectroscopy where it was found that the λ_{max} of the dye decreased systematically as electrolysis progressed. The voltammogram run on the completely electrolysed solution did not have the peak responsible for the reduction of the dye, confirming the UV evidence that the dye was completely electrolysed.

It was concluded that Procion Red MX 5B undergoes 4e reduction in phosphate buffer at pH range 3-11 at glassy carbon electrode. Isolation and identification of aniline by NMR from the completely electrolysed solution proved unequivocally that the dye Procion Red MX 5B can be electrodegraded into the corresponding aromatic amines. It is clear that decolourisation can be performed electrochemically and industrial applications are obvious. UV-vis spectroscopy complements the electrochemical and NMR evidence of decolourization.

Table of Contents

List of Figures

List of Symbols and Abbreviations

^{1}HNMR	proton nuclear magnetic resonance
α_a	anodic transfer coefficient
α_c	cathodic transfer coefficient
C_i	concentration of species *i*
C_o^∞	concentration of O in the bulk
C_o^s	concentration of O at the electrode surface
AR	analytical reagent
Analar	analytical reagent
COSY	correlated spectroscopy
CP	chemically pure
CV	cyclic voltammogram
CYV	cyclic voltammetry
D	diffusion coefficient
D_i	diffusion coefficient of species *i*
DME	dropping mercury electrode
DMF	dimethylformamide
E	electrode potential
E_e	equilibrium potential
E_p	peak potential (superscripts ^{a} and ^{c} indicate anodic or cathodic)
F	Faraday's constant
GC	glassy carbon
GCE	glassy carbon electrode
η	overvoltage or overpotential
IR	infrared spectrum
j	current density
j_o	exchange current density
j_p	peak current density (superscripts ^{a} and ^{c} indicate anodic or cathodic)
n	number of electrons
n_α	number of electrons transferred up to and including the rate determining step

NMR	nuclear magnetic resonance
$\overrightarrow{k}$	oxidation rate constant
PGE	pyrolytic graphite electrode
$\overleftarrow{k}$	reduction rate constant
SCE	saturated calomel electrode
K^{θ}	standard rate constant
TLC	thin layer chromatography
V	volume of the solution in the working electrode compartment
v	sweep or scan rate
WE	working electrode
x	distance from the electrode into the solution

Chapter 1

Introduction

Dyes are used in the textile finishing industry. Waste water from this industry is complex with respect to both the quantity and variability of the waste compounds. The highly coloured nature of the effluent poses a treatment problem that had no ready solution.

Water insoluble dyes generally exhibit good exhaustion properties and can be removed from the effluent by physical methods such as flocculation. When this effluent is discharged to a conventional sewage treatment works, some of the colour is removed by activated sludge processes. Thus although colour removal is a problem with all types of textile dyeing processes, it is the introduction of water soluble dyes, such as those containing a reactive group, which has resulted in colouration becoming a substantial treatment problem.

Reactive dyes are coloured components capable of forming a covalent bond between the dye molecule and the fibre. The reactive systems of these dyes react with hydroxyl groups on the cellulose substrate by nucleophilic substitution. The presence of water, and alkaline conditions required for the ionisation of the fibre , means that hydroxyl ions are also present in the dye bath and compete with the ionised cellulose as the nucleophiles. This results in hydrolysed dyes which can no longer react with the cellulose fibre and accounts for the low levels of exhaustion achieved with some reactive dyes. Thus effluent from reactive dyeing is often highly coloured (between 10 and 50 % of the dye will be present in the dyebath effluent) and difficult to treat with adsorption or flocculation methods due to the water soluble nature of the hydrolysed dyes.

Water soluble dyes pass through the treatment works and give rise to colouration of the receiving water bodies unless additional treatment steps are implemented. Dyes in an aquatic environment give shadow effects, which can result in a reduced rate of photosynthesis, in addition to aesthetic aspects. Light absorption by a dye molecule can lead directly to degradation, but generally commercial dyes will release the absorbed energy

to nearby molecules. This means that dyes that are released into the environment may serve as sensitizers of indirect photo effects. It is clear that conventional waste water-treatment processes do not achieve adequate colour removal and that alternative treatment options are required.

This brings us to the aim of this study which was to determine the possibility of electrochemical degradation of commercial reactive azo dyes into corresponding aromatic amines, thereby decolourising them. Orange II and methyl orange were the dyes used for preliminary experiments in preparation for the study of Procion Red MX 5B, an uninvestigated commercial reactive azo dye.

Cyclic voltammetry was one of the techniques used in the investigation of the electrochemical reduction of Procion Red MX 5B. This technique is known for its ability to generate a species during one redox scan and then probe its fate with a subsequent redox scan. It can also be used as an electroanalytical technique.

A three electrode system was used to study the electrochemistry of Procion Red MX 5B in the aqueous solution buffered with phosphate buffers of pH range 3-11. The working electrode was a glassy carbon disc, saturated calomel was the reference electrode and the counter electrode was either a spiral platinum wire or a graphite rod electrode.

The effect of pH on the reduction process of the dye was studied by running cyclic voltammograms of the dye at different pH's. The primary reduction process was shown to be diffusion controlled, i.e. electron transfer was rapid in this conditions.

The interdependence of the redox processes was studied by varying the potential window and changing the direction of the potential sweep. This was done in acidic media (pH 3 and 6), basic media (pH 8) and neutral media (pH 7) to determine the interrelationships between the six redox processes found.

Controlled potential bulk electrolysis could then be employed to confirm the electroreduction mechanism of the dye, as proposed on the basis of the information

deduced from cyclic voltammetry. Concomitant with this technique, spectroscopic techniques (ultraviolet-visible and nuclear magnetic resonance spectroscopy) were used to confirm the proposed electroreduction mechanism. Ultraviolet-visible spectroscopy was used to monitor the controlled potential bulk electrolysis, while conventional nuclear magnetic resonance spectroscopy was used to identify the species produced during the electrolysis processes.

Chapter 2

Theoretical Background

2.1 Electrode Reactions

The simplest electrode reaction is the one that converts, at an inert surface, two species O and R which are stable and soluble in electrolyte medium containing an excess of an inert background electrolyte. This electrochemical reaction can be presented as follows:

$$O + ne \rightleftharpoons R \qquad \text{.....(1)}$$

The electrode reaction represented above may appear simple but in general it has at least five separate steps:

1. Transport of O from the bulk solution to the interface
2. Adsorption of O onto the electrode.
3. Electron transfer at the electrode to form R.
4. Desorption of R from the surface of the electrode
5. Transport of R from the interface into the bulk of the solution

The rate of reduction and hence the cathodic current resulting from the movement of cation O to the electrode surface is determined by the slowest step of the overall sequence. In order to understand the characteristics of such an electrode reaction one needs to understand the mass transport and electron transfer processes.

2.2 Mass Transport

There are three modes of mass transport involved in electrode reactions viz. diffusion, migration and convection.

2.2.1 Migration

Migration is the movement of charged species due to a potential gradient and it is the mechanism by which charge passes through the electrolyte. In an electrochemical cell, the current through the external circuit must be balanced by the passage of ions through the solution between the electrodes. It is however not an important mass transport mode for the electroactive species even if it is charged. The forces that lead to migration are purely electrostatic and hence the charge can be carried by any ionic species in the solution. Consequently if electrolysis is being carried out with a large excess of background electrolyte, this carries most of the charge and very little of the electroactive species of interest is transported by migration.

2.2.2 Convection

Convection is the movement of species due to mechanical forces. It involves stirring of the electrolyte. This mode of transport is used in bulk electrolysis in order to maximize the flux of electroactive material to the surface of the electrode.

2.2.3 Diffusion

Diffusion is defined as the movement of species (neutral or charged) down a concentration gradient and it occurs whenever there is a concentration variation at the surface of the electrode. The change at the surface of the electrode is brought about by the electrochemical reaction (1). Hence close to the electrode surface there is always a boundary layer up 10^{-2} cm thick in which the concentration of O and R are a function of distance from the electrode surface.[1] The concentration of O in the bulk, C_o^{∞}, is higher than the concentration of O at the electrode surface C_o^{0}, while the opposite is the case for R and hence O diffuses to the electrode surface and R away from the electrode surface.

2.2.3.1 Linear Diffusion to a Planar[2] Electrode

In unstirred solution and in the presence of supporting electrolyte, diffusion is the only form of mass transport which needs to be considered for the electroactive species.

The simplest model is that of linear diffusion to a planar electrode and it is assumed that the electrode is perfectly flat and of infinite dimensions so that concentration variations can only occur perpendicular to the electrode surface. Diffusion may then be characterised by Ficks laws[3] in one dimensional form. The first law states that the flux of any species through a plane parallel to the electrode is given by:

$$flux = -D_i \frac{dC_i}{dx} \quad \text{.....(2)}$$

where D_i is the diffusion coefficient, x is the distance from the electrode and C_i is the concentration of the species i. The first law applied to the surface of the electrode, where $x = 0$, is used to relate the current to the chemical change at the electrode as shown in fig.2.1, i.e. equating the flux of O or R with the flux of electrons.

$$\frac{j}{nF} = -D_o\left(\frac{\partial C_o}{\partial x}\right)_{x=o} \quad \text{or} \quad \frac{j}{nF} = D_R\left(\frac{\partial C_r}{\partial x}\right)_{x=o} \quad \text{.....(3)}$$

where j is the current density, n the number of electrons and F is Faraday's constant.

The second law describes the change of concentration of the electroactive species with time as the potential of the working electrode is scanned through the potential range where reaction (1) occurs. The surface concentration of O will decrease as the potential is made more negative until the surface concentration becomes effectively zero (the reaction becomes diffusion controlled) and the surface concentration will remain zero at more negative potentials. The surface is, however, the only point in the space where the change in concentration occurs instantaneously, elsewhere, diffusion must play its role. Fig.2.2 shows the development of the concentration profiles during the experiment. Initially it can be seen that the flux to the surface (and hence the cathodic current density) increases with time because of the change of the potential and it continues to increase until the surface concentration becomes zero. Thereafter the situation is akin to a potential step experiment. The differential equation that describes the change in concentration with time for the potential step experiment is:

$$\frac{\partial C_o}{\partial t} = D\frac{\partial^2 C_o}{\partial x^2} \quad \text{.....(4)}$$

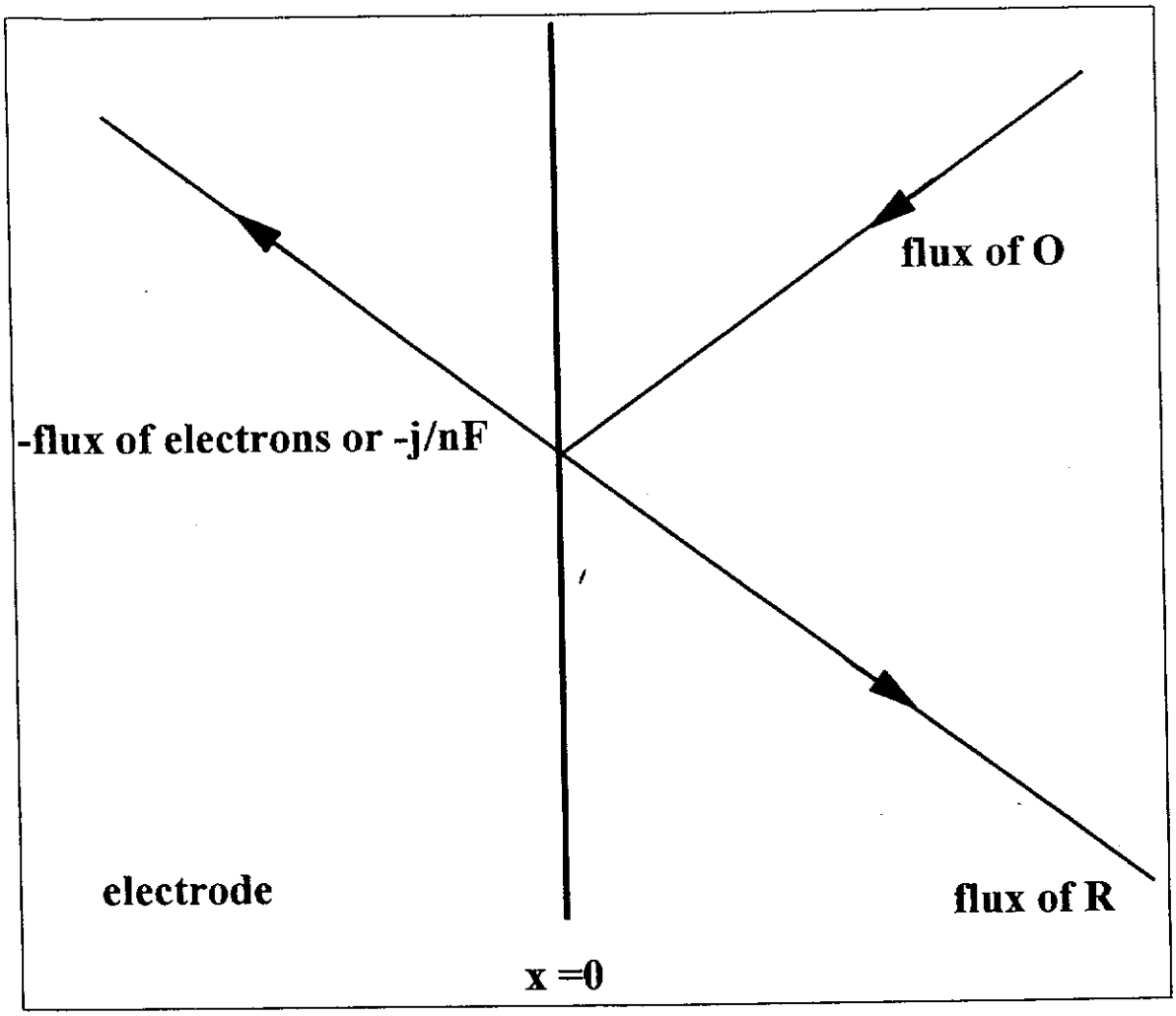

Fig. 2.1. The flux balance at the electrode surface for the reduction of O into R

The solution of this equation with the following boundary conditions is given below:

$t = 0$ and for all $x, C_o = C_o^{\infty}$
and for $t > 0$, at $x = 0, C_o^{\sigma} = 0$
and at $x = \infty, C_o = C_o^{\infty}$

$$j = \frac{nFD^{\frac{1}{2}}C_o^{\infty}}{\pi^{\frac{1}{2}}t^{\frac{1}{2}}} \quad \text{.....(5)}$$

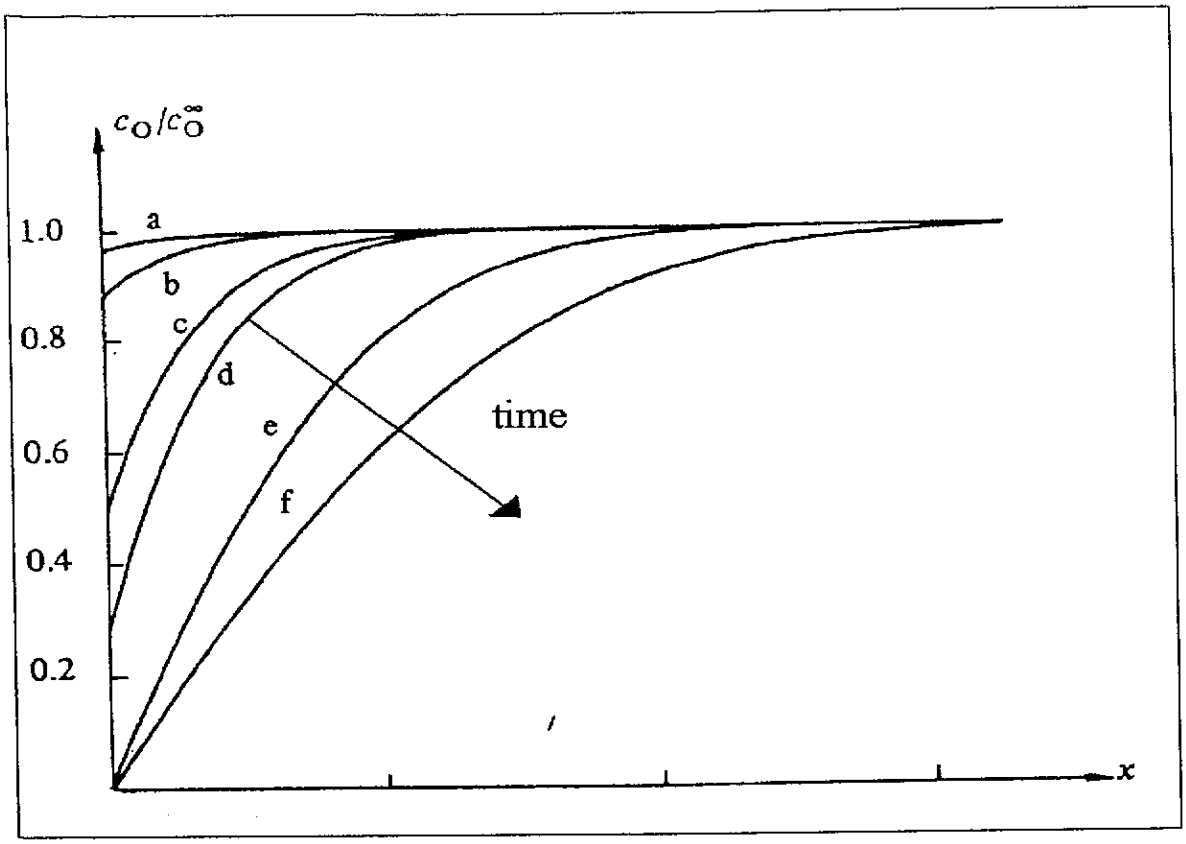

Fig.2.2. Development of the concentration profiles during the forward sweep of a cyclic voltammogram.

2.2.3.2 The Rate of Electron Transfer.

Having described the mass transport from the bulk to the electrode surface and vice versa the next step is to consider the rate at which the chemical change will occur at the electrode surface.

Rate of reduction = $\overleftarrow{k}(C_o)_{x=0}$ .....(6)

Rate of oxidation = $\overrightarrow{k}(C_R)_{x=0}$ .....(7)

where $\overleftarrow{k}$ is the reduction rate constant and $\overrightarrow{k}$ is the oxidation rate constant.

The rate of heterogeneous electron transfer would be expected to depend on the potential gradient at the surface of the electrode, driving the transfer of electrons between the

electrode and the solution. The gradient in turn depends on the potential at the electrode. It is found experimentally that the rate constants vary with potential according to the following equations[4].

$$\overrightarrow{k} = \overrightarrow{k_o} \exp\left(\frac{\alpha_a nF}{RT}E\right) \text{ and } \overleftarrow{k} = \overleftarrow{k_o} \exp\left(\frac{-\alpha_c nF}{RT}E\right) \quad ..(8)$$

where α_a and α_c are known as the anodic and cathodic transfer coefficients ($\alpha_a + \alpha_c = 1$ for $n = 1$) respectively. Assuming that the concentrations of the species at the surface of the electrode are the same as in the bulk solution, the rate of oxidation and reduction processes at the electrode may be converted to partial current densities simply by multiplying by nF which will convert dimensions to $A.cm^{-2}$. Hence the net current density can be expressed as:

$$j = \overrightarrow{j} + \overleftarrow{j} \quad \text{.....(9)}$$

where $\overleftarrow{j}$ is negative

$$j = nF\overrightarrow{k_o}C_R\exp\left(\frac{\alpha_a nF}{RT}E\right) - nF\overleftarrow{k_o}C_O\exp\left(\frac{-\alpha_c nF}{RT}E\right) \quad ....(10)$$

Equation (9) describes the current density as a function of the electrode potential E measured versus a reference electrode. It is commonly written in another form obtained by introducing the overpotential or overvoltage η which is defined as the deviation of the potential from E_e (equilibrium potential) for the O/R couple. The equation can be simplified by considering that at equilibrium i.e. at E_e :

$j = j_o = -\overleftarrow{j} = \overrightarrow{j}$ ie at $\eta = 0$ and the negative sign reflects the sign convention

that a cathodic current is negative

$$\eta = E - E_{\varepsilon} \quad \text{.....(11)}$$

Where j_o is the exchange current density

$$j_o = nF\overrightarrow{k_o}C_R\exp\left(\frac{\alpha_a nF}{RT}E\right) = -nF\overleftarrow{k_o}C_o\exp\left(\frac{-\alpha_c nF}{RT}E\right) \quad \text{...(12)}$$

Substitution of (11) into (10) and application of (12) gives

$$j = j_o\left(\exp\frac{\alpha_a nF}{RT}\eta - \exp\frac{-\alpha_c nF}{RT}\eta\right) \quad \text{.....(13)}$$

which is the Butler-Volmer equation, which is central to the discussion of electrode kinetics. This is a fundamental equation of elèctrode kinetics and it shows the way in which the current density varies with the exchange current density, overpotential and transfer coefficients.

At high positive overpotential where $\left|\overrightarrow{j}\right| >> \left|\overleftarrow{j}\right|$ the second term in (13) falls off and the current density is expressed as follows:

$$j = j_o\exp\frac{\alpha_a nF}{RT}\eta \quad \text{.....(14)}$$

$$\ln j = \ln j_o + \frac{\alpha_a nF}{RT}\eta \quad \text{.....(15)}$$

$$\eta = a + b\ln j \quad \text{.....(16)}$$

where $a = -\ln j_o\left(\frac{RT}{\alpha_a nF}\right)$ and $b = \frac{RT}{\alpha_a nF}$

Similarly at high negative overpotential where $\left|\overrightarrow{j}\right| << \left|\overleftarrow{j}\right|$:

$$\eta = a + b\ln j \quad \text{.....(16)}$$

where $b = \frac{RT}{\alpha_c nF}$

Equation (16) is known as the Tafel equation.

The third limiting form applies at very low overpotentials where $\eta << RT/\alpha_c nF$ and $\eta = RT/\alpha_a nF$. The two exponential terms in (12) may be expanded as Taylor Series and ignoring quadratic and higher order forms leads to :

$$j = j_o \frac{nF}{RT}\eta \quad \text{.....(17)}$$

The exchange current densities vary with the concentration of both O and R at the surface of the electrode such that it is convenient to quote the standard rate constant defined by :

$$K^{\varnothing} = \frac{j_o}{nF(C_o^{\infty})^{\alpha_a}(C_R^{\infty})^{\alpha_c}} \quad \text{.....(18)}$$

since $K^{\varnothing}$ is independent of the concentration of O and R . $K^{\varnothing}$ is the value of rate constant for the electron transfer at the standard potential E_e. Thus I-E characteristics are completely specified by $K^{\varnothing}$ and a transfer coefficient.

2.3. Cyclic Voltammetry.

Cyclic voltammetry involves sweeping the electrode potential, initially set a value where no electrode reaction occurs, at a known rate into a region where electrode reaction occurs, and then reversing the potential sweep. A faradaic current due to the electrode reaction is registered in the relevant zone of the applied potential where electrode reaction occurs. The sweep rate (v) in the forward and reverse directions is normally the same, so that the excitation waveform is actually a saw-tooth shown in fig.2.3[5]. The resulting electrochemical spectrum, which is also shown in fig.2.3, is known as a cyclic voltammogram.

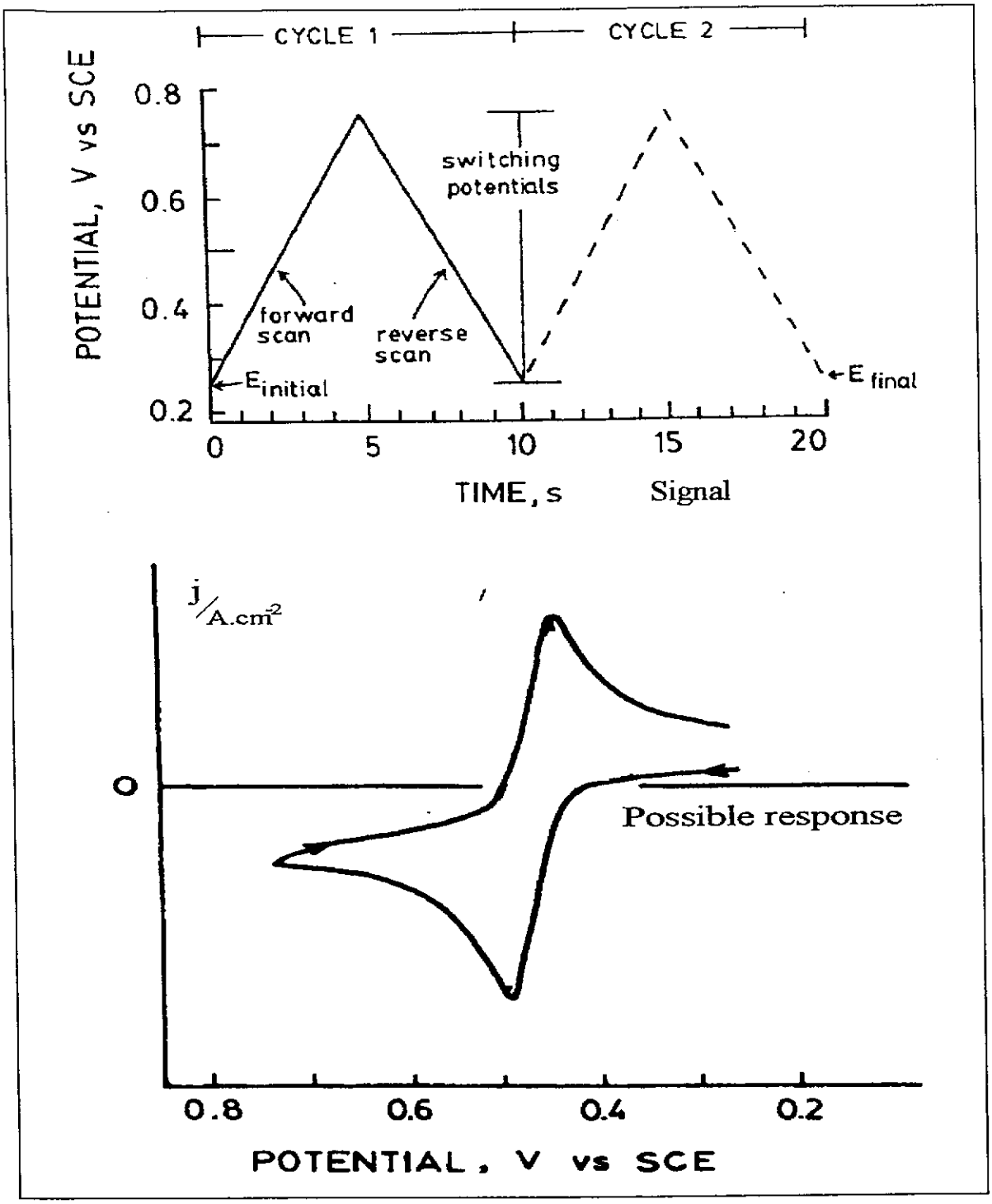

Fig.2.3. Typical potential profile and a possible response for a diffusion-controlled charge transfer reaction during cyclic voltammetry.

In cyclic voltammetry (CYV) ν_{anodic} and $\nu_{cathodic}$ are generally chosen to be equal and this is what has been done when recording voltammograms in this study. CYV can be used to study reversible, irreversible and quasireversible systems. These reaction systems will be discussed briefly in the following section

2.3.1 Reversible Systems.

The reversible electrochemical system is a system in which the electron transfer rates are significantly greater than the rate of mass transport and therefore Nernstian equilibrium is always maintained at the electrode surface. The model electrode reaction which will be considered in this section is a reduction process assuming that O is initially present in the solution. A typical cyclic voltammogram of a reversible system is shown in fig.2.4[6] where j_P^C refers to the cathodic current density resulting from the reduction of O into R. j_P^A is the anodic current density resulting from the reduction of R back into O. E_P^A is the anodic peak potential and E_P^C is the cathodic peak potential.

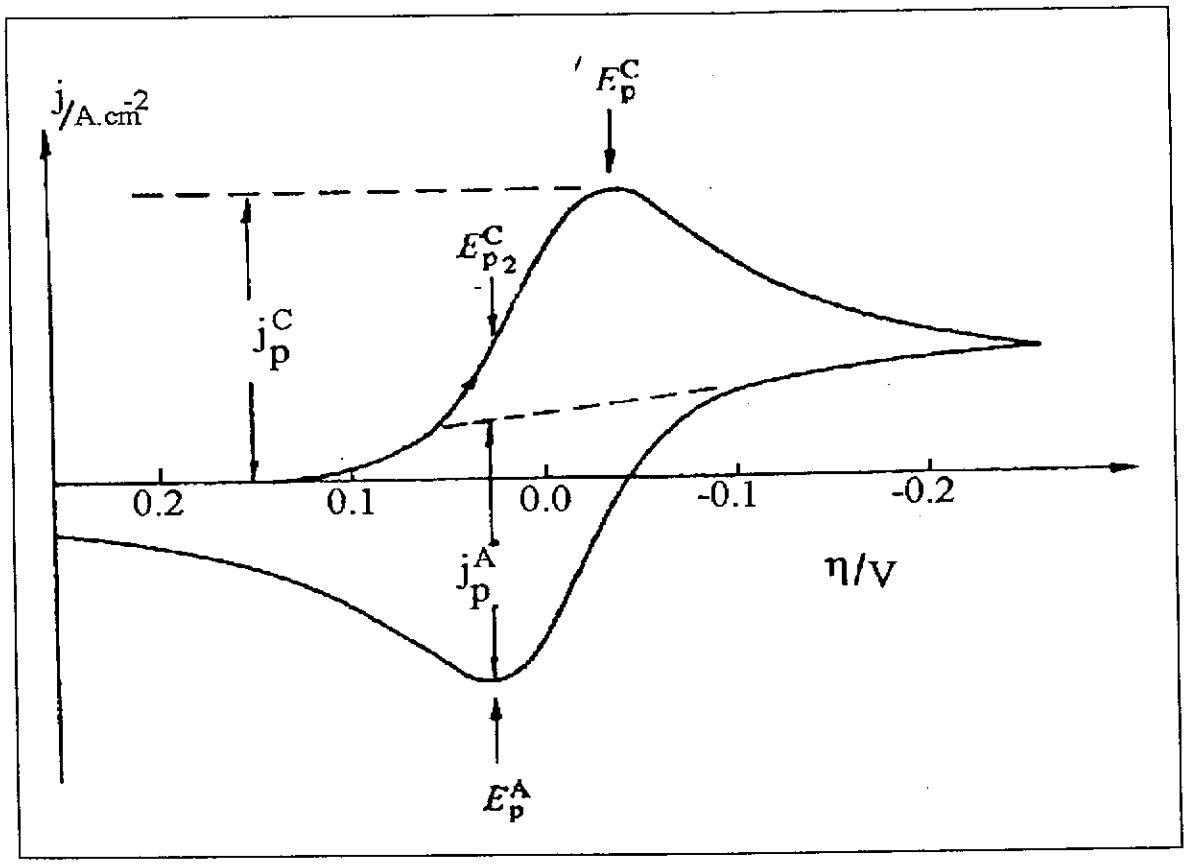

Fig .2.4. Cyclic voltammogram of a reversible process for reduction of O into R. Initially O is present in the solution.

It can be shown that at 25 °C:

$$j_p = -(2.69 \times 10^5) n^{\frac{3}{2}} C_o^{\infty} D^{\frac{1}{2}} v^{\frac{1}{2}} \quad \text{.....(19)}$$

where j_p is the peak current density in A.cm^{-2}, D is the diffusion coefficient in cm^2 . s^{-1}, ν is the scan rate in V/s and C_o^∞ is the concentration of electroactive species in mol.cm^{-3}. This is known as Randles-Sevcik equation. Thus the peak current is proportional to the concentration of electroactive species and to the square root of the scan rate. It must also be emphasised that for a reversible system a cyclic voltammogram can be obtained only if both R and O are stable.

The diagnostic tests for a reversible system at 25 °C can be summarised as follows:

- $j_p \propto \nu^{\frac{1}{2}}$
- E_p is independent of ν
- $\left|E_p - E_P/2\right| = \frac{56.6}{n} mV$
- $E_P^A - E_P^C = \frac{57.0}{n} mV$
- $\left|\frac{j_P^A}{j_P^C}\right| = 1$

2.3.2 Irreversible System

An irreversible system is a system in which the electron transfer rate is significantly less than the mass transfer rate i.e. Nernstian equilibrium is not maintained on the surface of the electrode. The typical voltammogram for an irreversible system is shown in fig.2.5. The peak current for an irreversible process at 25 °C is given by:

$$j_p = -(2.99x10^{-5})(n_C.n_\alpha)^{\frac{1}{2}} C_o^\infty D_o^{\frac{1}{2}} \nu^{\frac{1}{2}} \quad \text{.....(20)}$$

where n_α is the number of electrons transferred up to and including the rate determining step.

The most marked feature of an irreversible system cyclic voltammogram is the total absence of the reverse peak.[8] However such a feature on its own does not necessarily imply an irreversible electron transfer but could be due to a fast following chemical reaction. In this study the irreversible nature of the electrochemical reaction was proved by

carrying out bulk electrolysis while monitoring the disappearance of the electroactive material by UV-vis spectrophotometry.

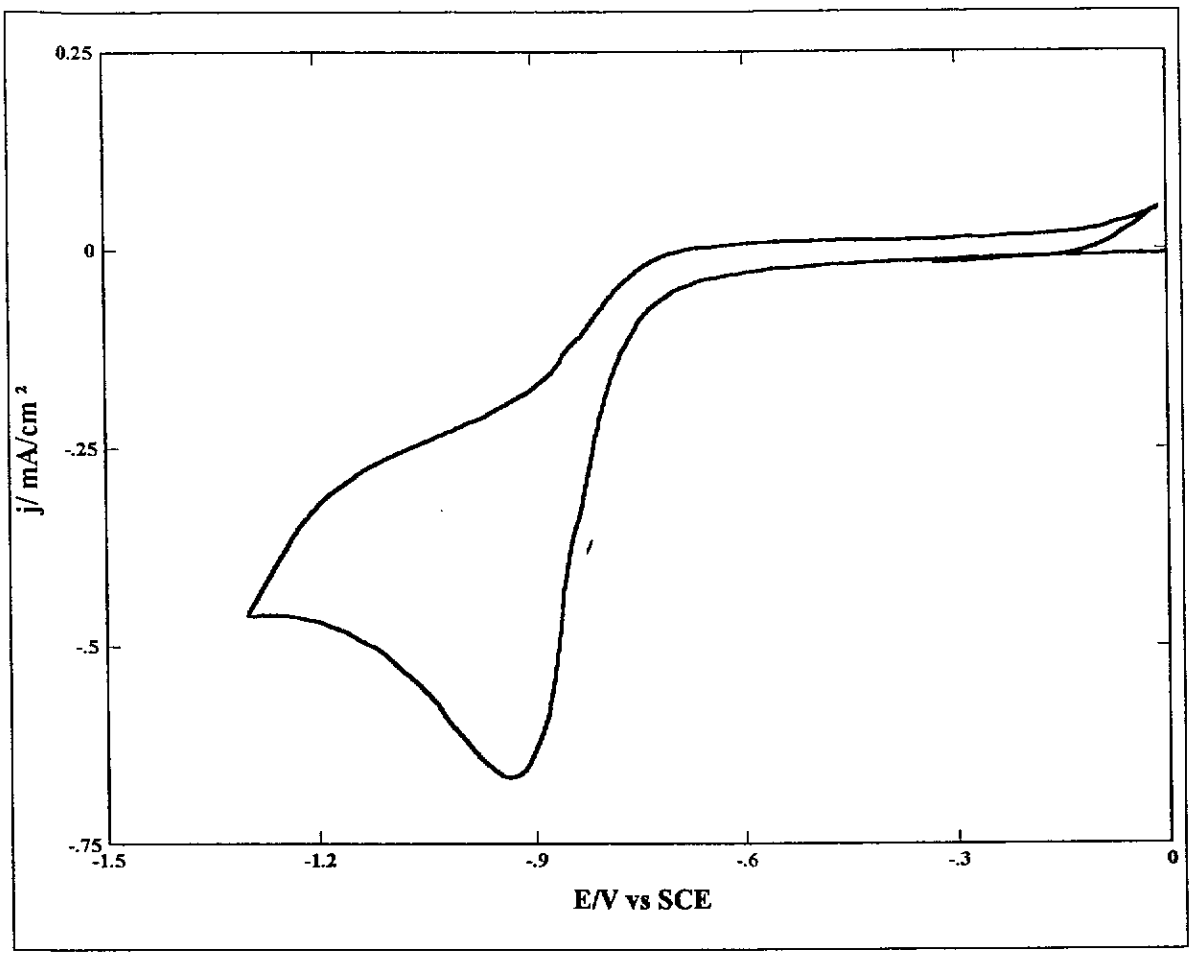

Fig. 2.5. Cyclic voltammogram of an irreversible reaction.

2.3.3 Quasi-reversible Reaction System

Quasireversible reaction represents the intermediate state between a reversible and an irreversible reaction. The extent of irreversibility increases with an increase in scan rate, while at the same time there is a decrease in the peak current to the reversible case and an increasing separation between anodic and cathodic peaks. Fig.2.6. is a graph showing the transition from a reversible to an irreversible system as the sweep rate is increased.[9] The diagnostic characteristics of a quasireversible system at 25 °C are :

- $|j_p|$ increases with $\nu^{0.5}$ but is not proportional to it.

- $\left|\frac{j_P^A}{j_P^C}\right| = 1$ provided $\alpha_c = \alpha_a = 0.5$
- ΔE_p is greater than 59/n mV and increases with
- E_P^C shifts with increasing ν

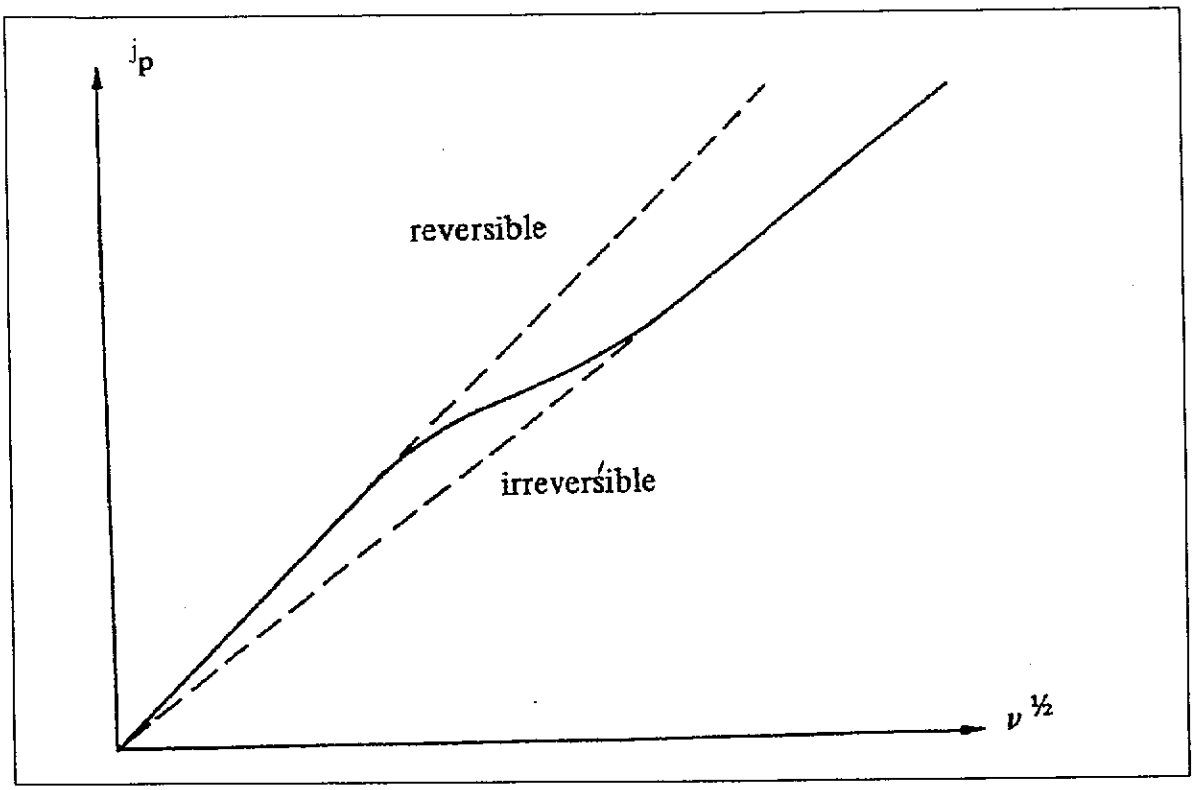

Fig.2.6. A plot of the dependence of the peak current density on the square root of the scan rate, showing the transition from reversible to irreversible behaviour with increasing ν.

2.4 Bulk Controlled Potential Electrolysis.

Controlled potential bulk electrolysis is widely used to determine the overall number of electrons involved in an electrode process. It is also used to prepare a sufficient quantity of the reaction products for identification by conventional analytical techniques. Once voltammetry has provided information about the electrode processes possible in the system, it remains to find out how the products are connected with these processes.[10]

In contrast to voltammetry where the volume of solution per unit electrode area is high, the volume: area ratio is small. One way in which a very small ratio can be obtained is by

employing a thin layer cell in which a thin film of solution is constrained between two parallel plates of which at least one is the working electrode, reference and counter electrodes are placed elsewhere. In such a cell electrolysis takes place in less than a minute which is considerably faster compared with a conventional cell.

In the conventional bulk electrolysis experiment a divided cell is used in which the working electrode (WE) is separated from the counter electrode by means of a glass frit or an ion exchange membrane, however an undivided cell can also be used if the counter electrode reaction will not interfere with the products from the WE. The WE compartment, which should permit stirring, is then filled with a known volume of solution containing a known concentration of electroactive species. The potential of the WE is then fixed at a value determined on the basis of steady state or cyclic voltammetry studies, usually a potential at which the reaction under investigation proceeds at a mass transport limited rate. The current, its integral and the charge are then monitored as a function of time, usually until the current drops to about 1% of its initial value. Samples for analysis are also removed at various stages of the electrolysis and at the end. For a simple reaction of the type:

$$O + ne \rightleftharpoons R$$

assuming a constant rate of stirring, the current should fall exponentially according to:

$$j(t) = j(0)\exp(-bt) \quad \text{.....(21)}$$

where $j(0)$ is the initial current at $t = 0$ and b is a constant related to the diffusion coefficient and cell and electrode dimensions. For a simple reaction, $\ln|j|$ should fall linearly with time t. The charge passed as a function of time, $q(t)$, is given by:

$$q(t) = \int_0^t j\,dt \quad \text{.....(22)}$$

and therefore :

$$q(t) = q(\infty)(1 - \exp(-bt)) \quad \text{.....(23)}$$

For a simple reaction $q(t)$ should vary linearly with time and $q(\infty)$ can be obtained by extrapolation to $j(t) = 0$. Any deviation from linear behaviour for either $\ln|j|$ vs t or $q(t)$ *vs* $j(t)$ indicates that a more complex reaction scheme is involved. The most important information provided by controlled potential electrolysis is the number of electrons involved in an electrochemical reaction i.e.

$$q(\infty) = nFcV \quad \text{.....(24)}$$

where c is the concentration of electroactive species and V is the volume of the solution in the working electrode compartment. The value of n is readily determined from (24) if c is known. In this study controlled potential bulk electrolysis was used to prepare sufficient products for analysis.

2.5 References

1. Southhampton Electrochemistry Group, Editor T. J. Kemp, **Instrumental Methods in Electrochemistry**, Ellis Harwood Limited, Chichester, (1985) p. 26
2. Southhampton Electrochemistry Group, Editor T. J. Kemp, **Instrumental Methods in Electrochemistry**, Ellis Harwood Limited, (1985) p. 27
3. Southhampton Electrochemistry Group, Editor T. J. Kemp, **Instrumental Methods in Electrochemistry**, Ellis Harwood Limited, (1985) p. 28
4. Southhampton Electrochemistry Group, Editor T. J. Kemp, **Instrumental Methods in Electrochemistry**, Ellis Harwood Limited, (1985) p. 24
5. P. T. Kissinger and W. R. Heineman,, **Laboratory Techniques in Electroanalytical Chemistry**, Marcel Dekker, Inc., New York, (1984) P. 87&88
6. Southhampton Electrochemistry Group, Editor T. J. Kemp, **Instrumental Methods in Electrochemistry**, Ellis Harwood Limited, (1985) p. 182
7. Southhampton Electrochemistry Group, Editor T. J. Kemp, **Instrumental Methods in Electrochemistry**, Ellis Harwood Limited, (1985) p. 183
8. Southhampton Electrochemistry Group, Editor T. J. Kemp, **Instrumental Methods in Electrochemistry**, Ellis Harwood Limited, (1985) p. 187
9. Southhampton Electrochemistry Group, Editor T. J. Kemp, **Instrumental Methods in Electrochemistry**, Ellis Harwood Limited, (1985) p. 188
10. L. Eberson and H. Schaafer, **Organic Electrochemistry**, Springer-Verlag, New York, (1971) p. 20

Chapter 3

Literature Review

A review of the chemistry of azo dyes and the electrochemical behaviour of azo dyes is presented.

A dye is defined as a chemical substance used to impart colour to a substrate from a solution or a fine dispersion. It is retained in the substrate by adsorption, mechanical retention or by ionic or covalent bonds.[1] Dyes give colour to the material onto which they have been anchored by selectively absorbing light of certain wavelengths and reflecting the remaining wavelength of the white light falling upon the surface. If therefore a dye absorbs strongly at the red end of the visible spectrum the light which will be reflected will be of a bluish hue.[2]

Dyestuffs are widely used for colouring diverse material such as paper, plastics, leather, wax polish, anodized aluminium and cosmetics. A few carefully selected dyes are also permitted as colourants in the manufacture of sweets, table jellies, custard powder, ice-cream and other foodstuffs. The most important application of dyes is to colour textile fibres. The dyes used for this purpose need to have a number of special properties. They must be reasonably cheap, applicable in solution or as a dispersion and be as fast as possible against light and laundering. They must also be capable of withstanding the finishing processes carried out on the textile during manufacture.

Dyes are conveniently classified according to their method of application and the types of fibre they are most suited for, but they can also be classified according to their chemical structures.[3] There are at least seven chemical classes of dye namely azo dyes, nitro and nitroso dyes, polymethine dyes, Aza[18] annulene dyes, di- and triaryl carbonium dyes, sulphur dyes, carbonyl dyes and pigments.

3.1 Azo Dyes

Azo dyes, of which there are over a thousand inclusive of all types with the common feature of one or more azo groups, constitute numerically the most important class of synthetic colouring matters and in money value they are second largest to the anthraquinoid vat dyes. Over 50 % of the dyes listed in the colour index belong to the azo class, and the proportion of the azo dyes has been stated variously as half to three-quarters of all the synthetic dyes now in use.[2] The azo dyes play a prominent part in almost every type of colour application.[4]

Azo dyes are characterised by a chromophoric azo group -N=N- whose nitrogen atoms are bonded to sp^2 hybridized carbon atoms. At least one of these carbon atoms belongs to an aromatic ring (usually a benzene or naphthalene derivatives) or heterocycle (pyralozone, thiazole), whereas the other carbon adjoining the azo group may be part of an enolizable aliphatic derivative (acetoacetic acid).

Due to the simple nature of synthesis, usually in aqueous medium, and the almost unlimited choice of starting material, an extremely wide variety of azo dyes is possible. The number of combinations is further increased by the fact that a dye molecule may contain several azo groups. This diversity of inexpensively produced azo dyes permits a wide variety of shades and fastness properties suitable for use on a variety of substrates. Naturally occurring azo dyes are unknown.

Azo dyes are named according to the number of azo groups in each molecule i.e. monoazo, bisazo, trisazo and tetrakisazo dyes for one, two, three and four azo groups respectively. Common and IUPAC names can be used to describe the structure of the azo compound. Azo dyes can be classified either according to chemical guidelines (characteristic chemical groups) or by colour aspects as applied in dye works. A rigid assignment to one of the two classification systems is possible but not advisable because of overlapping.[5] There is therefore scarcely any chemical class of azo dyes that belongs to a single colour class or vice versa. Moreover, many materials can be dyed with dyes from various colour groups. A

compromise between the two classification systems with emphasis on applications used in the dye works appears to be the most appropriate.

The importance of the azo dyes is due to their mode of application and to the fact that they represent a clearly defined group. They are briefly described here: disperse dyes; metal-complex dyes; organic pigments; reactive dyes. Reactive dyes will be dealt with more extensively.

3.2 Synthesis of Azo Dyes

The processes that are important in the production of azo dyes are: diazotization and coupling, condensation of nitro compounds with amines, reduction of nitro compounds and oxidation of amino compounds. Of all the industrially important processes, azo dyes are made by diazotization of a primary aromatic amine followed by coupling of the resultant diazonium salt with an electron-rich nucleophile. The modern dye stuff therefore owes a large debt of gratitude to Peter Greiss, the chemist who discovered the diazotization and coupling reactions in 1858. All other industrially employed processes are advantageous only where azo coupling cannot be utilized because of the unavailability of the starting compounds.

3.2.1 Diazotization.

The diazotization of an aromatic or heteroaromatic primary amine is the first of the two reaction steps by which practically all azo dyes are produced. Diazotization is defined as the reaction of the primary amine with nitrites preferably sodium nitrite, in aqueous mineral acid at around 0°C, whereby the amine is converted into the corresponding diazonium salt as shown in fig.3.1.

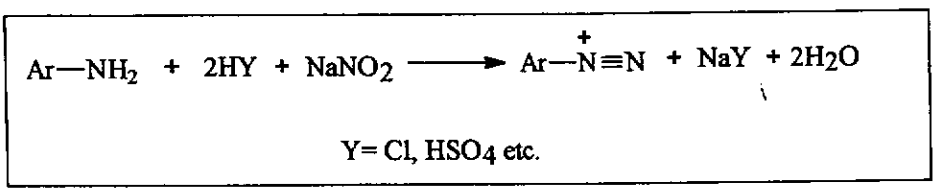

Fig.3.1. Diazotization of aromatic amine.

A higher proportion of hydrogen ions than two moles indicated in fig.3.1 is used in diazotization of weakly basic amines, since this results in the equilbria in the nitrous acid solution shifting towards the production of more electrophilic molecules. Diazotization of aromatic diamines gives bisdiazonium compounds and therefore the reaction is called bis-diazotization.[7]

The essential step in diazotization is the electrophilic nitrosation of the amino group of the primary aromatic amine as shown in fig.3.2 step 1. Formation of the diazonium ion (fig.3.2 step 3) then follows via the diazohydroxide (fig.3.2 step 2).

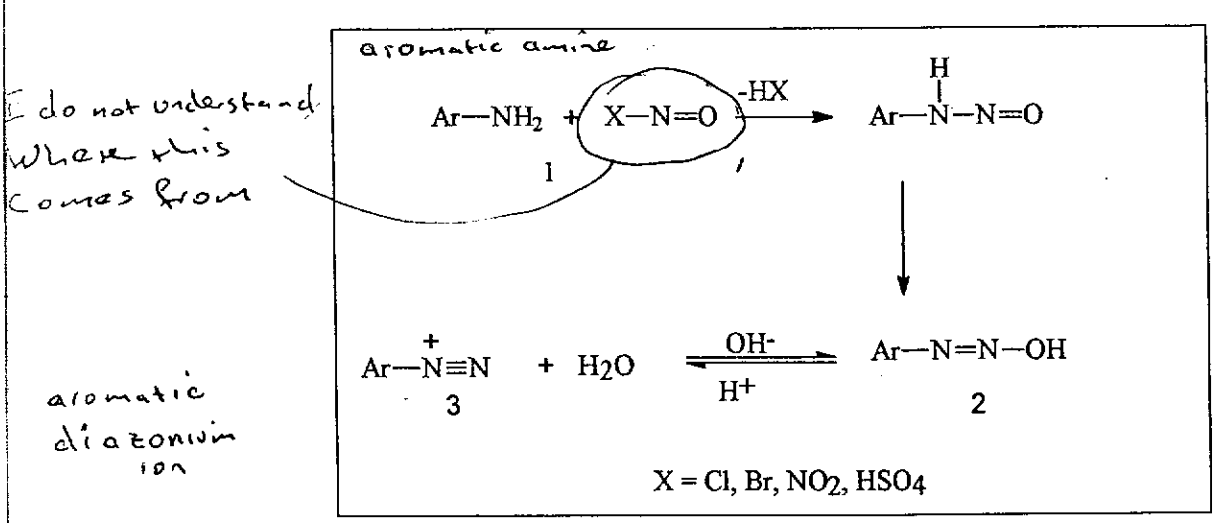

Fig.3.2. Mechanism of diazotization.

An excess of sodium nitrite must be avoided, since the nitrite can react with the coupling agents as well as with secondary or tertiary amines to form nitroso compounds during subsequent coupling. Excess nitrite can be detected with potassium iodide starch paper. The excess nitrite can be eliminated by adding amidosulfuric acid or urea.

3.2.2 Coupling

The azo-coupling reaction consists of an electrophilic substitution reaction of the diazonium compound with a nucleophilic partner (coupling component RH).

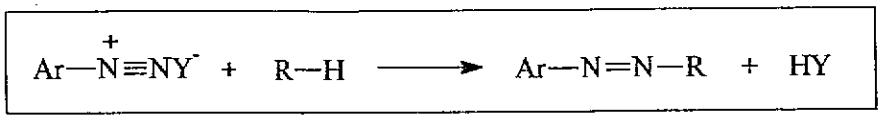

Fig.3.3. The azo coupling reaction.

Coupling components are aromatic systems with nucleophilic centers at the aromatic nucleus, particularly phenols, naphthols, and amines or enolizable compounds with reactive methylene groups. Phenol reacts as phenolates, naphthol as naphtholates, and amines as free bases. According to fig.3.3, free acid is formed during the coupling reaction. In order to maintain an optimal reaction sequence the pH of the medium must be kept constant by adding alkalis or buffers. Coupling under strongly alkaline conditions is not possible because the diazonium compound undergoes reverse reaction to form anti-diazotate as shown in fig.3.2 and the diazonium salt may react with the amine to form diazoamino compound (R-N=N-NH-Ar). Phenols and enols are therefore generally coupled in the weakly alkaline range (pH 7-9), and amines in the weakly acid range (pH 4-7).

Substituents with donor effects in the aromatic nucleus of the coupling components increase reactivity. Donor substituents on the diazonium salt lower its electrophilicity whereas electron-withdrawing substituents increase it.

The C atom with the highest electron-density is usually the preferred coupling position of a coupling component. Due to the directing influence of the hydroxyl or amino groups in the aromatic system, coupling takes place at the ortho or para positions. If these two positions are occupied, there is either no coupling or one of the substituents is exchanged. Coupling never occurs at the meta position in relation to the directing substituent. Components of the naphthalene derivatives generally couple more easily than benzene derivatives. Other reaction conditions besides pH also play an important role in azo coupling. Higher temperature generally has a negative effect on the coupling reaction since it favours the reaction of water with a diazonium salt as shown in fig.3.4.

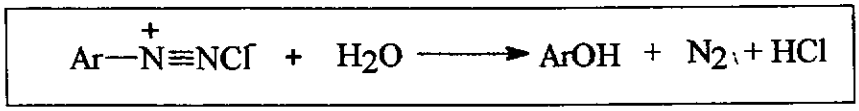

Fig.3.4. Reaction of diazonium salt with water.

Coupling can be accelerated by raising the pH and concentration of the reactants. In some cases the yield of azo dye can be increased by adding sodium chloride prior to the azo coupling.

3.3 Reactive Dyes

Reactive dyes are coloured compounds which contain one or two groups capable of forming a covalent bond between a carbon or phosphorus atom of the dye ion or molecule and an oxygen, nitrogen or sulphur atom of a hydroxy, amino, or mercapto group of the substrate respectively. Such covalent bonds are formed with the hydroxyl groups of cellulosic fibers; with amino, hydroxy and mercapto groups of protein fibers and with the amino groups of polyamide fibers. The development of reactive dyes has continued to be rapid, and the world demand for such material reached approximately 9.7000×10^7 Kg in 1990, valued at 1.5 billion rands. Reactive dyes thus constitute the largest monetary basis in the dye industry, accounting for approximately 17 % of the textile dye market by volume.[8]

3.3.1 Structure of Reactive Dyes.

The characteristic structural features of a reactive dye are shown schematically in fig.3.5.

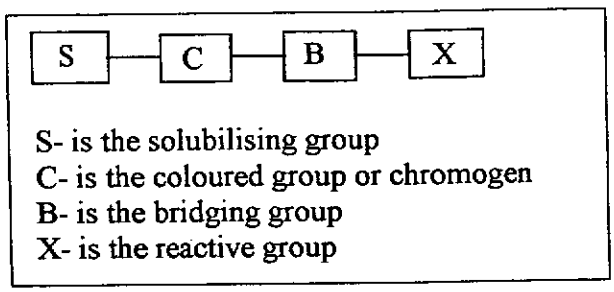

Fig.3.5. Structural features of a reactive dye

3.3.1.1 The Reactive Groups

The reactive group is the group that links the dye covalently to the reactive group of the fibre or the textile. The reactive groups on the dye can be classified according to their reaction mechanism with the reactive groups of the fibre or textile.

I. Those that react by a nucleophilic substitution mechanism based on the presence of labile halogeno substituents in a heteroaromatic system e.g. the chlorotriazinyl dyes shown in fig.3.6. The principal reactive systems of this type are the halogeno-substituted triazine, pyrimidine, pyrazine, quinoline, thiazole and pyridazone groups.[9]

II. Those that react by the addition of a nucleophilic group to the carbon-carbon double bond of the reactive system. In most instances the unsaturated reactive group is not present in the dye as supplied but is formed from a precursor in the presence of alkali. The most important

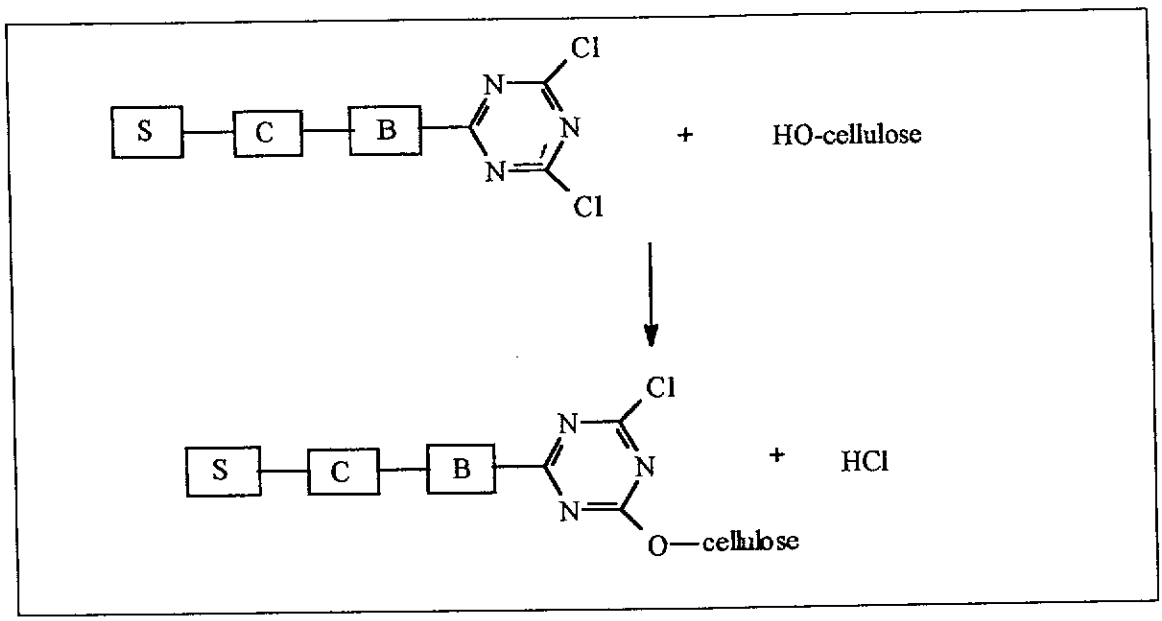

Fig.3.6. Reaction of the dichlorotriazinyl dye with the cellulose fibre

precursor for dyes of this type is the sulphuric acid ester of β-hydroxy ethylsulphone, which forms a vinylsulphone in the dyebath by elimination of sulphuric acid as shown in fig.3.7.

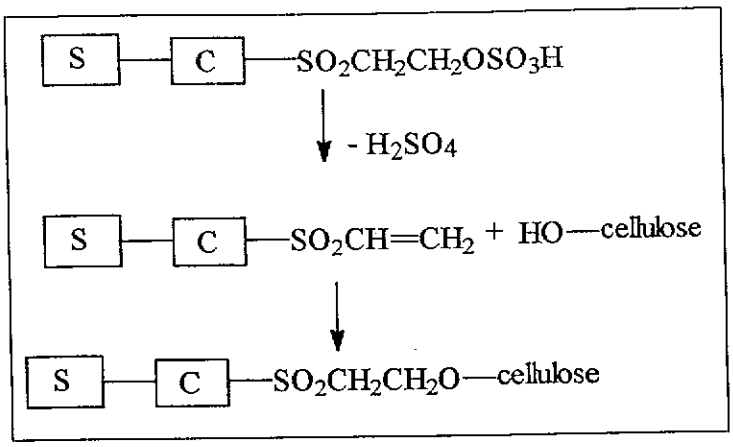

Fig.3.7. Reaction of the reactive dye with a cellulose

III. Groups that react via several addition and elimination steps with the nucleophilic group of the fibre. There are only two reactive groups in this class which have attained widespread industrial importance to date,, namely the α-bromoacrylamido group and its precursor, the α,β-dibromopropionylamido group. They are shown in fig.3.8.

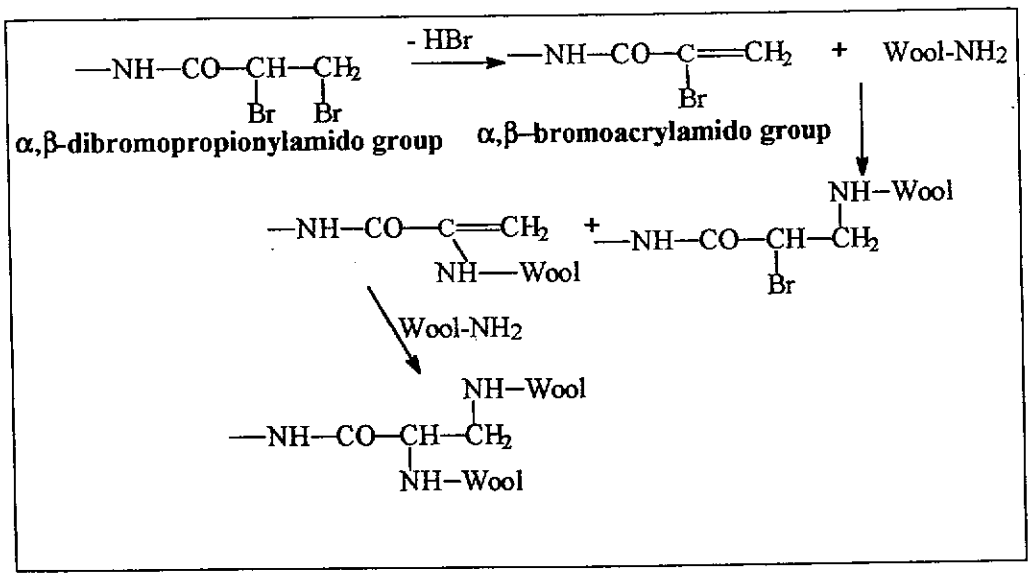

Fig.3.8. The reaction of α,β-bromoacrylamido group with wool

They are the most widely used reactive dyes for wool. They are able to react with two nucleophilic groups of the fibre. This leads to the crosslinking of wool, an effect consolidated by Ball et al.[10]

IV. Reactive groups which react by esterification of a phosphonic acid group (the phosphorus atom bonded to an aliphatic or aromatic carbon atom of the dye. The reactive

dyes with this group were discovered by McConnell[11] of Burlington Industries. They are designed to be used on cellulose polyester blends. Their reaction with cellulose is shown in fig.3.9.

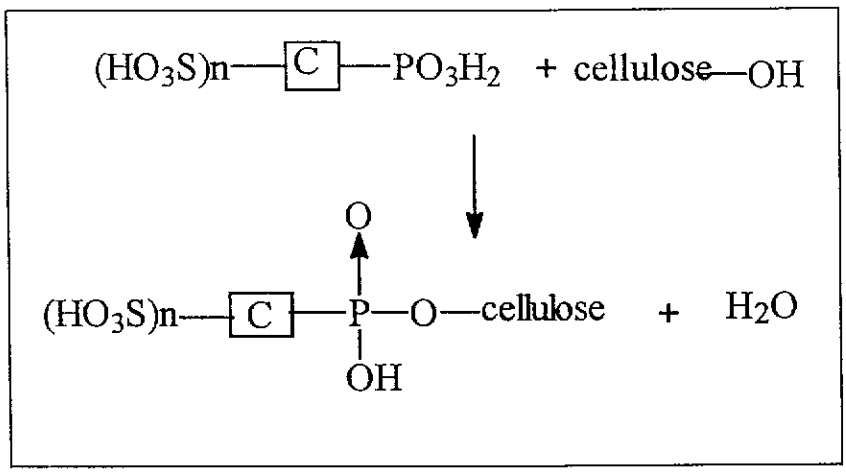

Fig.3.9. Reaction of cellulose with ester forming reactive group.

3.3.1.2 Chromogen or the Coloured Part

A chromogen is the part of the dye that gives colour to the dye. Virtually every conceivable chromophore has been used in the synthesis of reactive dyes. Most reactive dyes fall in the category of azo dyes. Almost every hue in the dye spectrum can be achieved by appropriate structural modification (mono- and bisazo dye, combinations involving either single or multiple aromatic and heterocyclic ring system). The typical azo reactive dye is shown in fig.3.10.

3.3.1.3 The Bridging Group.

The bridge link or the bridging group is the part of the reactive dye that links the chromogen and the reactive group. This part is necessary for synthetic reasons and it influences three principal factors:

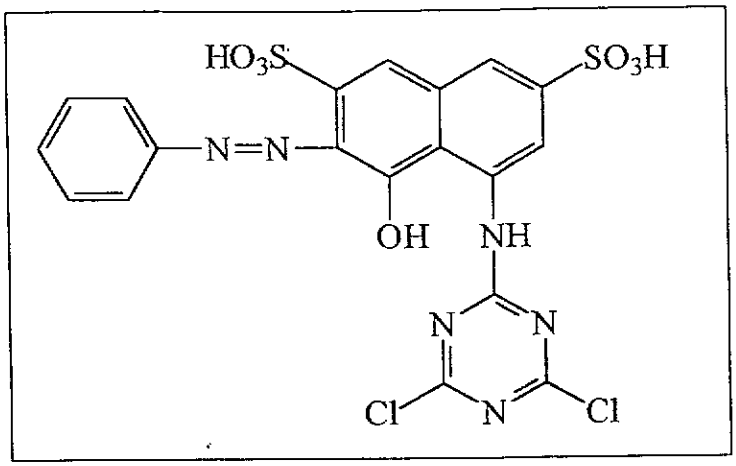

Fig.3.10. The chemical structure of Reactive Red 2

i) The reactivity of the reactive system. Dissociation of the imino bridge as shown in fig.3.11 reduces the reactivity of the reactive groups by several powers of ten. This results in lower fixation of the dye onto the substrate.

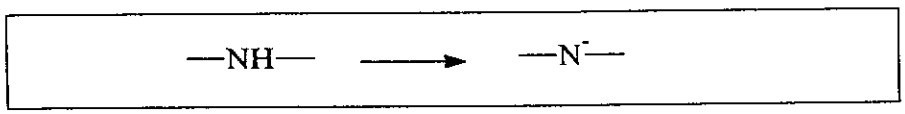

Fig.3.11. An imino linkage which is commonly found in many reactive dyes

ii) The proton on the imino bridge of the reactive group in fig.3.12 is in rapid tautomeric equilibrium with one of the several isomers containing protons at the heterocyclic nitrogen atom. Tautomeric forms have lower selectivity, i.e. a lower ratio of reactivities with the cellulose and with water. Therefore a given reactive group has the highest selectivity when the imino bridge is alkylated.

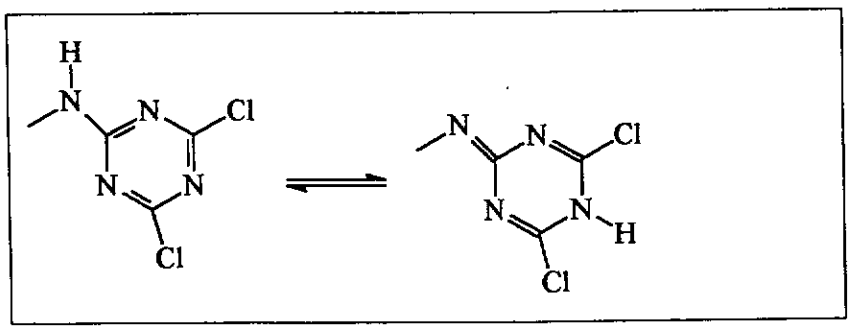

Fig.3.12. Tautomeric equilibrium of reactive group isomers containing the proton on the imino bridge.

iii) The stability of reactive dyeing: If the link between the chromogen and the reactive group can be splitted then the dye-fibre bond will be broken, leading to instability on reactive dyeing.

3.3.1.4 Water-solubilizing Group

Water-solubilizing groups are responsible for rendering the dye water soluble. With dyes for cellulose and protein fibers, one to four sulphonic groups are necessary to achieve solubility. The dye in fig.3.10 is a typical example of a reactive dye with sulphonic groups.

3.3.2 Synthesis of Reactive Azo Dyes

The synthesis of reactive azo dyes is almost similar to the synthesis of azo dyes. The difference lies in the condensation of the reactive group. The reactive group can be condensed with the coupling agent before coupling with the diazonium salt or it can be condensed after coupling.

The synthesized dyes are isolated from aqueous reaction media by salting out. Consequently the isolated dyes are never pure compounds as can be obtained for other dye classes.[12]

3.4 Electrochemical Behaviour of Azo Dyes in Aqueous Solution.

It is well known that any chemical reaction that involves addition or removal of electrons from a chemical compound can be carried out electrochemically, where change in free energy is controlled by means of the electrode potential using a potentiostat.

Chemical reduction of an azo compound is of interest here. Prolonged reduction first saturates the azo group, giving a hydrazo derivative, N-N and then breaks the N-N linkage to form two primary amine molecules.[13] If coupling has been used in preparation of the azo compound, the amines will therefore be the original amine from which the diazonium salt was coupled and the amino derivative of the amine or phenol with which the diazonium salt

was coupled, e.g. benzene azo-2-naphthol on complete reduction gives one equivalent of aniline and one equivalent of 1-amino -2- naphthol as shown in fig.3.13.

The reduction of p-dimethylaminoazobenzene by chemical methods has been studied by Jacobson[14] and Kunz[15], who found that the products of zinc reduction in HCl medium were amines, from the splitting of the azo bond by the addition of four hydrogen atoms. Catalytic reduction of azo compounds to the corresponding amines, or hydrazo compounds, can be achieved by proper choice of catalyst. Reduction of aromatic azo dyes is not unusual electrochemically. It is reported[16] that the azo group is reduced at the dropping mercury electrode (DME) to hydrazo or further to an amino derivative. Shikata and Tachi[17] made the earliest polarographic study of azo compounds. Their principal interest concerned the effect of various functional groups on the reduction potential of the azo bond. They described three reduction waves for p-dimethylaminoazobenzene which varied in height and potential as the pH is changed. Pittoni[18-19] also reported three waves in diluted acid solution for the same dye.

Laitinen and Kneip[20] found that p-aminoazobenzene undergoes four electron reduction to yield amines in acid solution at pH 1.9 in 50 % ethanol. Water soluble sulphonated azo dyes have been reduced electrochemically to amines at a stirred mercury cathode in both acidic and basic solution.[21] In strong alkaline media, a two electron polarographic wave was observed. Coulometric measurements showed an unstable hydrazo compound, which gave an anodic

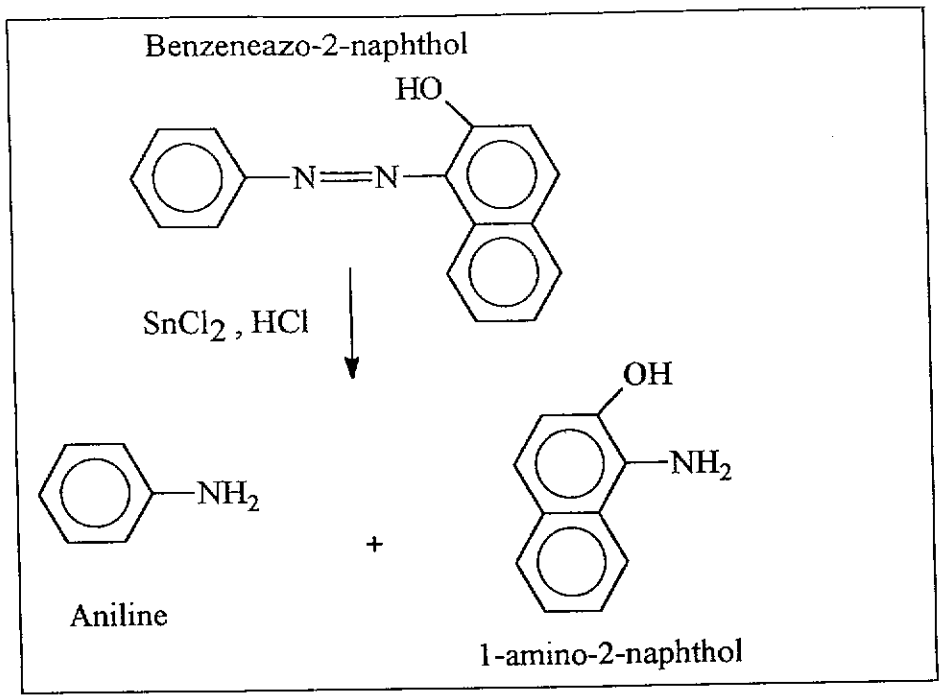

Fig.3.13. The chemical reduction of benzeneazo -2-naphthol.

wave and disproportionated slowly to give the original azo compound and amines. It was also found that the azo bond reduction peak height was directly proportional to the concentration of the dye. Reduction surpassing the hydrazo-derivative stage generally requires greater energy than the azo to hydrazo reaction and if the difference in energy is great enough the reduction may be represented by two waves. The second reduction peak potential will be more negative than the first one. In some cases one, in others two, or even three polarographic waves have been observed.[16]

Pontachrome Violet SW and Super Chrome Garnet Y are azo dyes that have been used by Willard and Dean[22] and Florence[23] for the polarographic determination of aluminium. The polarographic behaviour of Pontachome Violet SW and its lanthanide complexes was studied by Florence and Aylward.[24] They found that Pontachrome Violet SW undergoes four electron reduction yielding corresponding aromatic amines. The structure of Pontachrome Violet SW is shown in fig.3.14. Florence and Farrar[25] studied the polarographic behaviour of azobenzene and its p-sulphonic acids. The techniques employed included d.c., a.c, single sweep and kalousek polarography. Their results showed that the rate of the electrode reaction of the azo-hydrazo couple depended on the pH, the minimum rate occurring near pH 9 for azo benzene-4-sulphonic acid in aqueous media.

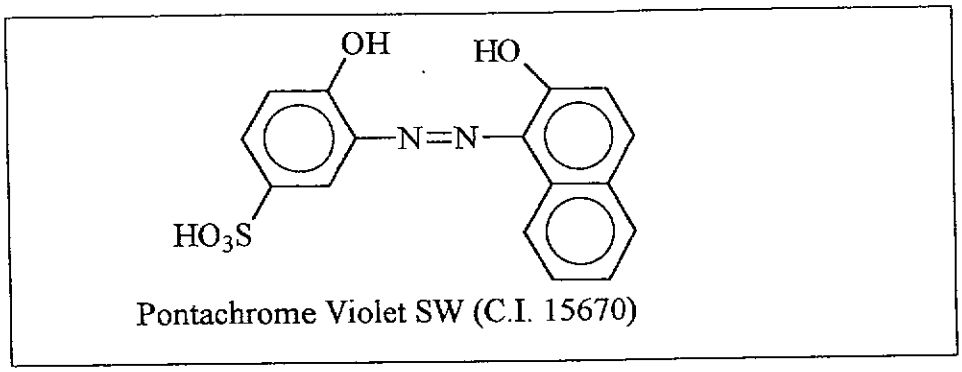

Pontachrome Violet SW (C.I. 15670)

Fig.3.14. The chemical structure of Pontachrome Violet SW (C.I. 15670)

At very low and high pH values, the couple approaches full reversibility at the DME. They proposed that the pH effect is due to strong adsorption of both the azo and hydrazo derivatives. The structure of azo benzene-4-sulphonic acid is shown in fig.3.15.

Florence[26] studied the effect of substituents on the electroreduction of several azo compounds and found that the number of electrons involved in the reduction of the azo compounds

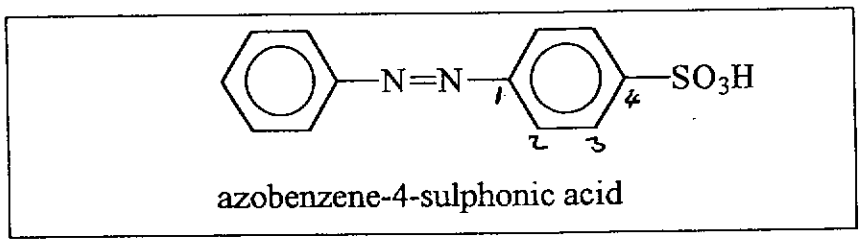

azobenzene-4-sulphonic acid

Fig.3.15. The chemical structure of azobeneze-4-sulphonic acid

depended on the electro-releasing ability of the substituent. In the para-substituted azobenzene series, the compounds undergo 2-electron reduction to a stable hydrazo derivative, only when strongly electron-donating groups are absent. Groups such as hydroxy, amino, and dimethylamino, which increase the electron density on the azo bond, bring about an increase in the polarographic step heights and lead to coulometric n values of four. An o-hydroxy group results in 4-electron reduction at all pH values in the compounds investigated. Florence[27] also studied the polarography of azo compounds and their metal complexes. He describes the work carried out in attempt to elucidate some unexplained aspects of the electrochemistry of aromatic azo dyes and their metal complexes

in aqueous media and to substantiate results already known. The electrochemical behaviour of hydroxy azo compounds was studied in 50 % ethanol. It was found that 3',3- dihydroxy azobenzene gave n = 2 at all pH values and controlled potential coulometric reduction at a large mercury pool produced a hydrazo derivative, but ortho and para dihydroxy gave $3 \leq n \leq 4$, and in basic media both gave n = 2. This means that the hydroxy group at the meta position does not increase the electron density on the N-N bond to activate it to consume 2 more protons and the opposite is the case for ortho and para positions.

Nitro derivatives produced 2-electron waves at all pH excerpt at pH 13 where 4-hydroxy-4'-nitro azobenzene and 1-(4-nitrophenyazo)-2-naphthol gave n = 3.5 and 2.4 respectively. Nitro groups are electron-withdrawing and therefore they diminish the electron density on the hydrazo bond leading to a stable hydrazo compound. A polarographic study of heterocyclic azo compounds by Florence, Johnson and Bartly[28] consolidated the view that electron-withdrawing substituents stabilize the hydrazo derivative. They found that the hydrazo derivatives of the heterocyclic azo dyes were more stable with respect to disproportionation than the benzene and naphthalene derivatives. They attributed the stability of hydrazo derivative to the strongly electron-withdrawing properties of pyridyl and the thiazolyl groups. The structures of some of the compounds they studied are shown in fig.3.16.

Goyal and Jain[29] studied the polarographic behaviour of some aryl azoisoxazoles. They found that these compounds undergo 2-electron reduction to form stable hydrazo compounds. They also attributed the stability of the hydrazo derivative to the electron-withdrawing effect of isoxazoles.

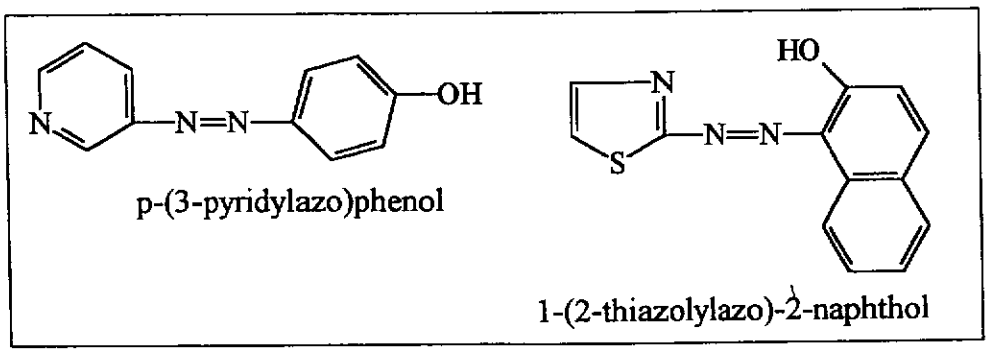

Fig.3.16. The chemical structures of heterocyclic azo compounds.

Florence[27] also studied the electroreduction of p-bisazobenzene which was considered the prototype of the azo compounds studied, because it embodied most of the electrochemical behavioural characteristics of the compounds studied. At all pH's the first stage in the reduction of p-bisazobenzene is a 2-electron reduction step in which one of the azo groups is reduced to a hydrazo bond. The reduction of this azo bond takes place in the presence of a strongly electron-withdrawing substituent viz. the p-phenylazo group. The resulting p-phenylazo hydrazobenzene shown in fig.3.17. was stable, and had no tendency to disproportionate in the pH range 3 to 9.

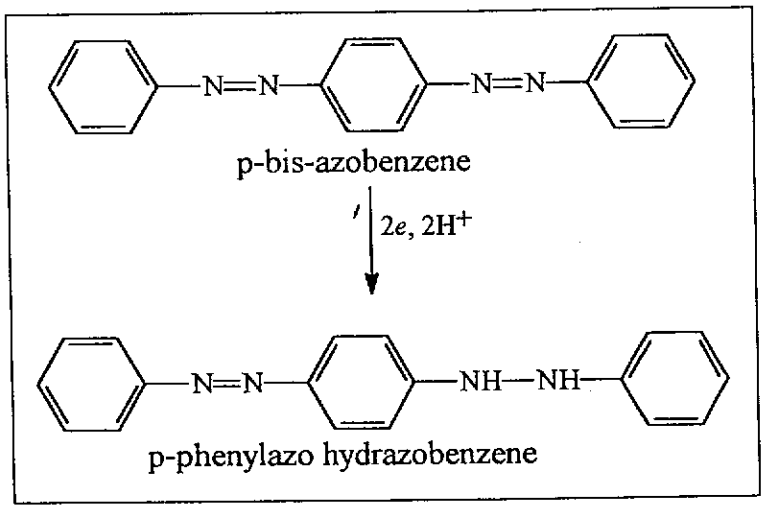

Fig.3.17. Two electron reduction of p-bis-azobenzene

Reduction of the second azo group occurs with the strongly electron-donating p-phenylazo group present. Exhaustive controlled-potential electrolysis at a potential corresponding to the plateau of the second wave gave n = 7.81 which meant that the p-bisazobenzene was being reduced to corresponding amines.

Hart and Smyth[30] studied the polarographic behaviour and analysis of some azo dye. The dyes studied included CI Direct Orange 34, Acid Red 73, Direct Blue 84 and CI Direct Red 80. They results suggested that these dyes are reduced into corresponding amines in acidic solution.

Gupta and Raina[31] investigated the polarographic behaviour of some azo compounds. They found that the products of electrochemical reaction were different in acid and alkaline ranges. In acid media, the uptake of 2e followed by a fast proton attack on the hydrazo

derivative is the major step. The protonated hydrazo derivative may undergo cleavage of N-N to form diimine derivative which is reduced to an amine by further consuming proton, and an electron, as shown in fig.3.18.

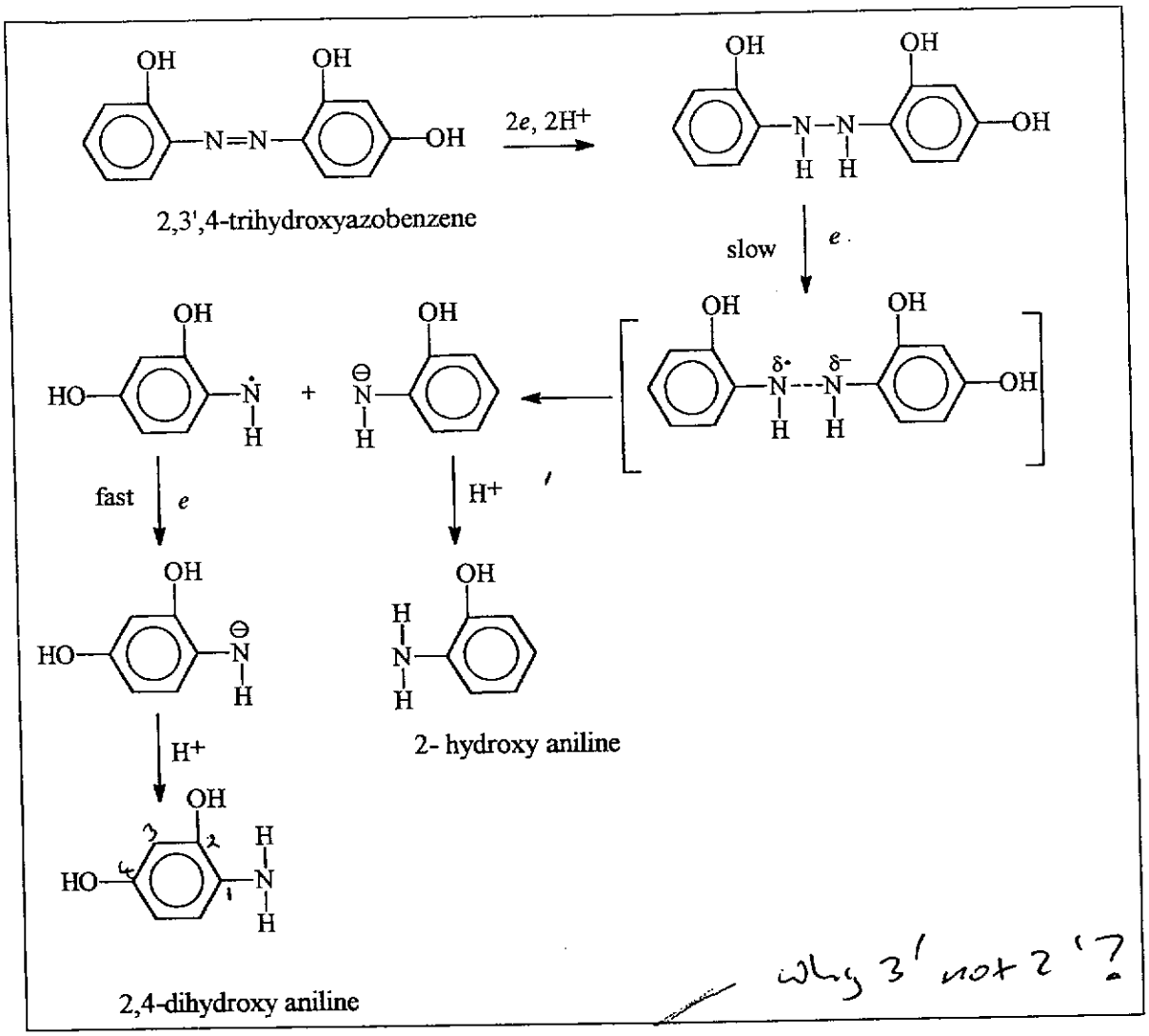

Fig.3.18. The proposed reduction mechanism of 2,3',4-tryhydroxyazobenzene

In alkaline media they found that the reduction half wave potential had shifted towards the negative value. They suggested that the first step is similar to the acid media first step, followed by base attack, simultaneously undergoing homogenous reaction with the hydrazo compound for further electron-reduction and formation of aniline derivatives. Hence only one 2e wave would be possible at pH values where the reaction is fast enough to transfer hydrazo derivatives to the corresponding amines and azo compounds. Goyal, Malik and Marthur[32] studied the electrochemical reduction 4-hydroxy-5-[(2-hydroxy-1-naphthalenyl)azo] -3- [(4-sulpho-1-naphthalenyl)azo]-2,7-naphalene

disulphonic acid commonly known as Fast Sulphone Black-F shown in fig.3.19. Electrochemical behaviour of this dye was studied in phosphate buffers of pH range 2.0 to 11.0 at a DME and a pyrolytic graphite electrode (PGE). The aim of choosing this dye for their study was to investigate the effect of electron-donating and electron-withdrawing groups on the ease of the reduction of azo groups. The dye possesses an electron-donating hydroxy group on one side of an azo group and an electron-withdrawing sulphonate group attached on to the other azo moiety as can be seen from fig.3.19. The first 4e, $4H^+$ reduction causes cleavage of the azo group attached to the naphthalene ring having an electon-donating hydroxyl group only. The electron-withdrawing sulphonate group at a meta position reduces the electron density on the azo bond causing it to consume 2 electrons. On the other hand the presence of an electron-donating hydroxyl group at the ortho position increases the electron density at the hydrazo bond after 2-electron reduction thereby activating it to take two protons and 2 electrons.

In cyclic voltammetry at a scan rate of 80 mV/s, two well defined peaks were observed at pH > 4.0. At pH < 4.0 the peak potentials of the two peaks were so close that only one peak was observed. When the direction of the sweep was reversed additional peaks were observed,

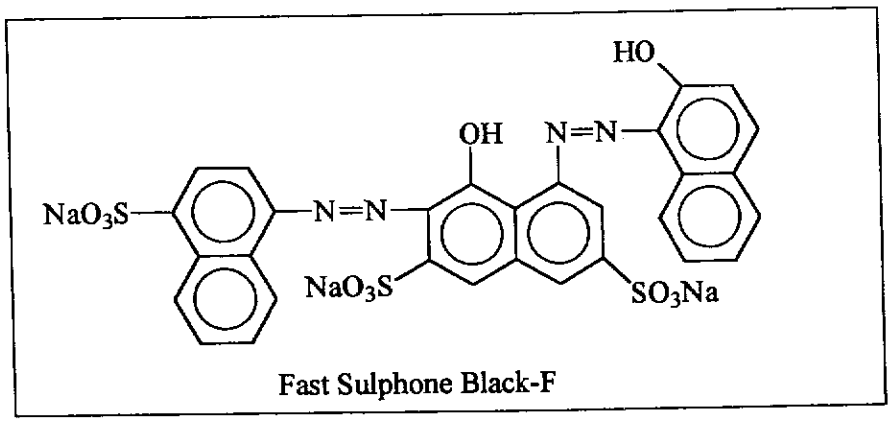

Fast Sulphone Black-F

Fig.3.19. The chemical structure of Fast Sulphone Black-F dye.

and in the reverse cycle another reduction peak was observed. They also observed that the polarograms at pH > 9.0 exhibited only one peak whereas voltammograms at PGE exhibited two reduction peaks. They attributed this difference to the nature of the two electrodes used in their investigation. They also found that the dye undergoes 8-electron

reduction at pH < 4.0 at a mercury cathode, whereas in the pH range 4.0-6.0 the first wave corresponded to six electron transfer and the second to a two electron transfer. At higher pH, both waves involve a 4-electron transfer, and at pH > 9.2 again a single wave corresponding to 8 electron processes is observed. Fast Sulphone Black-F undergoes 8-electron reduction at PGE in the pH range 4-8.

The progress of controlled potential reduction of Fast Sulphone Black-F was monitored by both cyclic voltammetry and visible spectra in the region 250-800 nm. Fast Sulphone Black-F exhibits two well defined bands at 475 nm and 600 nm in the pH range 2.0-11.0. The absorbance at λ_{max} decreased systematically and no intermediate capable of absorbing at longer or shorter wavelength was generated. Cyclic voltammograms of completely electrolysed solution showed a total absence of reduction peaks meaning that the dye chromophores had been destroyed.

The products of electrolysis were analysed by infrared spectra (IR) and thin layer chromatography (TLC) and were found to be the corresponding amines from the fission of the azo bonds, and hence it was concluded that the electroreduction of Fast Sulphone Black-F does not stop at the hydrazo stage but gives the corresponding aromatic amines as products.

Goyal, Srivastava and Nautiyal[33] studied the electrochemical behaviour of 4-(2-hydroxy-1-naphthylazo) benzenesulphonic acid, which they termed Naphthol Red-J and is commonly known as Orange II, in phosphate buffers of pH range 2.5-11.0 at a DME and PGE. The techniques employed included polarography, cyclic voltammetry and coulometry. Orange II has an electron-withdrawing sulphonate group at the para position and an electron-donating hydroxyl group at the ortho position to the azo bond as seen in fig.3.20. They found that Orange II like Fast Sulphone Black-F undergoes 4e reduction giving corresponding aromatic amines. They also found that the electroreduction mechanism of Orange II is the same for DME and PGE. The aromatic amines, sulphanilic acid and 1-amino-2-naphthol were identified in the completely electrolysed solution by comparison of their retention times with the authentic samples. The cyclic voltammogram

of completely electrolysed solution showed the absence of the dye reduction peak in the case of Fast Sulphone Black-F.

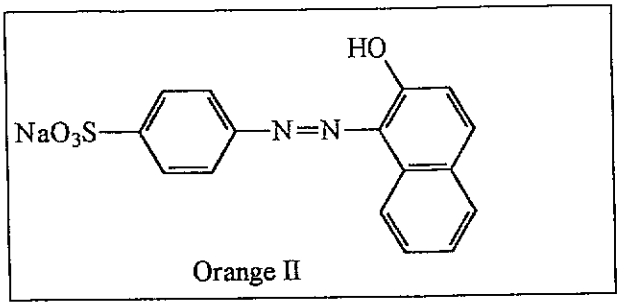

Fig.3.20. The chemical structure of Orange II

Sahm, Knittel and Schollmeyer[34] electrochemically analysed reactive dyes with monoazo and monoanthraquinone structures. They demonstrated the application of voltammetric techniques to the detection of reactive dyes. They pointed out that the electrochemical characterization of the behaviour of reactive dyes was not available in the literature. They studied Azo Red I shown in fig.3.21. and Azo Red II whose structure they did not know.

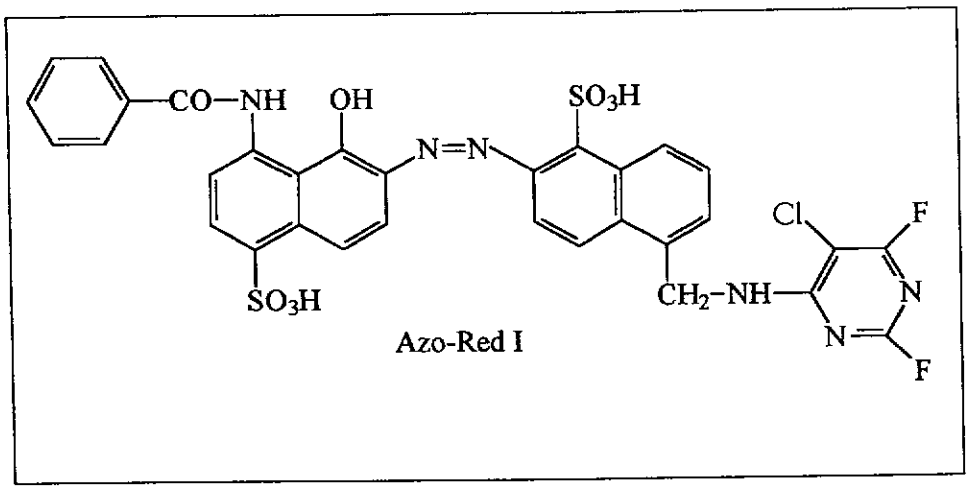

Fig.3.21. The chemical structure of Azo-Red I

The aim of their study was to provide basic knowledge for the development of sensors for monitoring these dyes and their hydrolysed forms. They concluded that reactive dyes can be determined quantitatively by direct current polarographic methods down to the range 10^{-5} mol/L. Reduction peaks are due to the reduction of the azo group [reduction potential at about -0.2 V vs saturated calomel electrode (SCE) in acid medium]. Solid electrodes such

as glassy carbon (GC) can be used and the detection limit is higher than that of direct current polarography but sufficient for most purposes.

Gupta, Raina and Bhat[35] studied the polarographic reduction of 34 azo compounds in variety of buffers at different pH values. Their focal point was the electron-releasing and electron-attracting effect of the substituents on the half wave potentials of the dyes. They found that substituents bring about electron-density variation at N=N, viz., -COOH, $-SO_3H$, facilitate a single 2-electron reduction of an azo group, simultaneously lowering the basicity of N-atoms to the extent that there are not protonated easily. Electron-donating substituents produce an increase in electron density at the azo bond and many electrons are needed for reduction.

Goyal and Bansal[36] studied the electrochemical behaviour of 2-(4'-hydroxybenzeneazo) benzoic acid at a PGE. The electrochemical behaviour of this dye was studied under conditions closer to those of biological systems in order to determine its stability. It was found that in the acidic pH range, the 2-electron, 2-proton reduction of this dye gives a hydrazo intermediate. The strongly repelling hydroxy group weakens the NH-NH bond and causes disproportionation of the intermediate to give the corresponding aromatic amines namely p-aminophenol and o-aminobenzoic acid.

3.5 Electrochemical Behaviour of Azo Dyes in Nonaqueous Solution.

Aylward, Garnet and Sharp[37] studied the electroreduction of azobenzene in dimethylformamide (DMF). They pointed out that azobenzene and hydrazobenzene are strongly adsorbed at the DME in aqueous solution and Nygard proposed[38] that adsorption makes a significant contribution to the electrode process. In DMF the reduction of azobenzene is not complicated by the adsorption, also reduction can be studied in the presence and in the absence of proton donors. Aylward et al[37] showed that azobenzene is reduced at a DME in two diffusion-controlled one electron steps in a 0.1 M solution of tetraethylammonium perchlorate in DMF. The product of the 2-electron reduction was diamagnetic, which they called a dianion. On addition of phenol, a weak proton donor the 2-electron reduction steps shifted from negative potential to positive potentials read against

the Ag/Ag+ reference electrode and the peaks overlapped into one peak as the concentration of phenol was increased. This explains why the reduction of the azo compounds in aqueous solution is pH dependent. They[39] later proposed the mechanism of reduction in DMF shown in fig.3.22.

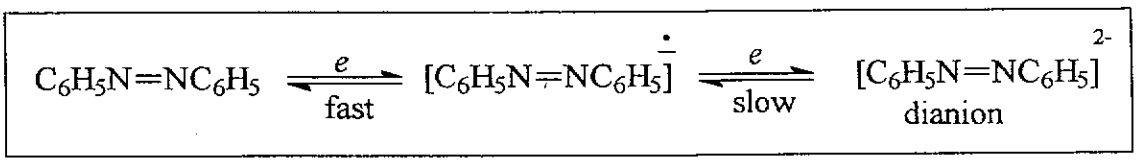

Fig.3.22. Reduction mechanism of azobenzene in DMF.

Sadler and Bard[40] studied the electrochemical reduction of azo compounds including azobenzene in DMF solutions by polarography, cyclic voltammetry at a platinum electrode, controlled potential electrolysis, electron spin resonance spectroscopy and ultraviolet spectroscopy. Their results support the mechanism shown in fig.3.22. Furthermore the two one electron steps were found to be reversible. In the presence of excess proton donors, the diamagnetic anion forms a hydrazo compound, ie. hydrazobenzene for azobenzene reduction as shown in fig.3.23 and in the absence of proton donors it decomposes slowly to form

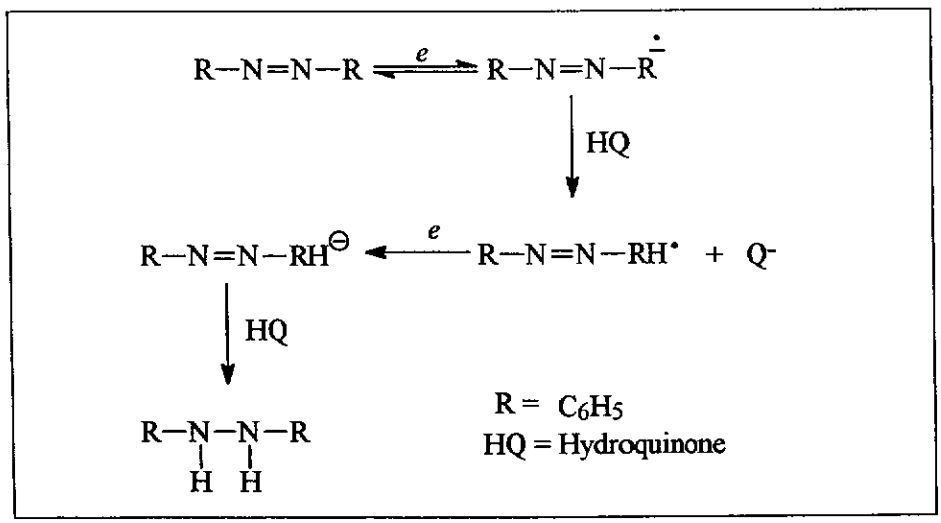

Fig.3.23. Reduction of azobenzene in the presence of a proton donor, hydroquinone.

the corresponding arylhydrazine or abstract a proton from the solvent to form a protonated anion as shown in fig.3.24.

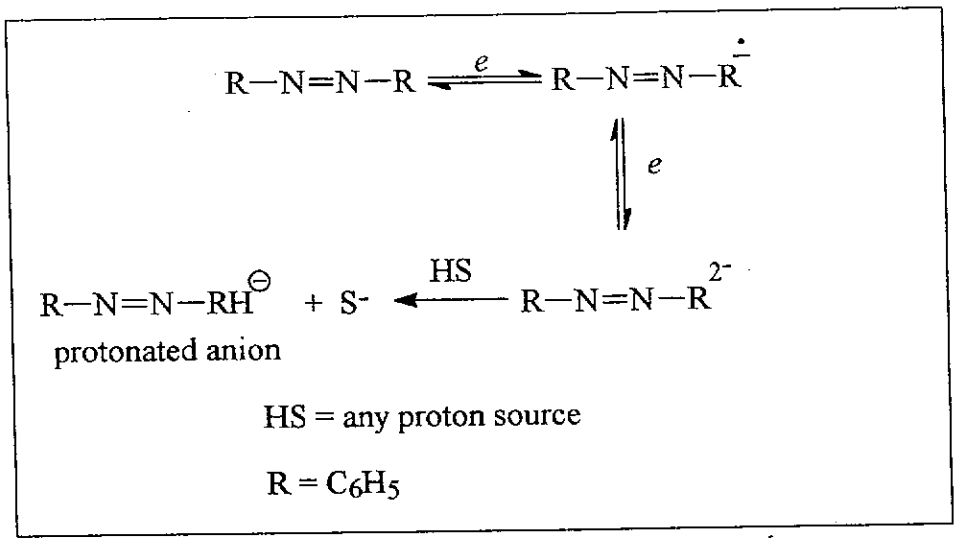

Fig.3.24. The reduction of azobenzene in the absence of the proton donor.

Boto and Thomas[41] studied the dc and ac polarographic behaviour of several 4-monosubstituted azobenzenes in acetonitrile. Here two one electron reduction steps were also reported. They found that the first step was reversible but in contrast to Sadler and Bard[40]s observation the second step was not reversible. The only compound that exhibits a reversible second one electron reduction step was 4-nitro azobenzene. The reversibility of the second one electron reduction step for this compound is attributed to the electon-withdrawing effect of the nitro group which tends to draw electrons out of the π-electron system, hence facilitating easier electron addition to the azo bond. The electron-withdrawing effect stabilizes the dianion shown in fig.3.25., by lowering the electron density of the dianion towards proton attack.

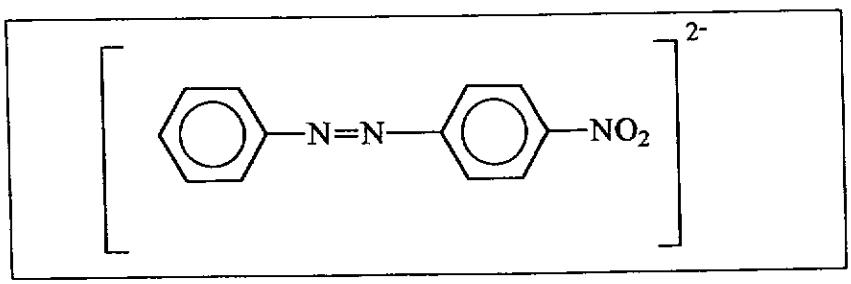

Fig.3.25. The chemical structure of 4-nitroazobenzene dianion.

Boto and Thomas[42] continued with the study of substituted azobenzene in acetonitrile. They focused attention on the identification of the reduction products of azobenzene and 4-nitroazobenzene. Their objective was to see if the product of the second one electron reduction step was a stable dianion, as postulated by Aylward et al.[37], or the monoprotonated anion. Their results indicated that two electron reduction product was not a dianion but a monoprotonated anion in agreement with the work of Sadler and Bard[40] in DMF. Although both electron steps are reversible, the observed irreversibility of the second wave is due to the very fast, irreversible protonation of the product during the second charge transfer step.

Acetonitrile is considered to be the major source of protons in this step as the final product, the monoprotonated anion, was obtained by electrolysis of 2 mM azobenzene in solvent containing less than 0.5 mM water. On the other hand, the results obtained for 4-nitroazobenzene indicated as shown in fig.3.25 that the stable dianion is the product of the two one-electron reduction steps. The polarogram of the product showed two anodic peaks corresponding to the two step oxidation back to the parent compound. The oxidation peaks appeared at essentially the same potentials as the corresponding reduction peaks of the parent compound, as would be expected for reversible electron transfer reactions. The highly coloured two electron reduction product obtained can be compared with the much less coloured two electron product from azobenzene, indicating that the products are of quite different nature, since such a marked colour change and intensity would not be expected to be simply due to the presence of one nitro group in the molecule. Evan et al[43] pointed out that the chemically formed dianion of the aromatic azo compounds in tetrahydrofuran are highly coloured species. They attributed the stability of the dianion of 4-nitroazobenzene to the presence of strongly electron-withdrawing nitro group which delocalizes the negative charge. The dianion of 4-nitroazobenzene is thus a weaker base than the initially produced dianion of azobenzene and so cannot abstract a proton from the solvent.

3.6 References

1. F. D. Snell and L. S. Ettre, **Encyclopaedia of Industrial Chemical Analysis**, Vol. 12, John Wiley & Sons, USA., (1971) p. 1
2. K. Venkataraman, **The Chemistry of Synthetic Dyes**, Vol.1, Academic Press Inc., New York, (1952) p. 409
3. P. Tooley, **Fuel, Explosives and Dyestuffs**, John Murray Ltd, London, (1971) p. 212.
4. E. N. Abrahart, **Dyes and their Intermediates**, Edward Arnold Ltd, London, (1977) p.72
5. W. Gerhartz, Y. S. Yamamoto, F. T. Campbell, R. Pfefferkorn and J. F. Rounsaville, **Ullmann's Encyclopaedia of Industrial Chemistry**, 5th edn, Vol. A3, VCH Publishers, Weinheim, Federal Republic of Germany, (1985), p. 247
6. Heinrich Zollinger, **Color Chemistry**, VCH Publishers, Weinheim, Federal Republic of Germany, (1987) p. 86
7. W. Gerhartz, Y. S. Yamamoto, F. T. Campbell, R. Pfefferkorn and J. F. Rounsaville, **Ullmann's Encyclopaedia of Industrial Chemistry**, 5th edn, Vol. A3, VCH Publishers, Weinheim, Federal Republic of Germany, (1985), p. 248
8. Barbara Elvers, Stephen Hawkins, William Russey and Gail Schulz, **Ullmann's Encyclopaedia of Industrial Chemistry**, 5th edn, Vol. A22, VCH Publishers, Weinheim, Federal Republic of Germany, (1993) p. 651
9. Clifford Preston, **The Dyeing of Cellulosic Fibres**, Dyes' Company Publications Trust, West Yorkshire, England, (1986) p.147
10. P. Ball, U. Meyer and H. Zollinger, **Crosslinking Effects in Reactive Dyeing of Wool and Silk, *Text. Res. J.***, 56, (1986) p. 447
11. B. L. McConnell, L. A. Graham and Swidler R.A., **A New Reactive System for Continuous Dyeing and Printing of Celluose and Blends, *Text. Res. J.***, 49(8), (1979) p. 458

12. D. R. Waring and Geoffrey Hallas, **The Chemistry and Application of Dyes.**, Plenum Press, New York, USA., (1990) p. 85

13. F. G. Mann and B. C. Saunders, **Practical Organic Chemistry**, 4th edn, Longman Singapore Publishers Ltd, Singapore, (1974) p. 210

14. P. Jacobson, **Summary of Results of the Rearangement of Hydrazo Compounds, with Consideration of their Importance,** ***Ann.***, 428, (1922) p. 76

15. P. Jacobson and R. Kunz, ***Ann.***, 303, (1898) p. 353

16. I. Rusznak, F. Peter and G. Y. Palyi, **Study of the Structure of Some Azo-Compounds with Polarographic Method.,** ***Acta Chim. Hung. Tomus.***, 35, (1963) p. 199

17. M. Shikata and I. Tachi, **The Electrolytic Reduction Potentials of Organic Compounds.** ***C.A.***, 31, (1937) p. 6087

18. A. Pittoni, **Behaviour of Methyl Orange at the Dropping-Mercury Electrode,** *C. A.*, 43, (1949) p. 7835g

19. A. Pittoni, **Polarographic Studies on Dimethyl Yellow,** *C. A.*, 44, (1950) p. 8268a

20. H. A. Laitinen and T. J. Kneip, **Polarographic and Coulometric study of p-Dimethylaminoazobenzene,** ***J. Am. Chem. Soc.***, 78, (1956) p. 736

21. L. P. Hubbuch and A. Lowry, ***Trans. Am. Electrochem. Soc.***, LV, (1929) p. 227

22. H. H. Willard and J. A. Dean, **Polarographic Determination of Aluminium,** ***Anal. Chem.***, 22(10), (1950) p. 1264

23. T. M. Florence, **Determination of Aluminium in Thorium Compounds by Linear Sweep Oscillographic Polarography,** ***Anal. Chem.***, 34(4), (1962) p. 496

24. T. M. Florence and G. H. Aylward, **Electrochemical Studies on Eriochrome Violet B and its Lanthanide Complexes,** ***Aust. J. Chem.***, 15, (1962) p. 65

25. T. M. Florence and Y. J. Farrar, **Polarography of Azobenzene and its P-sulphonic Acid,** ***Aust. J. Chem.***, 17, (1964) p. 1085

26. T. M. Florence, **Polarography of Aromatic Azo Compounds,** ***Aust. J. Chem.***, 18, (1965) p. 608

27. T. M. Florence, **Polarography of Azo Compounds and their Metal Complexes,** ***J. Electroanal. Chem. Interfac. Electrochem.***, 52, (1974) p. 115

28. T. M. Florence, D. A. Johnson and G. E. Bartley, **Polarography of Heterocyclic Azo Compounds an their Metal Complexes,** ***J. Electroanal. Chem.***, 50, (1974) p.113

29. R. N. Goyal and Rajeev Jain, **Polarographic Investigations of Some Arylazoisoxales,** ***J. Electroanal. Chem.***, 79, (1977) p. 407

30. J. P. Hart and W. F. Smyth, **Polarographic Behaviour and Analysis of Some Azo Dyes of Biological Importance,** ***Analyst.***, 105, (1980) p. 929

31. P.N. Gupta and Anju Raina, **Polarographic Behaviour of Some Azo Compounds, Indian.** ***J. Chem. Soc.***, LXII, (1985) p. 363

32. R. N. Goyal, W. U. Malik and N. C. Marthur, **Electrochemical Reduction of Fast Sulphone Black-F, a Bisazo Dye,** ***J. Electroanal. Chem.***, 235, (1987) p. 225

33. R. N. Goyal, S. K. Srivastava and A. P. Nautiyal, **Electrochemical Behaviour of Naphthol Red-J, an Azo Dye,** ***Indian J. Chem.***, 26(A), (1987) p. 871

34. Uwe Sahm, Dierk Knittel and Eckhard Schollmeyer, **Electrochemical Investigations on the Analysis of Reactive Dyes with Monoazo- and Monoanthraquinone Structures,** ***Fresenius J. Anal. Chem.***, 338, (1990) p. 824

35. P. N. Gupta, A. Raina and V. K. Bhat., **Polarographic Reduction of Aromatic Azo Compounds.,** ***Asian J. Chem.***, 2(1), (1990) p. 73

36. R. N. Goyal and V. Bansal, **Electrochemical Behaviour of 2-(4'-hydroxybenzeneazo)benzoic acid at Pyrolytic Graphite Electrode,** ***J. Electroanal. Chem.***, 385, (1995) p. 25

37. G. H. Aylward, J. L. Garnett and J. H. Sharp, **Electroreduction of Azobenzene in dimethyformamide, Review of Polarography** ***(Japan)***, 14, (1967) p. 322

38. B. Nygard, **Azobenzene-Hydrazobenzene-Polarographic Reversibility Problem,** ***Arkiv for Kermi.***, 20, (1963) p. 163

39. G. H. Aylward, J. L. Garnett and J. H. Sharp, **Alternating and Direct Current Polarography of Azobenzene in Indifferent Electrolyte in Dimethylformamide,** ***Anal. Chem.***, 39(4) (1967) p. 457

40. J. L. Sadler and A. J. Bard, **The Electrochemical Reduction of Aromatic Azo Compounds,** ***J. Am. Chem. Soc.***, 90(8), (1968) p. 1979

41. K. G. Boto and F. G. Thomas, **The Dc and Ac Polarography of Some Substituted Azobenzenes in Acetonitrile,** ***Aust. J. Chem.***, 24, (1971) p. 1484

42. K. G. Boto and F. G. Thomas, **The Polarography of Some Substituted Azobenzenes in Acetonitrile,** ***Aust. J. Chem.***, 26, (1973) p. 1251

43. A .G. Evans, J. C. Evan, P. J. Emes, C. L. James and P. J. Pomeroy, **Reactions of Radical Anions,** ***J. Chem. Soc. B***, (1971) p. 1484

Chapter 4

Experimental

4.1 General

NMR spectra were recorded at room temperature on a Varian 300 MHz spectrometer using deuterated solvents: $CDCl_3$, CD_3OD and D_2O. UV-vis absorption spectra were recorded on a Varian Cary 1E UV-vis spectrophotometer using water as a solvent. Elemental analysis was done by Dr. P. Boshoff at Cape Technikon.

4.2 Synthesis of Procion Red MX 5B

1.26 ml of aniline was dissolved in 8.4 ml of 50 % HCl. The solution was cooled to 5 °C and diazotized using 5.6 ml of 2.9 M $NaNO_2$.

5 g of recrystallized 4-amino-5-hydroxy -2,7-naphthalenedisulphonic acid dissolved in 94 ml of water was added dropwise to a suspension of cyanuric chloride prepared by mixing 3 g of cyanuric chloride with water-acetone solution (1:1) at 0-2 °C. The pH of the mixture was allowed to fall to 1.8. The solution was stirred for an hour and thereafter filtered to remove unreacted cyanuric chloride.

The filtered solution was diluted with 500 mL of water and mixed with the diazotized aniline. The pH was slowly raised to 6.8-7.0 at 0-4 °C by dropwise addition of 0.1 molar sodium carbonate during 45 minutes. The red solution was evaporated at reduced pressure. The residue was doubly recrystallized from water and ethanol. The yield of the dye was 2.99 g and the percentage yield was 35 %. Elemental analysis of hydrolysed dye dihydrate was as follows: calculated C: 37.14, H: 2.62, N: 13.68, S: 10.44, observed C: 37.80, H:2.74, N:13.09, S: 10.61. The structure of the dye was also confirmed by the ^{1}HNMR spectroscopy. The aromatic region of the ^{1}HNMR spectrum (Appendix I, spectrum 1) integrated to eight protons which is in accordance with the structure shown in

fig 4.1. Also according to ^{1}HNMR spectroscopy (appendix I, spectrum 1) fig 4.1 should show three singlets, a doublet and 2 triplets. This is as expected.

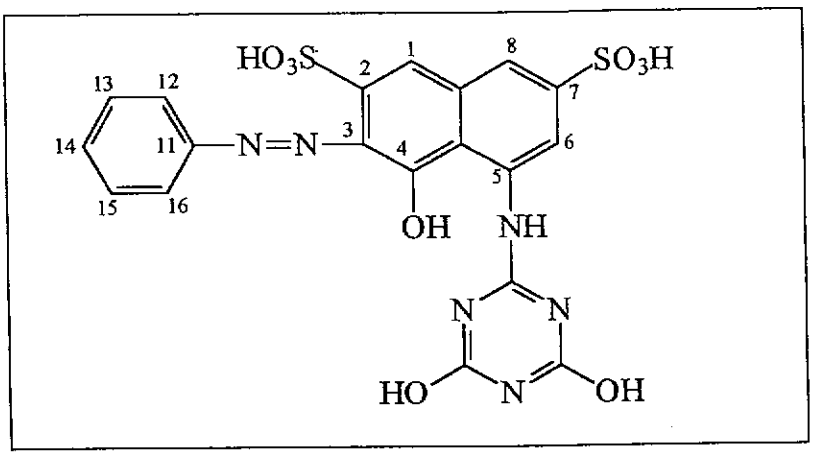

Fig.4.1. Chemical structure of hydrolysed Procion Red MX 5B

The ^{1}HNMR data below confirm the structure of Procion Red MX 5B:

δ 9.00 (H-8 singlet) δ 7.56 (H–1, singlet) δ 7.44 (H-6 singlet) δ 7.35 (2H-12,16, doublet J = 7.81 Hz) δ 7.17 (2H-13, 15, triplet, J = 7.69 Hz) δ 7.02 (H-14, triplet, J = 7.44 Hz)

4.3 Synthesis of Methyl Orange

4.3.1 Synthesis of Sulphanilic Acid

40 ml of conc. sulphuric acid was added cautiously in small portions to 20 ml of aniline. The mixture was swirled gently and kept cool in a cold water bath. The mixture was then placed in an oil bath and heated at 180-190 °C for five hours in a fume hood.

The mixture was removed from the oil bath, cooled to 50 °C and poured carefully into 400 g of crushed ice to encourage precipitation of sulphanilic acid. The mixture was allowed to stand for 10 minutes and the precipitated sulphanilic acid was collected on a Buchner funnel.

4.3.2 Purification of Sulphanilic Acid

The crude sulphanilic acid was dissolved in 450 ml of boiling water and 4 g of activated charcoal was added to decolourise the solution.The hot solution was filtered through a hot Buchner funnel and collected in a heated Buchner flask.The filtrate was cooled in order to encourage recrystallization of pure sulphanilic acid.Crystallized sulphanilic acid was collected on a Buchner funnel and washed with 10 ml of water. Sulphanilic acid was thereafter dried in an oven at 120 °C and cooled over anhydrous $CaCl_2$ in a dessicator.The yield was 19.20 g and the percentage yield was 50.6 %. Fig.4.2. shows the structure of sulphanilic acid. ^{1}HNMR spectroscopy was used to confirm the structure of the acid.The aromatic region of the ^{1}HNMR spectrum (appendix I spectrum 2) integrated to four protons which is in accordance with the structure shown in fig. 4.2.The ^{1}HNMR also shows two doublets which were expected from fig.4.2. since sulphanilic acid is symmetrical.

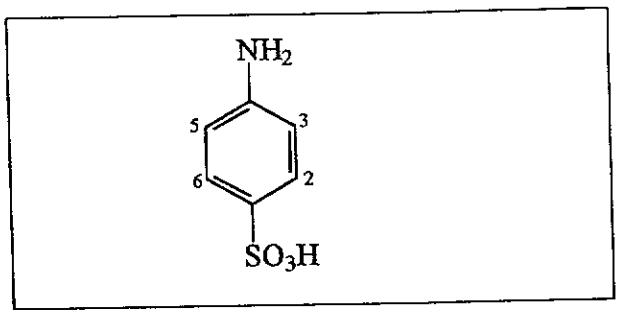

Fig.4.2. Chemical structure of sulphanilic acid

The ^{1}HNMR data below confirm the structure of sulphanilic acid:

δ 7.71 (2H-2,6, doublet, $J_{5,6}$ = 8.61 Hz) δ 7.30 (2H- 3,5, doublet, $J_{2,3}$ = 8.61 Hz)

4.3.3 Diazotization of Sulphanilic Acid

50 ml of 5 % Na_2CO_3 stock solution was diluted to 100 ml and 11.0 g of sulphanilic acid was added. The solution was warmed and additional 5-10 ml of 5 % Na_2CO_3 solution was added to dissolve sulphanilic acid completely. 20 ml of 2.5 M $NaNO_2$ was added to sodium sulphanilate solution and the solution was then cooled to 3-5 °C in an ice water slush. 16 ml of 60 % HCl was added while stirring the solution vigorously.

4.3.4 Coupling

6 ml of dimethyl aniline, thoroughly mixed with 3 ml of glacial acetic acid in a test-tube, was added to a beaker containing diazonium salt solution and the mixture was allowed to stand for 5-10 minutes with occasional stirring. The solution was finally made alkaline by adding 20 ml of 8.8 M NaOH. 20 g of NaOH was added to completely precipitate methyl orange. The precipitate was collected with suction on a Buchner funnel and recrystallized from hot water. The recrystallized methyl orange was washed with ethanol and finally with diethyl ether. The percentage yield was 41.32 %.

fig.4.3. shows the structure of methyl orange confirmed by ^{1}HNMR. The ^{1}HNMR spectrum of methyl orange (appendix I spectrum 3) integrates to 14 protons which is in accordance with fig.4.3. The spectrum shows two doublets which integrate to four protons, a triplet which integrates to four protons and a singlet which integrates to six protons, but according to the structure in fig.4.3. we should have 4 doublets and a singlet. Irradiation experiment (appendix I, spectrum 4) on the triplet confirmed the interaction of the triplets with the doublets which means that the triplet on the spectrum is the result of the two missing doublets that have overlapped, hence the triplet integrates to four protons.

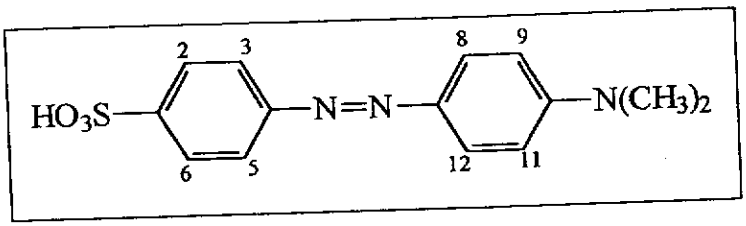

Fig.4.3. The chemical structure of methyl orange

The ^{1}HNMR data below confirm the structure of methyl orange :

δ 7.98 (H-2,6, doublet, J = 8.35 Hz) δ 7.87 (H-12,8,3,5, triplet, J = 8.61 Hz) δ 6.87(H-9,11, doublet, J = 9.22 Hz) δ 3.13 [$N(CH_3)_2$]

4.4 Synthesis of Orange II

4.4.1 Diazotization

10.51 g of the synthesized sulphanilic acid was placed together with 2.65 g of Na_2CO_3 in a beaker and 100 ml of water was added. The mixture was warmed until it was clear and 10 ml of 5.4 M $NaNO_2$ was added. The resulting solution was poured slowly with stirring in a beaker containing 10.5 ml of conc. HCl and 60 g of crushed ice.

4.4.2 Coupling

7.20 g of 2-naphthol was dissolved in 40 ml of cold 10 % NaOH solution. A cooled and well-mixed suspension of diazotized sulphanilic acid was added with stirring. After 10 minutes of stirring the solution was heated until all the solid had dissolved. 20 g of NaCl was added to salt-out the dye and the solution was heated until the salt had dissolved. The solution was allowed to cool in air for an hour and thereafter cooled in ice until crystallization was complete. The product was collected in a Buchner funnel and dried in an oven at 80-100 °C.

The crude product was dissolved in a minimum volume of boiling water, allowed to cool to 70 °C and ethanol was added to crystallize the dye. The pure dye stuff was filtered from the cold solution and washed with a little ethanol and thereafter dried in a vacuum oven. The yield was 14.83 g (85 %). Fig.4.4. shows the structure of Orange II. ^{1}HNMR spectroscopy was used to confirm the structure of Orange II. The ^{1}HNMR spectrum of Orange II (appendix I, spectrum 5) integrates to ten protons which is in accordance with fig.4.4. The assigning of protons was done with the aid of COSY spectrum (appendix I, spectrum 6)

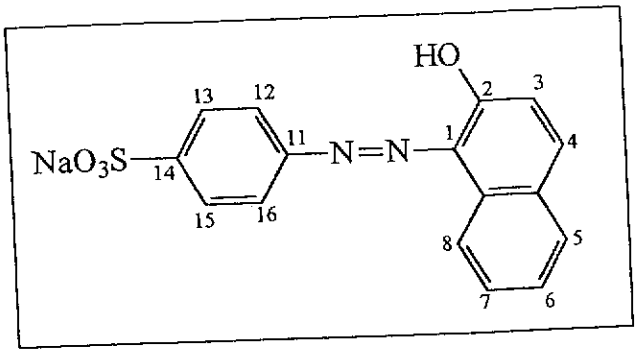

Fig.4.4. Chemical structure of Orange II

The ^{1}HNMR data below confirm the structure of Orange II:

δ 6.82 (H-3, doublet, J = 9.53 Hz) δ 7.46 (H-7, triplet, J = 8.73 Hz) δ 7.61 (H-6, triplet, J = 7.08 Hz) δ 7.68 (H-8, doublet, J = 7.70 Hz) δ 7.83 (H-12, 16, 4, multiplet) δ 8.00 (H-13, 15, doublet, J = 8.73 Hz) δ 8.58 (H-5, doublet, J = 7.82 Hz)

4.5 Electrochemical Reduction of Procion Red MX 5B

10.51 mM Procion Red MX 5B solution was prepared in 50 ml of pH 7.06 buffer solution. The dye solution was electrolysed for 186 minutes at -0.965 V vs SCE. The working electrode was a graphite rod (diameter 1.862 cm, height 3.652 cm) with the geometrical area of 24.09 cm^2. A graphite rod was the counter electrode and saturated calomel electrode was the reference electrode. After electrolysis, the solution, which had lost its red colour, was extracted with chloroform. The organic layer was vacuum evaporated and a residue of 0.0299 g was obtained. A ^{1}HNMR spectrum shown in appendix I (spectrum 7), revealed that the residue was aniline and therefore the percentage yield was 61 %.

Fig 4.5 shows the structure of aniline. The ^{1}HNMR spectrum of aniline integrates to seven protons which is in accordance with fig.4.5. It also shows two triplets, a doublet and a singlet expected from fig 4.5. The authentic ^{1}HNMR spectrum of aniline is shown in appendix I (spectrum 8)

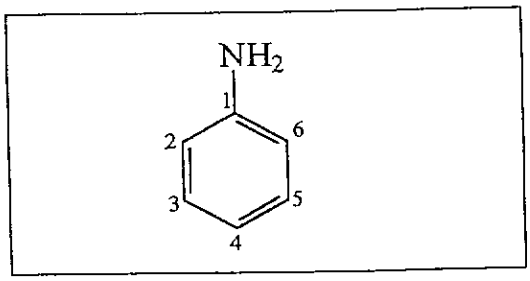

Fig.4.5. Chemical structure of aniline

The ^{1}HNMR data below confirm the structure of aniline:

δ 7.14 (H-3,5, triplet, J = 7.94 Hz), δ 6.75 (H-4, triplet, J = 7.39 Hz), δ 6.68 (H-2,6, doublet J = 7.63 Hz) δ 3.38 singlet (NH)

4.6 Buffer Solutions

Acetate/perchloric, acetate/acetic acid and phosphate buffer solutions were used for the study of the redox behaviour of Orange II, methyl orange and Procion Red MX 5B (Reactive Red 2). The following chemicals were used for the preparation of the buffer solutions: CH_3COONa, CH_3COOH, $HClO_4$; Analar (B. D. H), H_3PO_4 ;CP, $KHPO_4$ AR, Na_2HPO_4 and $Na_2HPO_4.7H_2O$ of 99 % purity, Na_3PO_4; CP. The pH's of the buffer solutions were measured using Zeiss pH meter (pH 300).

Reagent grade water (resistivity 18 MΩ.cm) was used to prepare the solutions. The reagent water was obtained from a Milli -Q-system (Milli- Q^{50} ultra pure water system, Cat. No ZFMQL 5001) where tap water is passed through a reverse osmosis membrane, an activated carbon cartridge to remove dissolved inorganic impurities and finally through a polymeric membrane filter which removes all the particles larger than 0.2 μm.

4.6.1 Preparation of Acetate/acetic Acid and Acetate/perchloric Acid Buffer Solutions.

Acetate/acetic acid and acetate/perchloric acid buffers were used for the study of Orange II and methyl orange redox behaviour. The pH of the buffer solutions prepared was 4.70.

0.2 M sodium acetate solution was titrated with 0.2 M acetic acid to prepare acetate/acetic acid buffer or with 0.2 M perchloric acid to prepare acetate/perchloric acid buffer.

4.6.2 Preparation of Phosphate Buffer Solutions.

The preparation of different pH buffer solutions is shown in table 4.1. The buffer strength of the solutions was 0.2 M.

Expected pH	H_3PO_4 (ml)	KH_2PO_4 (g)	$Na_2HPO_4.7H_20$ (g)	Na_2HPO_4 (g)	Na_3PO_4 (g)	Measured pH
3.02	0.65	13.60				3.29
3.77	0.10	13.60				4.07
5.00		12.92		0.21		5.06
6.00		9.20	2.80			6.04
7.00		2.36	7.40			7.06
8.00		0.28	8.78			8.04
9.10				4.74		9.19
10.00				4.46	0.37	10.46
10.60				4.08	0.87	10.84

Table 4.1. Preparation of different phosphate buffer solution with 0.2 M buffer strength.

4.6.3 Preparation of Dye Solutions.

The dye solutions were prepared from a stock solution prepared in water, by pipetting required volume of the stock solution into a volumetric flask and filling with a particular buffer solution.

4.7 The Cell

Fig 4.6 shows the cell (capacity 170 ml) used for electrochemical experiments and fig. 4.7 shows the central part of the cell holder. As shown in fig. 4.7 the central part of the cell holder has five inlets.

The following items were inserted in the inlets:

1. Luggin capillary and reference electrode assembly. A SCE (reference electrode) was placed in a reservoir above the Luggin capillary and separated from the solution via ungreased wetted stopcork. The reservoir contained saturated KCl drawn in by applying a water pump pressure to the side arm. This prevented the formation of bubbles. The reference electrode assembly shown in fig 4.8 was then inserted in inlet number 1. The Luggin capillary tip was placed 0.5 - 3 mm from a working electrode.

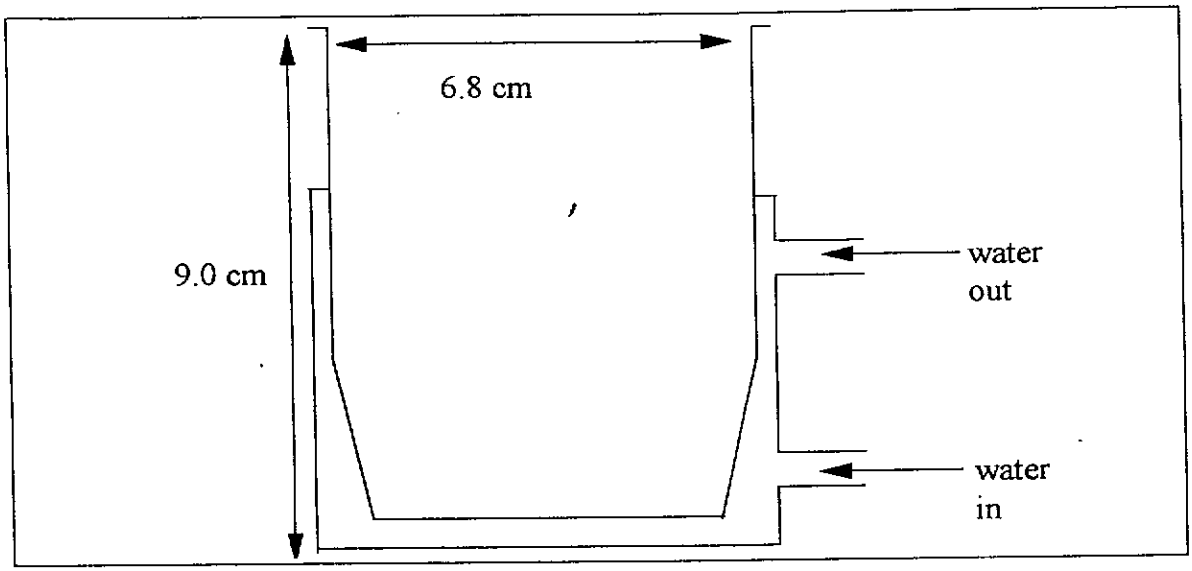

Fig.4.6. The cell

2. The working electrode. The graphite rod (bulk electrolysis) or a glassy carbon disk (diameter 0.264 cm, cyclic voltammetry) was inserted in the inlet number 2.

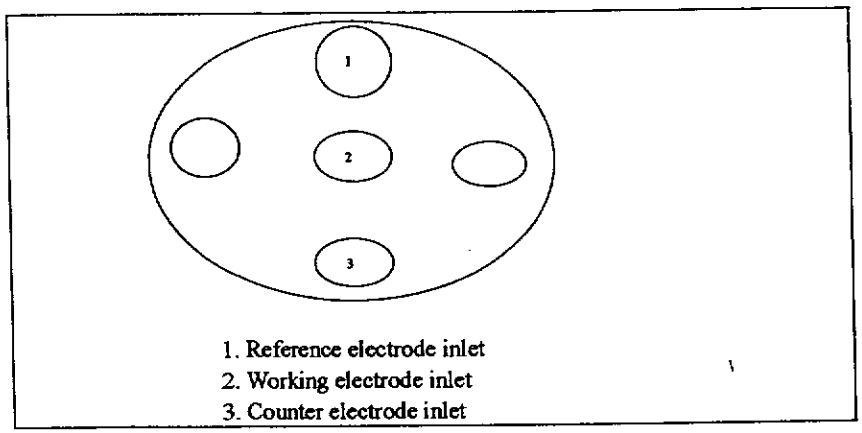

Fig.4.7. The lid of the cell holder

3. A counter electrode. A spiral platinum electrode or a graphite rod was inserted in the inlet number 3. These electrodes were ultrasonically cleaned in water. One of the two remaining inlets was used for deaeration of the solution for 10 minutes before any voltammogram was recorded and taking the samples for UV-vis spectroscopy analysis. These two inlets were securely stoppered to prevent the ingress of atmospheric oxygen during the course of the experiment.

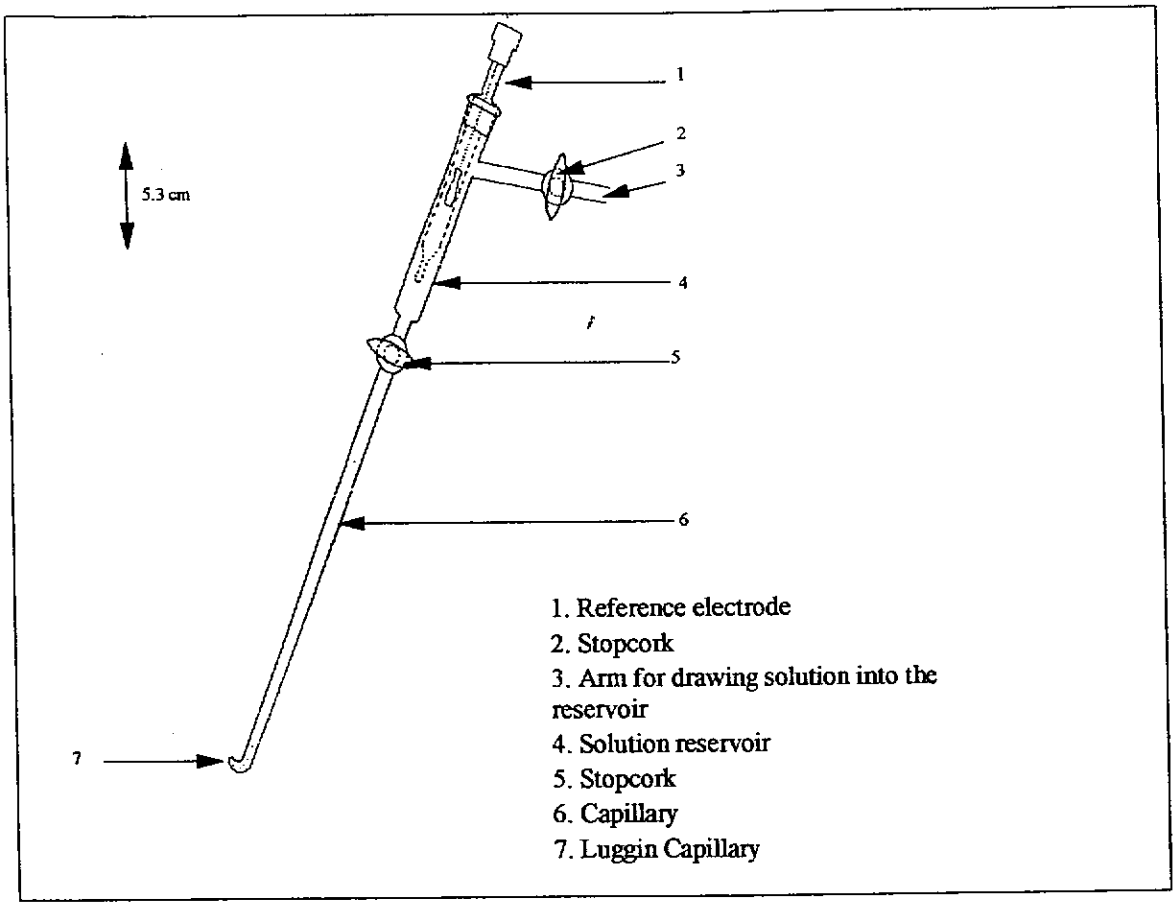

Fig.4.8. Diagram of the assembled reference electrode apparatus.[2]

4.8 Construction of the Working Electrode.

An insulated copper wire was secured at the back of a glassy carbon rod (4 - 6 mm) using silver epoxy cement (Emerson and Cuming, Belgium). The contact between the rod and the copper wire was then checked with a multitester. The carbon rod (with the attached wire) was then secured to a double -sided tape on a flat surface. A hollow cylindrical teflon mould was then pressed firmly onto the adhesive tape so that the carbon rod was centred

inside it. The mould was then filled with resin (Araldite-M-Resin mixed with HY- hardener in the ratio 5:1) that had been degassed in an oven for a minute at 100 °C and finally in a vacuum dessicator. The resin was then cured in the oven at 100 °C for 60 minutes. After curing the resin, the electrode was removed from the mould and checked for bubbles between the edge of the electrode and the cured resin. If bubbles were found the electrode was discarded. If no bubbles were found, the cured resin/electrode was inserted into a teflon holder. The mould was designed in such a way that the cured resin will fit snugly inside the teflon holder. Fig. 4.9 shows the constructed electrode and its dorsal side. The area of the electrode was 0.0549 cm^2.

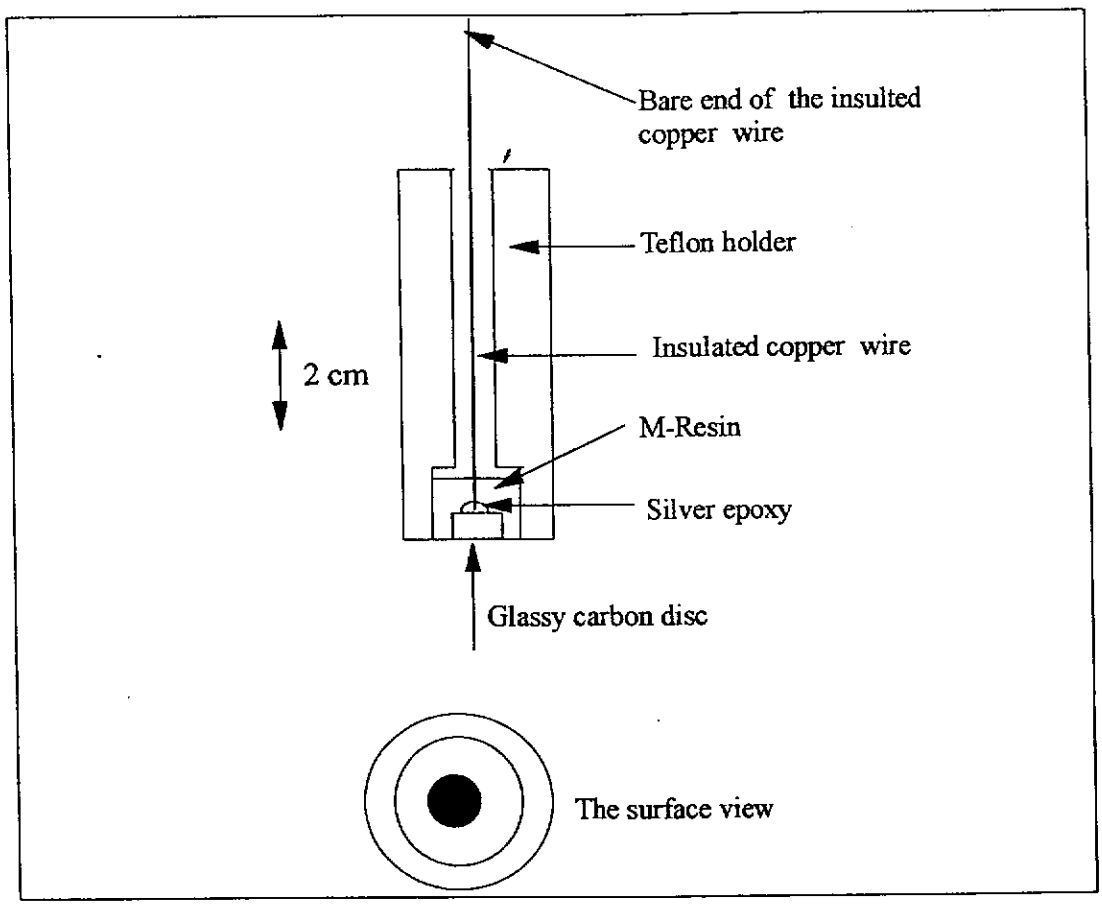

Fig.4.9. An assembled working electrode.

4.9 Instrumentation

Fig 4.10. shows the experimental arrangement of equipment and electrical connections. Electrode potential was controlled by a BAS CV-27 potentiostat. The electrodes were directly connected to the potentiostat.

Voltammograms were monitored as current-time and potential-time waveforms (simultaneously) on a Nicolet 3091 twin-channel digital storage oscilloscope. Preliminary voltammograms were monitored and recorded on a PL 3 chart recorder (LLOYD instruments). A program[3] collver8 was used to collect the digital data from the oscilloscope via an RS-232 serial interface to an 80-386 PC computer. Collver8 automatically assigned filenames (by incrementing a number) to data files and thus required a minimum attention from the user between experiments.

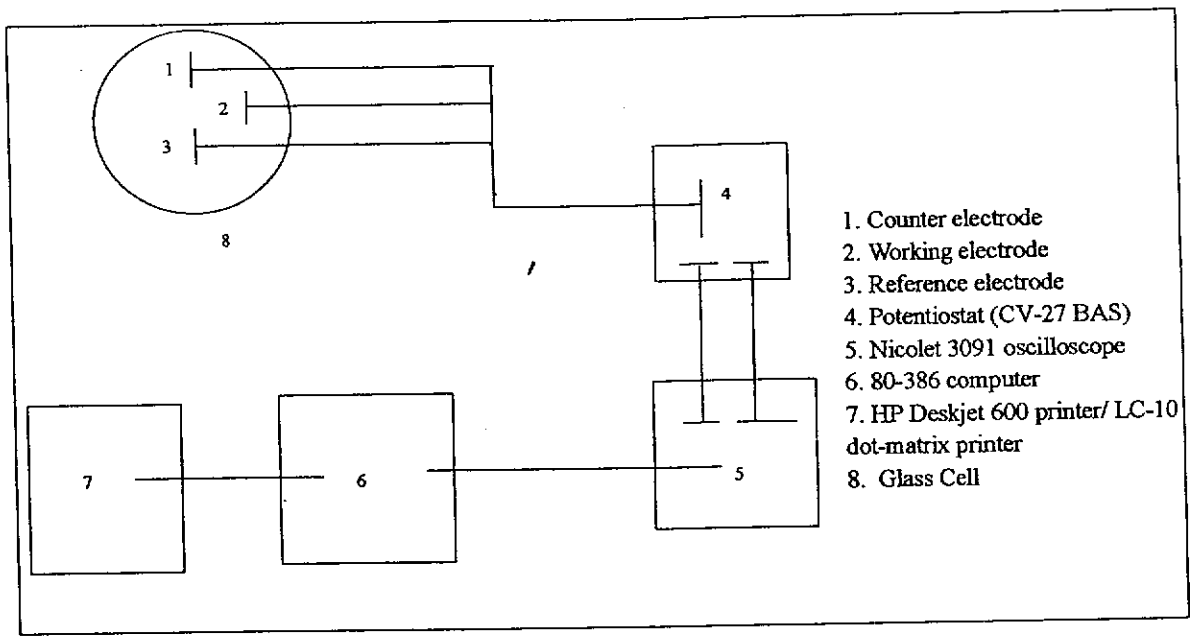

Fig.4.10. Schematic arrangement of experimental equipment and electrical connections.

The digital raw data files were then processed to numeric data which can be imported into any spreadsheet. The processed data files were filtered to produce a smooth voltammogram by the Matlab program[4] shown in appendix II.

4.10 Procedure for Electrochemical Measurements.

Electrochemical measurements can be influenced significantly by the pretreatment of the electrode and thus a standard pretreatment was developed. The working electrodes were polished on abrasive paper (SiC) ranging from 800 to 1200 and then with 6 μm, 3 μm and finally with 0.25 μm Metadi II diamond paste (Beuhler Ltd) using a Struers Planopol-2/PdM-Force polishing system. The pastes were spread on the cloth using

Metadi fluid (Beuhler Ltd cat. no 40-6032). A minimum quantity of 6 μm and 3 μm diamond pastes were spread on Dp-cloths (Struers) and 0.25 μm paste was spread on NFW (437) type cloth (Kemet).

The electrodes were ultrasonically cleaned in water after each change of grade of polishing disc. On completion of polishing, the electrode was fitted into a cell holder inlet. The reference electrode assembly and the counter electrode were then fitted into their inlets and the cell with solution was fitted on the holder. Nitrogen was bubbled into the solution for at least 10 minutes before the experiment.

4.10.1 Cyclic Voltammetric Experiment

A supporting electrolyte voltammogram was taken before each analyte voltammogram was recorded. The recording of the supporting electrolyte voltammogram ensured that there was no electroactive species on the surface of the electrode and served as the background. The concentrations of dye solutions were ~1 mM.

The electrochemical windows of the buffers were different. The phosphate electrochemical window ranged from -1.30 to 1.25 V whereas acetate/acetic and acetate/$HClO_4$ ranged from 0.80 to 1.10 V against SCE. The scan rate used was 150 mV/s. The potential was scanned from the rest potential in a positive or negative direction.

4.10.2 UV-vis Spectroscopy and Bulk Electrolysis Experiments.

Bulk electrolysis of 1.0046 mM Procion Red MX 5B solution was performed for 110 minutes at constant potential. The bulk electrolysis experiment was monitored by UV-vis spectrophotometry by recording the spectrum after 10 and 20 minutes. The electrolysing potential was -0.965 V vs SCE. A PAR 363 model potentiastat was used and it had a current capacity of 1000 mA compared to 10 mA for the BAS CV-27 potentiostat. This potentiostat was not used in conjunction with the Nicolet storage oscilloscope and the computer during the bulk electrolysis experiments.

4.11 References

1. G. D. Christian and W. C. Purdy, **The Residual Current in Orthophosphate Medium, *J. Electroanal. Chem.***, 3, (1962) p. 363

2. F. J. Graham, **Electrochemical Study of the Passivation of Stainless Steels**, MSc. Thesis, University of Natal, Durban, South Africa (1986) p.54

3. C. H. L Tonkinson, **The Transpassive Behaviour of the Anodic Film of Fe-Cr Alloys**, MSc. Thesis, University of Natal, Durban, South Africa (1993) p. 154-178

4. Dr. J. Sikora, **Personal Communication**, Pennstate University, USA

Chapter 5

Results and Discussion

5.1. Preliminary Experiments and Results

Preliminary experiments were performed to determine optimum conditions for studying redox behaviour of reactive azo dyes particularly Procion Red MX 5B (Reactive Red 2) chemically known as 5-[4,6 -dichloro triazin -2- yl amino) -4- hydroxy -3- phenylazo, 2,7 naphthalene disulphonic acid. Orange II (fig.4.4) and methyl orange (fig.4.3) were the chosen azo dyes for preliminary experiments. They were chosen because they are soluble in water though methyl orange is not very soluble compared with Orange II. Their chemical structures contain sulphonic acid groups, also found on the chemical structure of Reactive Red 2 (fig.4.1), the dye of interest. Orange II has a hydroxy group ortho to the azo bond. The same group is found on the same position on Reactive Red 2 chemical structure.

Cyclic voltammetry was the technique used to study the basics of Orange II and methyl orange redox behaviour.

5.1.1 Electrochemistry of Methyl Orange

Florence et al[1] reported part of the voltammetric behaviour of methyl orange in aqueous solution buffered at pH 4.7 using 0.2 M acetate buffer at a rotated PGE. The concentration of the dye was 5.0 x 10^{-5} M. They reported that methyl orange undergoes electroreduction as well as electrooxidation. The value of *n* involved in the electroreduction was found to be between 2 and 4. The half wave potentials of oxidation and reduction peaks were 0.695 V and -0.361 V vs SCE respectively.

In our investigation of 1.14 mM methyl orange, a stationary GCE was used vs SCE. The dye solution was prepared in pH 4.70 acetate-perchloric acid buffer solution. Acetate-perchloric buffer solution was used instead of acetate buffer solution because it has the same electrochemical potential window at the GCE vs SCE, since acetic acid vaporises.

Fig 5.1 shows the cyclic voltammogram of methyl orange. The voltammogram was initiated at 0.29 V where no electrochemical reaction takes place and scanned in the negative direction and thereafter cycled between -0.80 V and 1.10 V for 25 cycles.

The voltammogram shows four major peaks : A, B, C and D and their half wave potentials are -0.35 V, 0.29 V, 0.72 V and 0,24V respectively.

Peaks A and C half wave potentials are 3 % away from -0.361 V and 0.695 V which are the half wave potentials of methyl orange reported by Florence et al[1]. They did not report peaks B and D half wave potentials, because they used single sweep voltammetry without a reverse scan to investigate the electrochemistry of methyl orange. In fact peak D appeared during the second cycle as can be seen from fig.5.1. This could mean that the electrochemical reaction at peaks A, B or C produced an electroactive species which is electroactive in the same potential window as methyl orange.

The appearance of peaks A and C in fig.5.1 proved that the experimental set-up and conditions were satisfactory, but peaks B and D suggested that an investigation on a dye whose voltammetric behaviour had been studied by cyclic voltammetry be performed. The dye selected was Orange II.

5.1.2 Electrochemistry of Orange II

Redox behaviour of Orange II was reported by Goyal, Srivastava, and Nautiyal[2]. The techniques used to study this dye included cyclic voltammetry. They studied Orange II in phosphate buffers of pH range 2.5 -11.0 at DME and PGE versus SCE.

Fig.5.2 shows the cyclic voltammogram (CV) of 0.815 mM Orange II prepared in pH 4.70 acetate-perchloric acid buffer. The CV was initiated at 0.29 V and scanned in the negative direction and thereafter cycled between -0.81 V and 1.05 V.

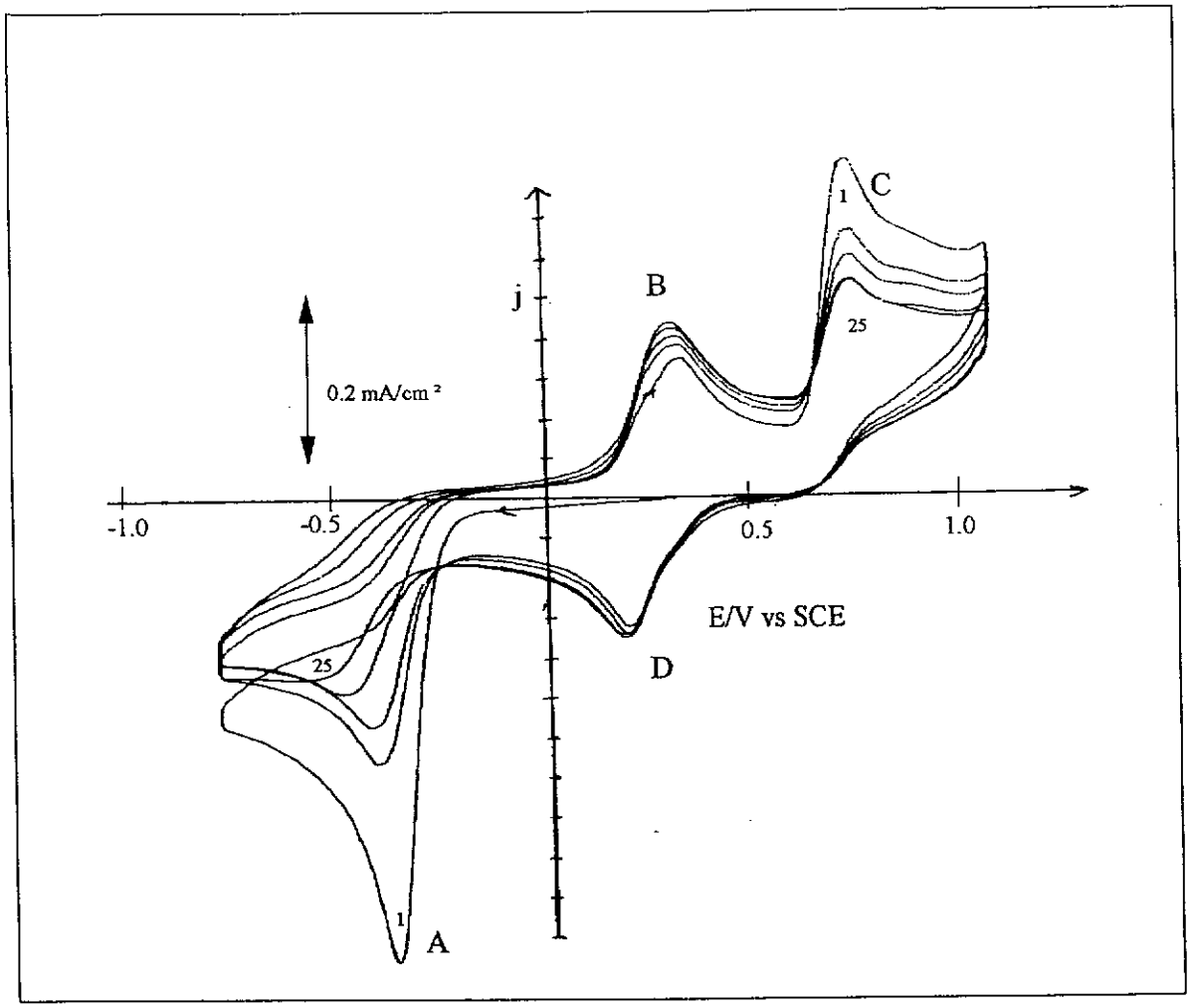

Fig.5.1. Cyclic voltammogram of 1.14 mM methyl orange in pH 4.70 acetate-perchloric buffer solution run at the GCE (glassy carbon electrode) vs SCE.

Initial potential : 0.29 V

Positive limit: 1.10 V

Negative limit: -0.81 V

Scan rate: 150 mV/s

The CV shows four major peaks: A, B, C and D as in our methyl orange CV (fig 5.1) and two minor peaks E and F. The voltammogram in fig.5.2 is similar to what Goyal et al found, but they didn't report peaks C and E.

Goyal et al[2] reported that cathodic peak A appears as a result of the electroreduction of Orange II giving corresponding aromatic amines. They also reported that cathodic peak D and anodic peaks B and F appear as a result of oxidation and reduction of the compounds formed at cathodic peak A.

Since they never reported C and E a CV of Orange II was run between -0.35 V and 1.10 V to see the effect of peak A's absence on C. The CV is shown in fig.5.3.

The CV shows peaks C, D and B but peaks F and E are now absent. The CV shows that anodic peak C is independent of peak A. This means that Orange II undergoes independent oxidation as methyl orange a fact not observed by Goyal et al[2]. The absence of peaks E and F confirms their dependence on peak A, whereas the appearance of peaks D and B during the second cycle confirms their dependence on the process that occurs at peak C.

Fig 5.4 shows the CV of Orange II run between -0.81 V and 0.50 V. The CV was initiated at 0.29 V and scanned in the positive direction and cycled between -0.81 V and 0.50 V. It shows cathodic peak A, which appeared during the first cycle, peak B appeared during a reverse scan, peak B and E appeared during the second cycle. The dependence of peak B, D, E and F on A confirmed what Goyal et al reported. Also peak A is a typical irreversible cyclic voltammetric peak which also confirms the electroreduction of Orange II into corresponding amines by splitting the azo bond (fig.5.5).

The cyclic voltammograms of methyl orange and Orange II recorded confirmed that the experimental conditions and set-up were good enough to investigate the uninvestigated dye namely Reactive Red 2 or Procion Red MX 5B.

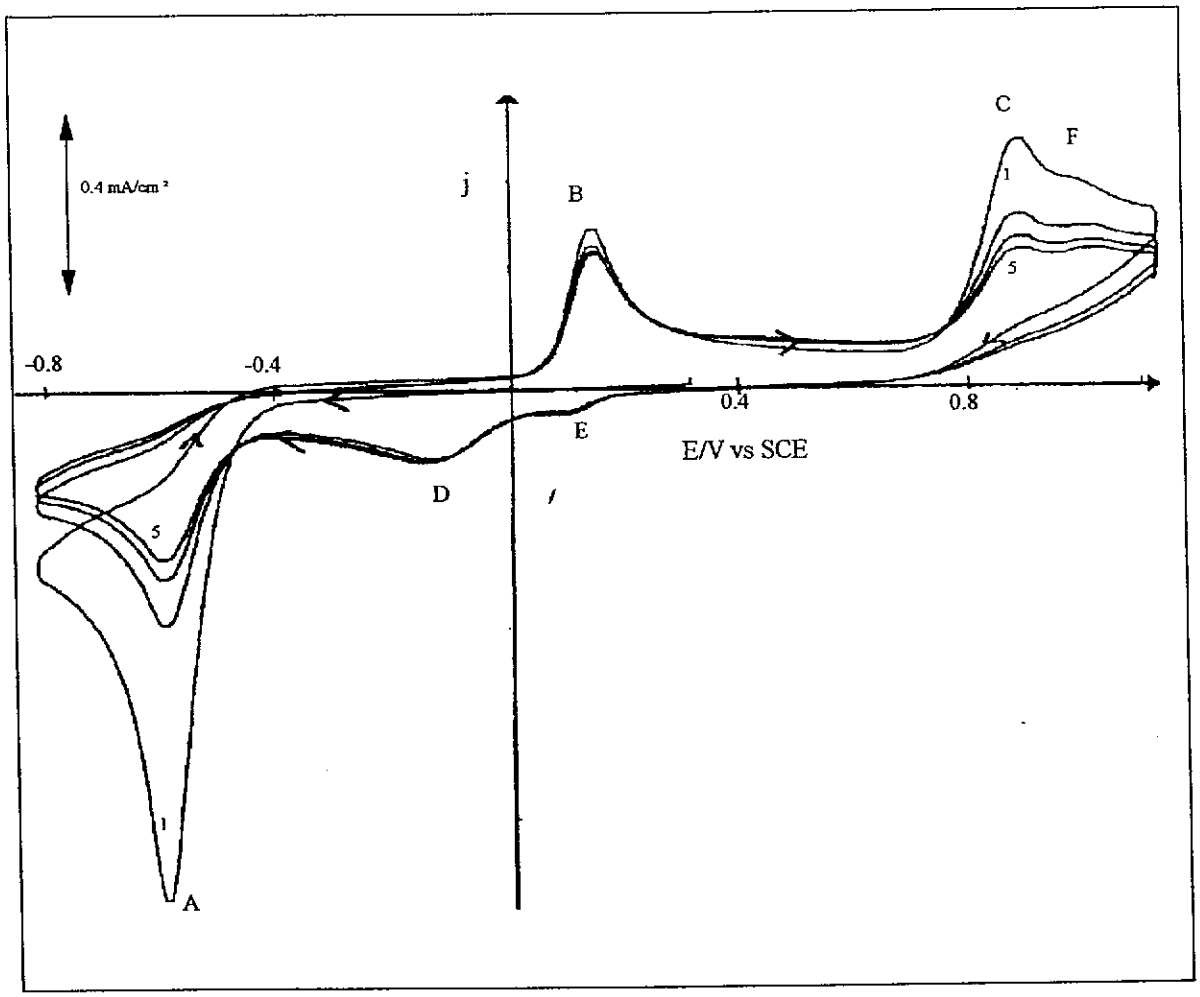

Fig.5.2. A CV of 0.815 mM Orange II run in pH 4.70 acetate-perchloric acid at the GCE vs SCE.

Initial potential : 0.29 V

Positive limit: 1.10 V

Negative limit: -0.81

Scan rate: 150 mV/s

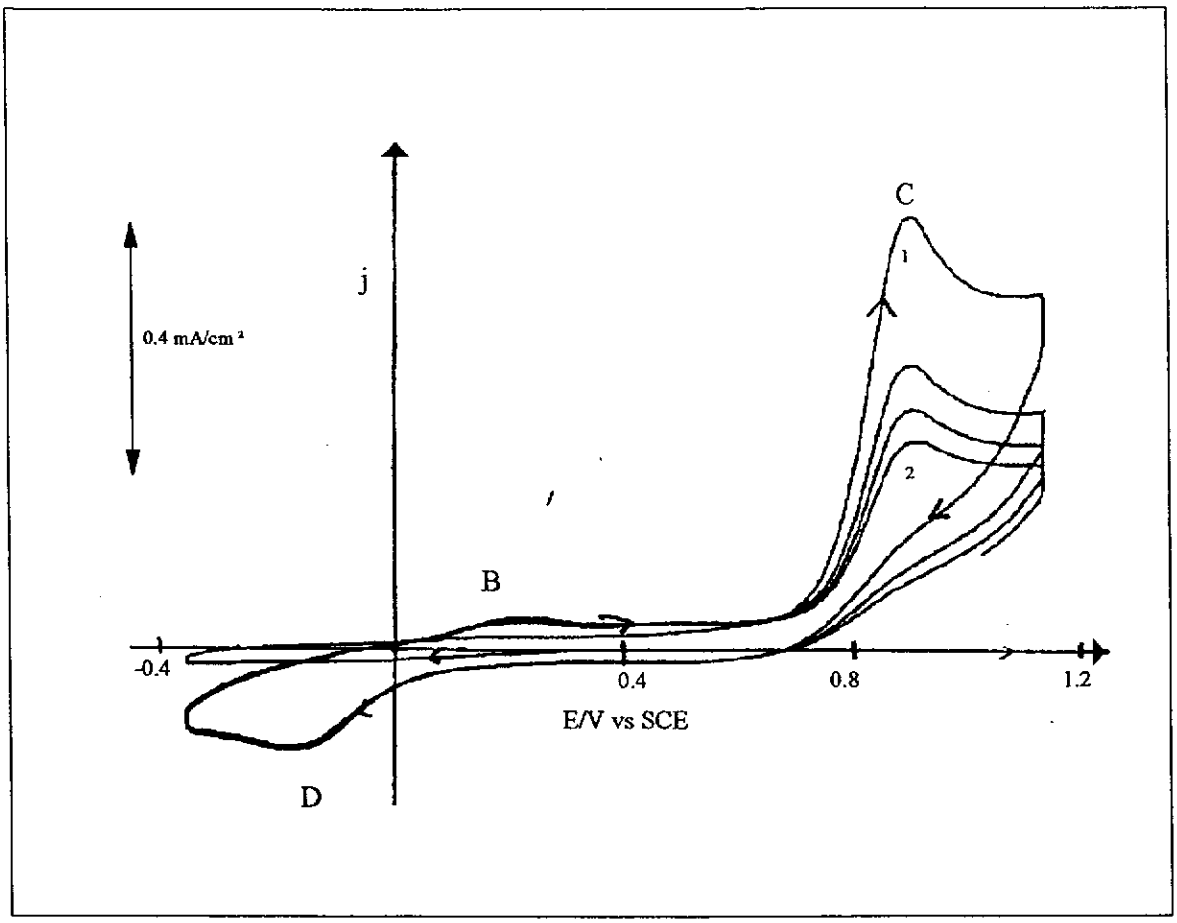

Fig.5.3. A CV of Orange II run in pH 4.70 perchloric acetate buffer at the GCE vs SCE.

Initial potential : 0.29 V

Positive limit: 1.10 V

Negative limit: -0.35 V

Scan rate: 150 mV/s

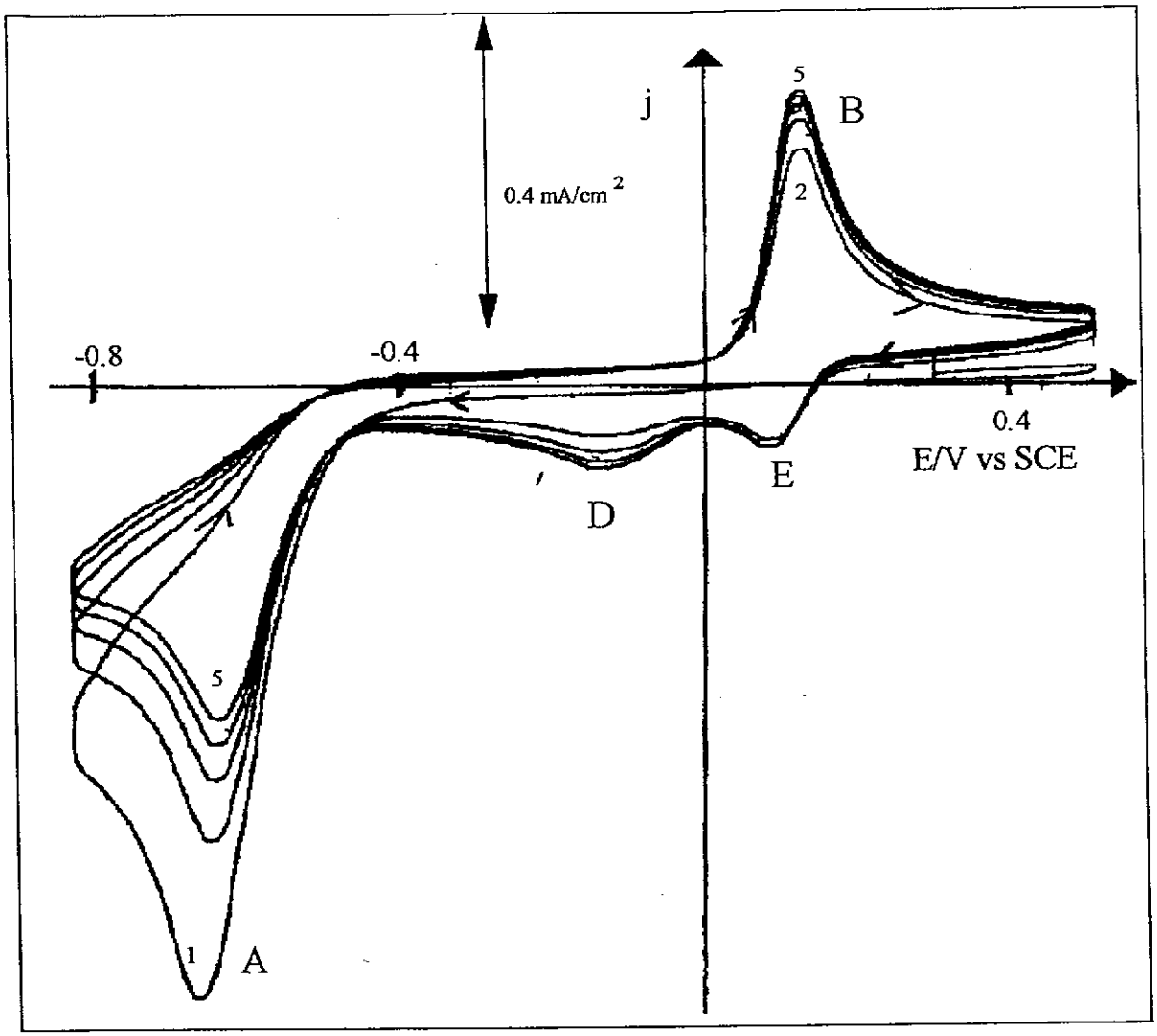

Fig.5.4. A CV of Orange II run in pH 4.70 acetic acid-perchloric acid buffer at the GCE vs SCE.

Initial potential : 0.29 V

Positive limit: 0.50 V

Negative limit: -0.81 V

Scan rate: 150 mV/s

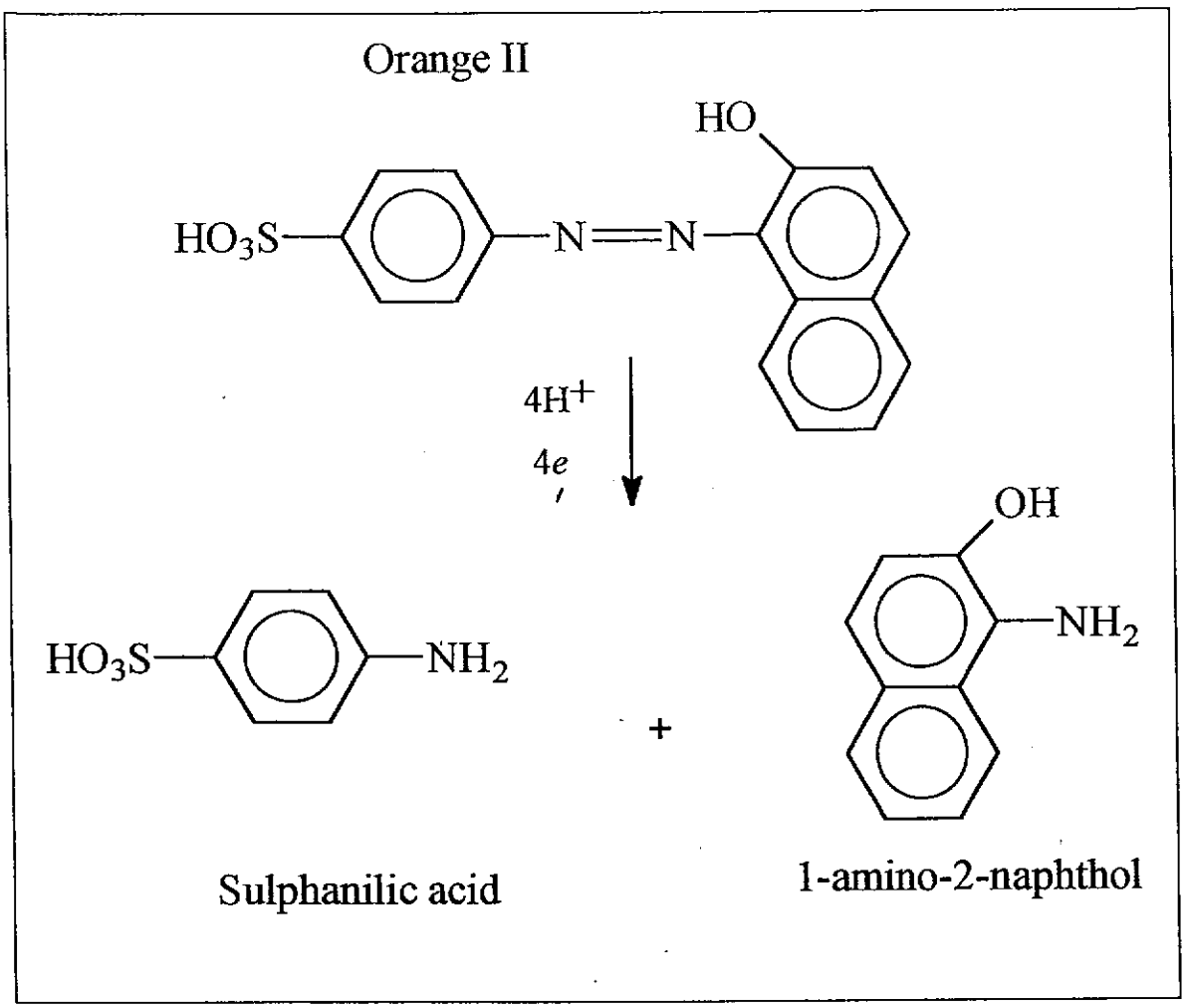

Fig.5.5. The electroreduction mechanism of Orange II

5.2. Redox Behaviour of Procion Red MX 5B

Procion Red MX 5B has been reported to undergo chemical and biological reduction into corresponding aromatic amines. In biological reduction, under anaerobic conditions, micro-organisms are the reducing agents. In this system nitrates have to be removed before the dye could be reduced since micro-organisms prefer nitrates to the dye. Chemical reduction is achieved using stannous chloride in HCl with methanol as a solvent[3].

Since it is known that any chemical reduction or oxidation reaction has a electrochemical analogue, redox behaviour of Procion Red MX 5B was investigated with the aim of reducing it into corresponding aromatic amines. The redox behaviour of Procion Red MX 5B was studied in phosphate buffers over pH range 3-11.

5.2.1 Cyclic Voltammetry of Procion Red MX 5B at pH 3, 4 and 5

Fig.5.6 shows the CV of Procion Red MX 5B run at pH 3.29. The voltammogram was initiated at 0.00 V where no electrode reaction takes place, scanned in the negative direction and cycled between 1.25 V and -1.30 V. The concentration of the dye was 1.0046 mM. During the first sweep in the negative direction, peak I was observed. When the direction was reversed peaks II and IV were observed. During the reverse cycle peaks V and VI were observed. It is worth noting that peak VI was absent during the first cycle and only appeared during the second cycle.

A CV was recorded by initiating the sweep in the positive direction, to confirm whether peaks II, IV, V and VI were related to peak I since it appeared first as seen in fig.5.6.
The CV is shown in fig.5.7. During the first cycle peak II was absent confirming its dependence on peak I, but peak IV was present confirming its independence. When the direction of the scan was reversed peaks V and VI were absent confirming their dependence on prior reduction at the potential of peak I.
The dependence of peaks II, V and VI on peak I was further confirmed by fig 5.8 which shows a CV of Procion Red MX 5B run between 1.25 V and -0.50 V excluding the potential of peak I.

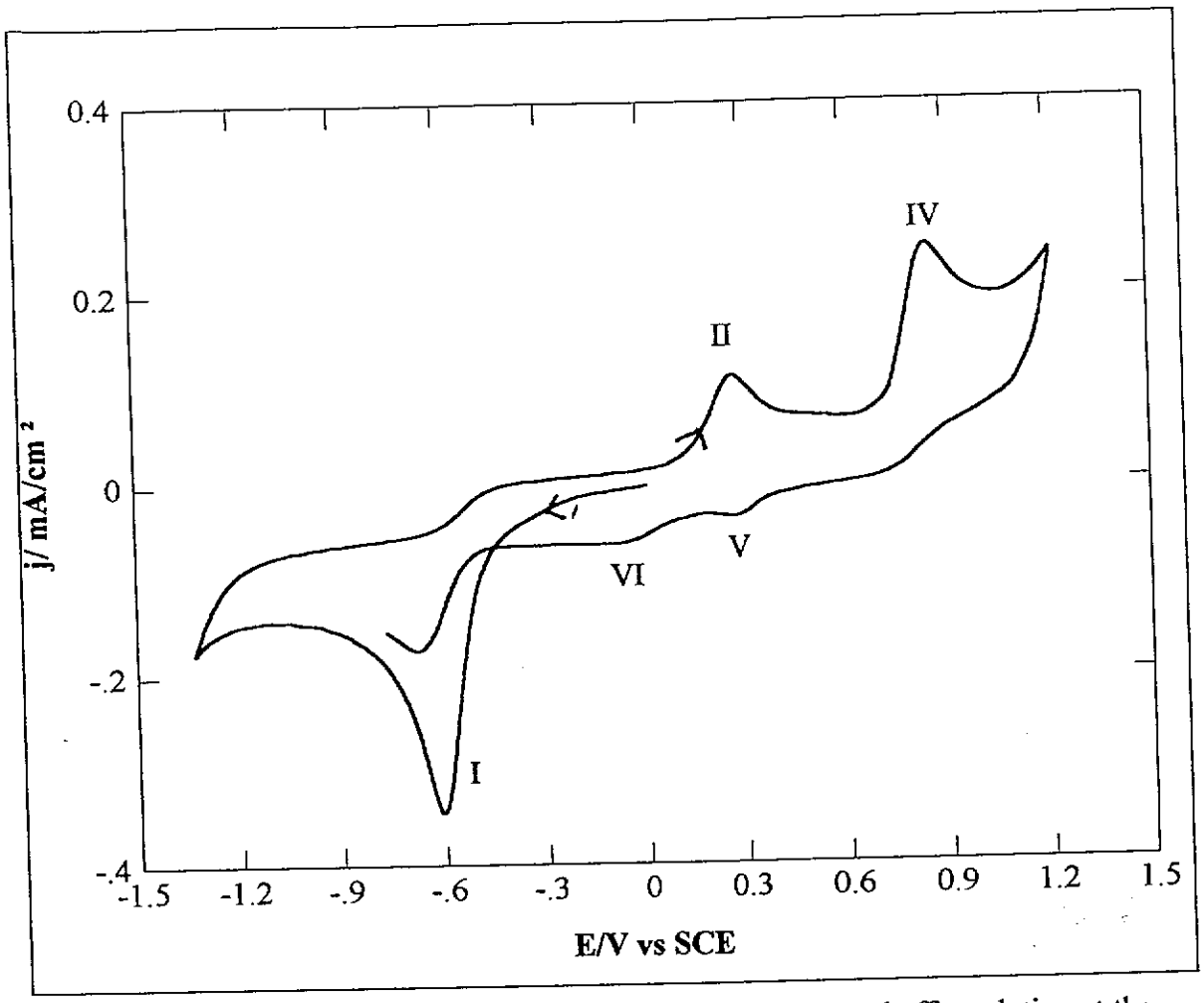

Fig.5.6 A CV of Procion Red MX 5B run in pH 3.29 phosphate buffer solution at the GCE vs SCE

Concentration of Procion Red MX 5B: 1.0046 mM

Buffer strength: 0.2 M

Initial potential: 0.00 V

Positive limit: 1.25 V

Negative limit: -1.30 V

Scan rate: 150 mV/s

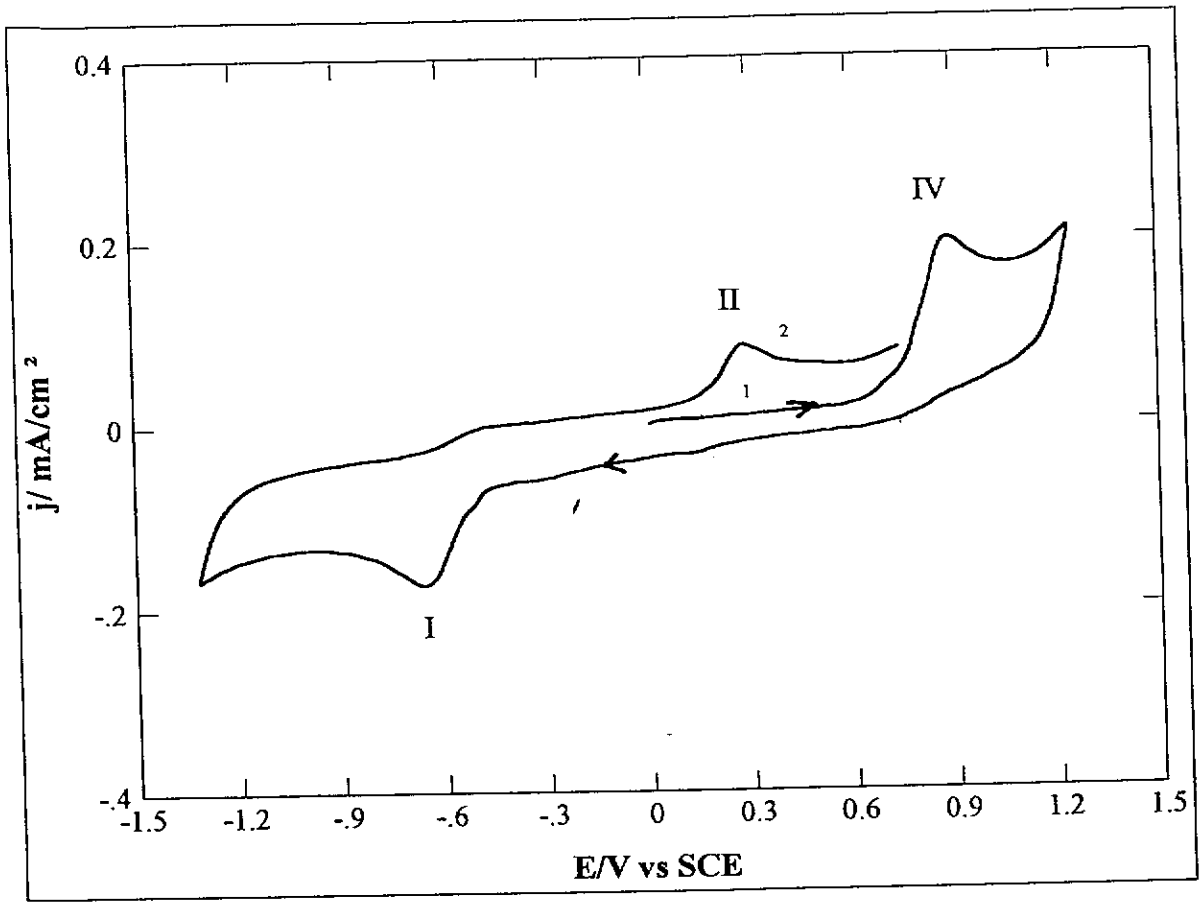

Fig.5.7. A CV of Procion Red MX 5B run phosphate buffer at the GCE vs SCE.

Concentration of Procion Red MX 5B: 1.0046 mM

Buffer strength: 0.2 M

Initial potential: 0.00 V

Positive limit: 1.25 V

Negative limit: -1.30 V

Scan rate: 150 mV/s

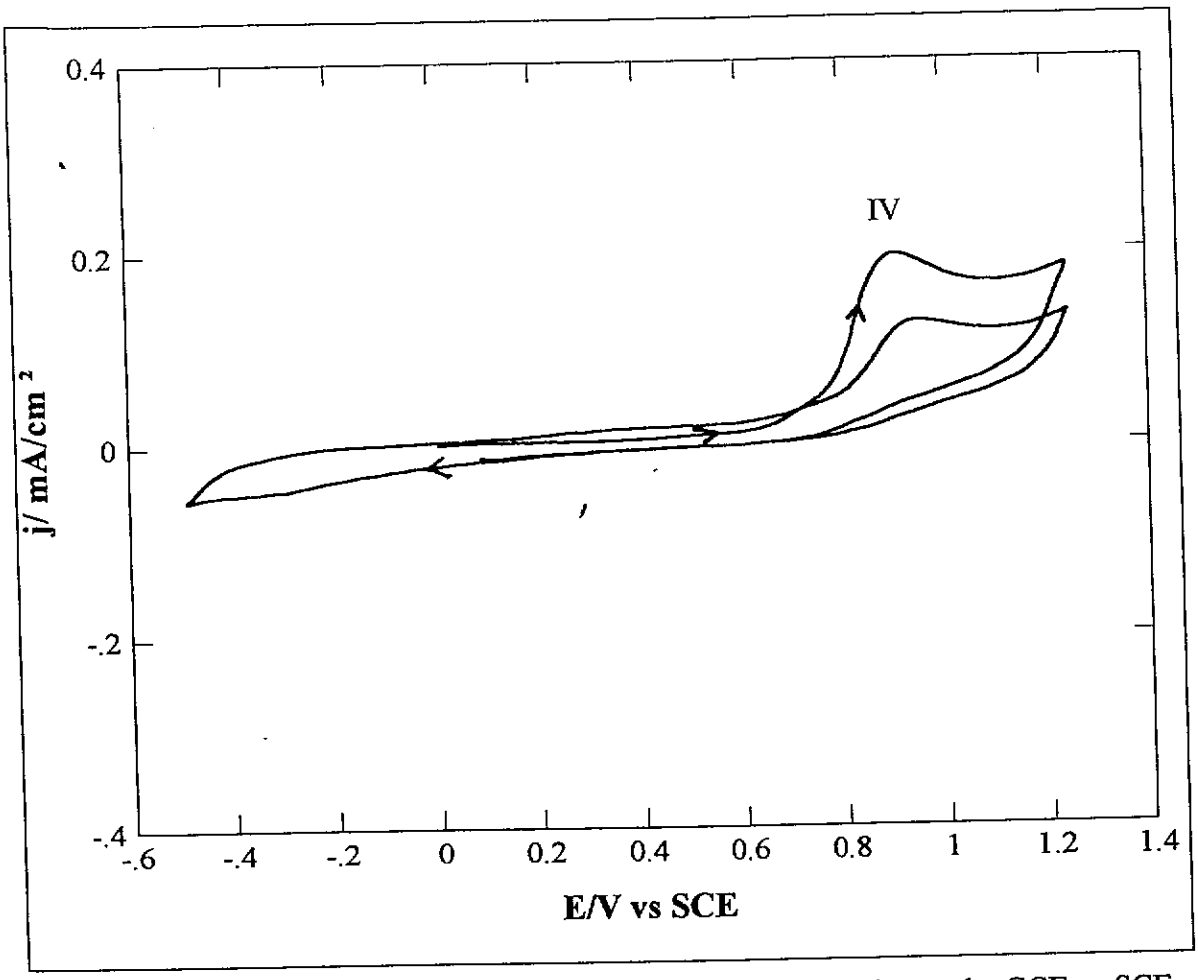

Fig.5.8. A CV of Procion Red MX 5B run in pH 3.29 buffer solution at the GCE vs SCE excluding peak I potential region.

Concentration of Procion Red MX 5B: 1.0046 mM

Buffer strength: 0.2 M

Initial potential: 0.00 V

Positive limit: 1.25 V

Negative limit: -0.50 V

Scan rate: 150 mV/s

The CV was initiated in the positive direction and on reaching the positive limit the scan was reversed and thereafter cycled between the positive and negative limits. Since peak I potential was excluded, peak IV alone was expected to be seen. As found, peak IV was the only peak that appeared in fig.5.8.

A CV was also run to positively confirm the dependence of peaks II, V and VI on peak I. This was done by excluding the peak IV potential region. Peaks II, V and VI were expected to be seen. The CV was initiated at 0.00 V in the negative direction and cycled between -1.30 V and 0.70 V. The CV is shown in fig.5.9 and it shows peaks I, II and VI but peak V is absent.

A CV was run at pH 4.07 phosphate buffer solution to see if it would be different from the CV run at pH 3.29 (fig.5.6). The voltammogram was initiated at 0.40V and scanned in the negative direction and thereafter cycled between 1.25 and -1.30 V. The CV is shown in fig.5.10 and shows peaks I, II, IV, V and VI as in fig.5.6. The only significant difference is the shift of peak I to more negative potentials.

A CV run at pH 5.06 showed an extra peak labelled peak III, as shown in fig.5.11. The voltammogram was initiated in the negative direction and cycled between -1.30 V and 1.25 V. The other peaks appeared as in fig.5.6. Peak III was found to depend on peak I like peaks II, V and VI by initiating the sweep of the voltammogram in the positive direction. The CV is shown in fig. 5.12. Fig.5.11 showed an increase in peak I height.

The increased peak height is a result of the precipitation that has been found to occur from pH 3.29 to pH 6.04. The degree of precipitation was found to decrease as pH increases hence the increase in peak I height. This was due to the potassium salt (KH_2PO_4) used in the preparation of the buffer solution. Table 4.1 shows that high concentration of this salt was used in pH 3.29 to pH 6.04. In fact Procion Red MX 5B solution prepared in 0.2 molar phosphoric acid didn't show any sign of precipitation.

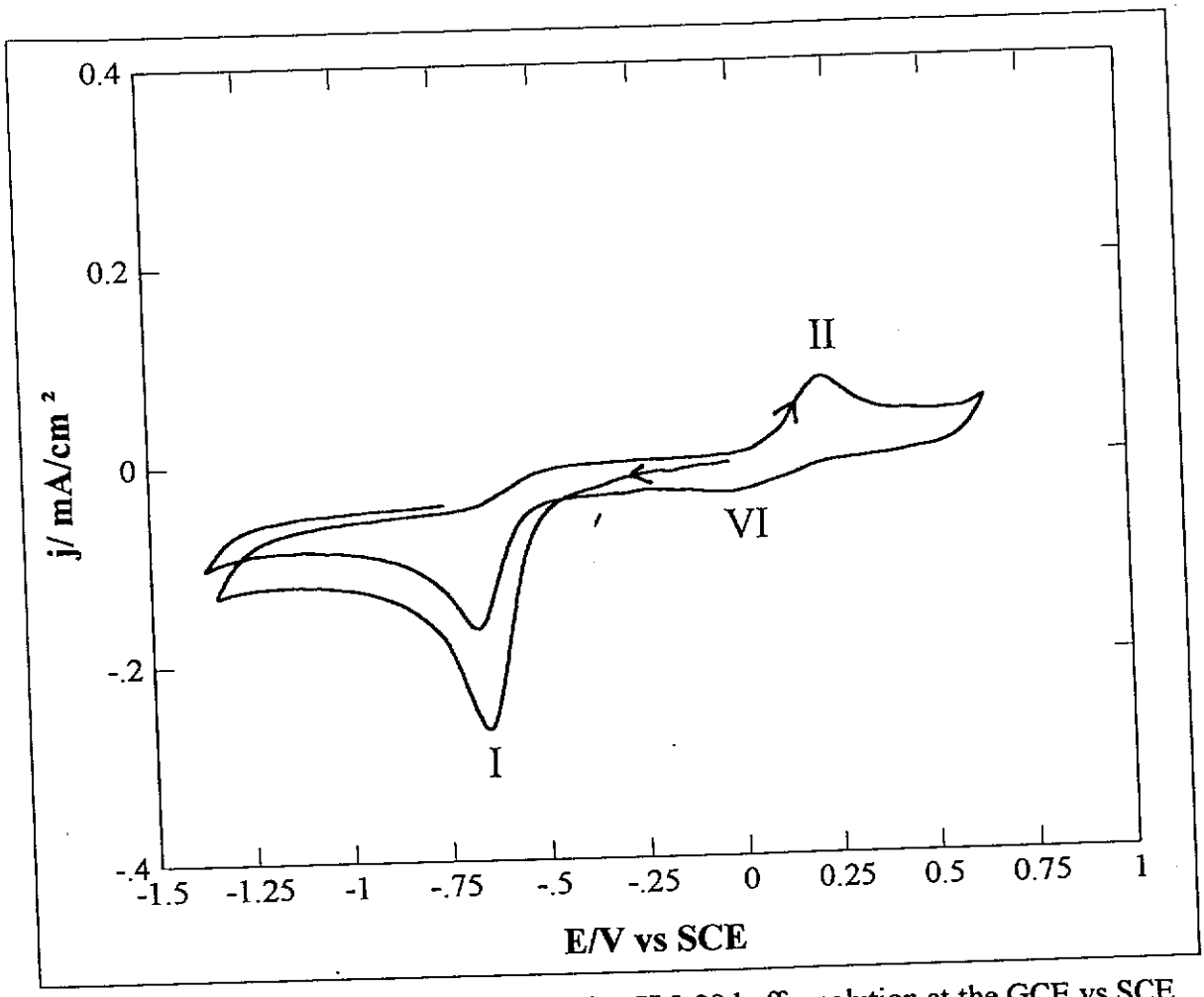

Fig.5.9. A CV of Procion Red MX 5B run in pH 3.29 buffer solution at the GCE vs SCE excluding peak IV potential region.

Concentration of Procion Red MX 5B: 1.0046 mM

Buffer strength: 0.2 M

Initial potential: 0.00 V

Positive limit: 0.70

Negative limit: -1.30

Scan rate: 150 mV/s

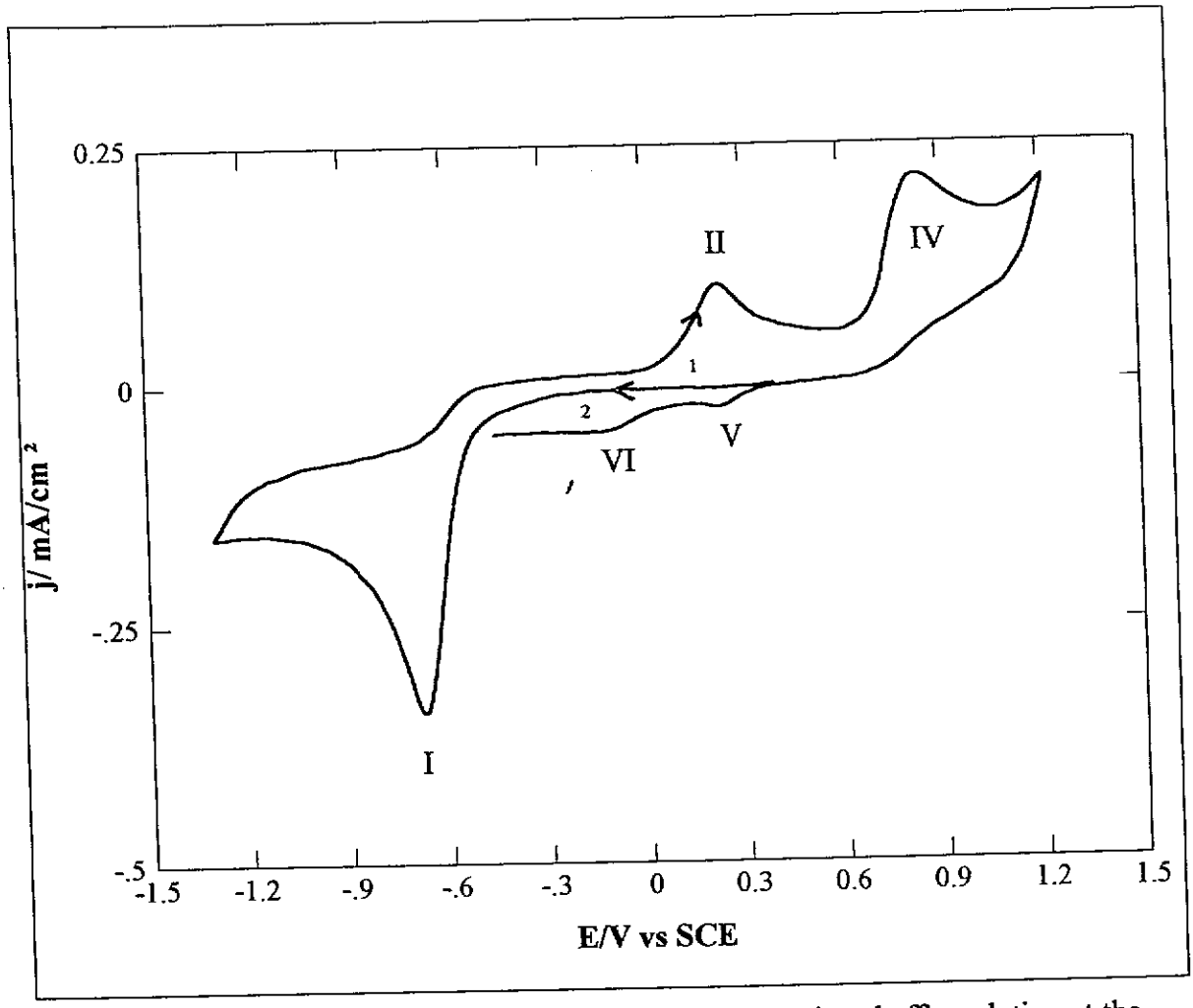

Fig.5.10. A CV of Procion Red MX 5B run in pH 4.07 phosphate buffer solution at the GCE vs SCE.

Concentration of Procion Red MX 5B: 1.0046 mM

Buffer strength: 0.2 M

Initial potential: 0.40 V

Positive limit: 1.25

Negative limit: -1.30

Scan rate: 150 mV/s

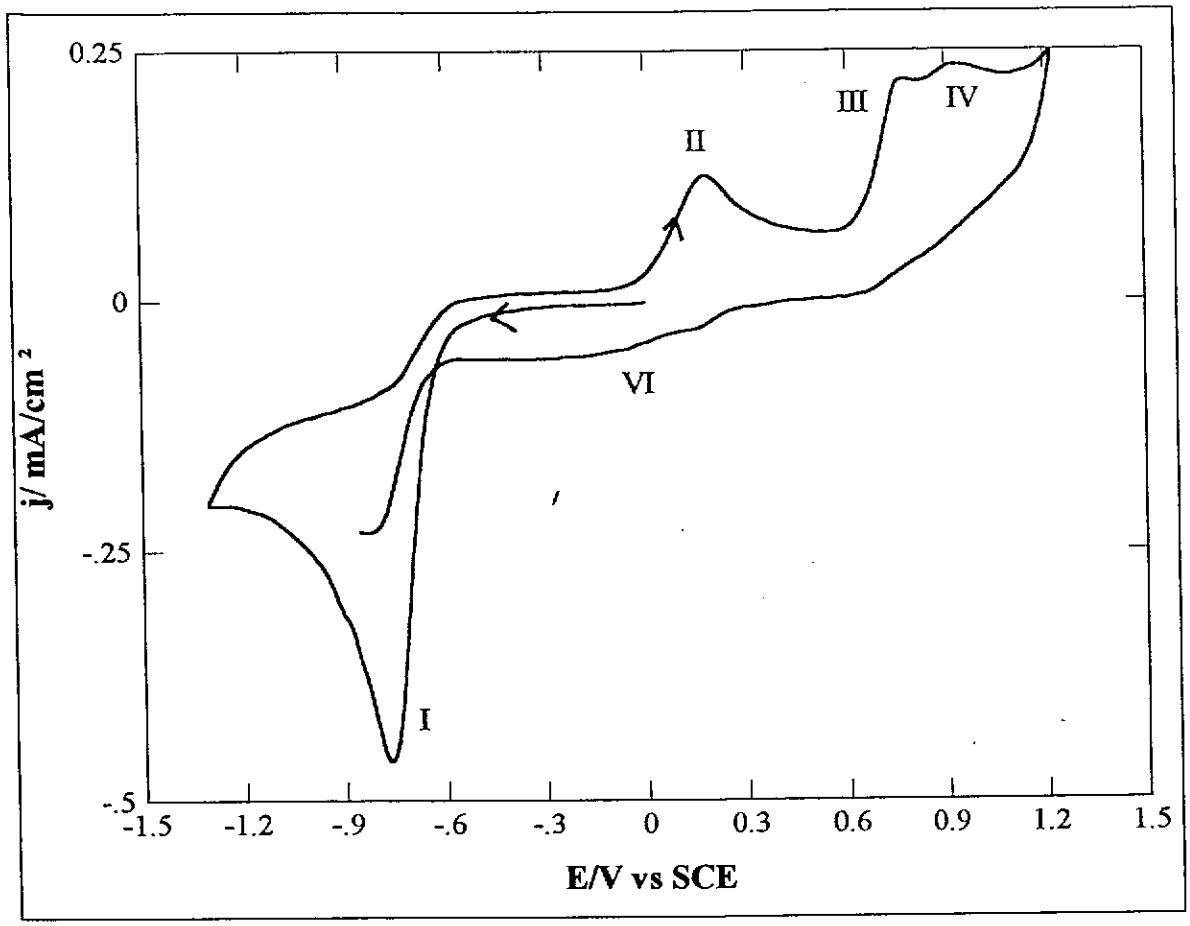

Fig.5.11. A CV of Procion Red MX 5B run in pH 5.06 phosphate buffer solution at the GCE vs SCE.

Concentration of Procion Red MX 5B: 1.0046 mM

Buffer strength: 0.2 M

Initial potential: 0.00 V

Positive limit: 1.25

Negative limit: -1.30

Scan rate: 150 mV/s

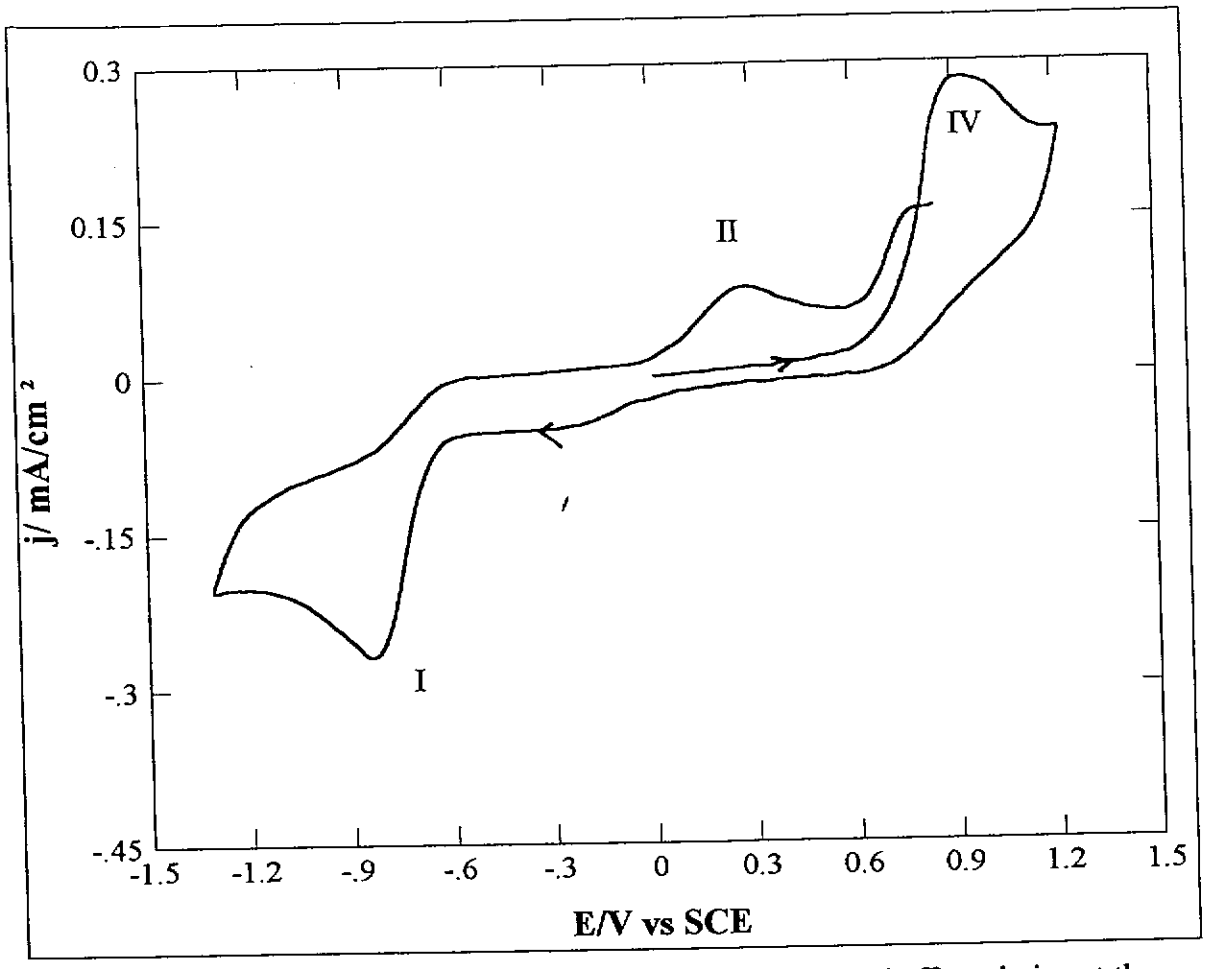

Fig.5.12. A CV of Procion Red MX 5B run in pH 5.06 phosphate buffer solution at the GCE vs SCE

Concentration of Procion Red MX 5B: 1.0046 mM

Buffer strength: 0.2 M

Initial potential: 0.00 V

Positive limit: 1.25

Negative limit: -1.30

Scan rate: 150 mV/s

5.2.1.1 Discussion

Peak I is a typical irreversible cathodic peak of the azo dye which was exhibited by Orange II and fast Sulphone Black[4]. These dyes were reported to undergo electrochemical reduction giving corresponding aromatic amines. The dependence of peak II, III, V and VI on peak I could mean that Procion Red MX 5B was reduced at peak I giving products that are electroactive in the same electrochemical potential window. The shift of Peak I potential as pH increases means that the reduction of Procion Red MX 5B is pH dependent.

The disappearance of peak V as pH increases shows that the formation of some of the products is pH dependent. The appearance of peak III at the pH 5.07 proves the peak potential dependence on the pH. This could mean that peak III was masked by peak IV at pH 3.29 and 4.06. Further investigation could not be carried out because of precipitation of the dye in these pH's.

5.2.2 Cyclic Voltammetry of Procion Red MX 5B at pH 6, 7 and 8.

Fig.5.13 shows the CV of Procion Red MX 5B run in pH 7.06 phosphate buffer. The cyclic voltammograms run at pH 6.04 and 8.04 are essentially the same as fig.5.13. The only difference is that peak I had changed its position since it has been established that its peak potential depends on the pH, i.e. it becomes more negative as the pH increases. Fig.5.13 shows the same peaks as the voltammogram in fig 5.11 except that peak V has disappeared, confirming that the product responsible for the peak depends on the pH for its formation. The dependence of peak II and VI was also found to be the same as in pH 3, 4 and 5. This is confirmed by the CV shown in fig.5.14.

The dependence of peak III on peak I was confirmed by its absence on fig.5.15 and it also proves the independence of peak IV. The CV in fig.5.15 was initiated in the positive direction and cycled between 1.25 V and -1.30 V.

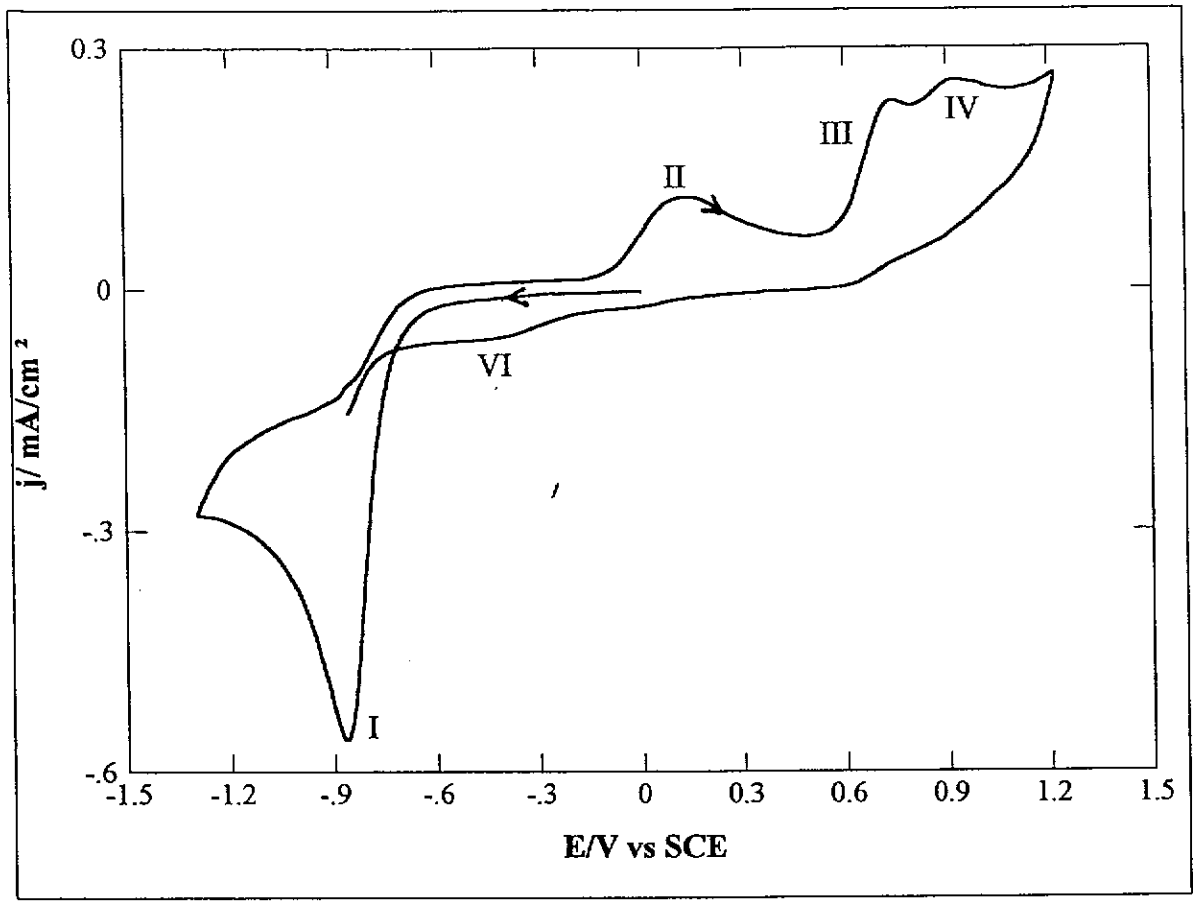

Fig.5.13. A CV of Procion Red MX 5B run in pH 7.06 phosphate buffer solution at the GCE vs SCE.

Concentration of Procion Red MX 5B: 1.0046 mM

Buffer strength: 0.2 M

Initial potential: 0.00 V

Positive limit: 1.25 V

Negative limit: -1.30 V

Scan rate: 150 mV/s

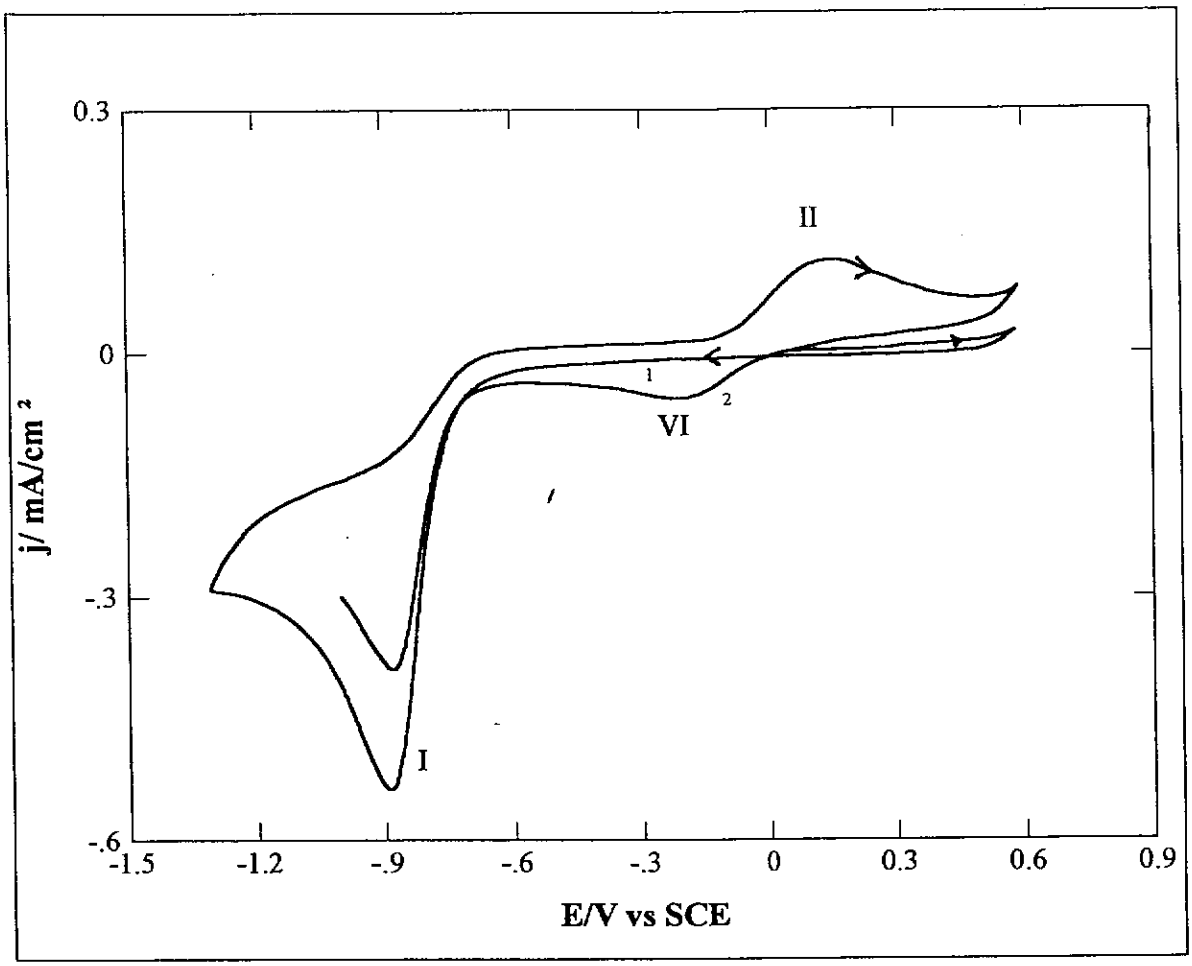

Fig.5.14. A CV of Procion Red MX 5B run in pH 7.06 phosphate buffer solution at the GCE vs SCE excluding peak III and IV potential region.

Concentration of Procion Red MX 5B: 1.0046 mM

Buffer strength: 0.2 M

Initial potential: 0.00 V

Positive limit: 0.60 V

Negative limit: -1.30 V

Scan rate: 150 mV/s

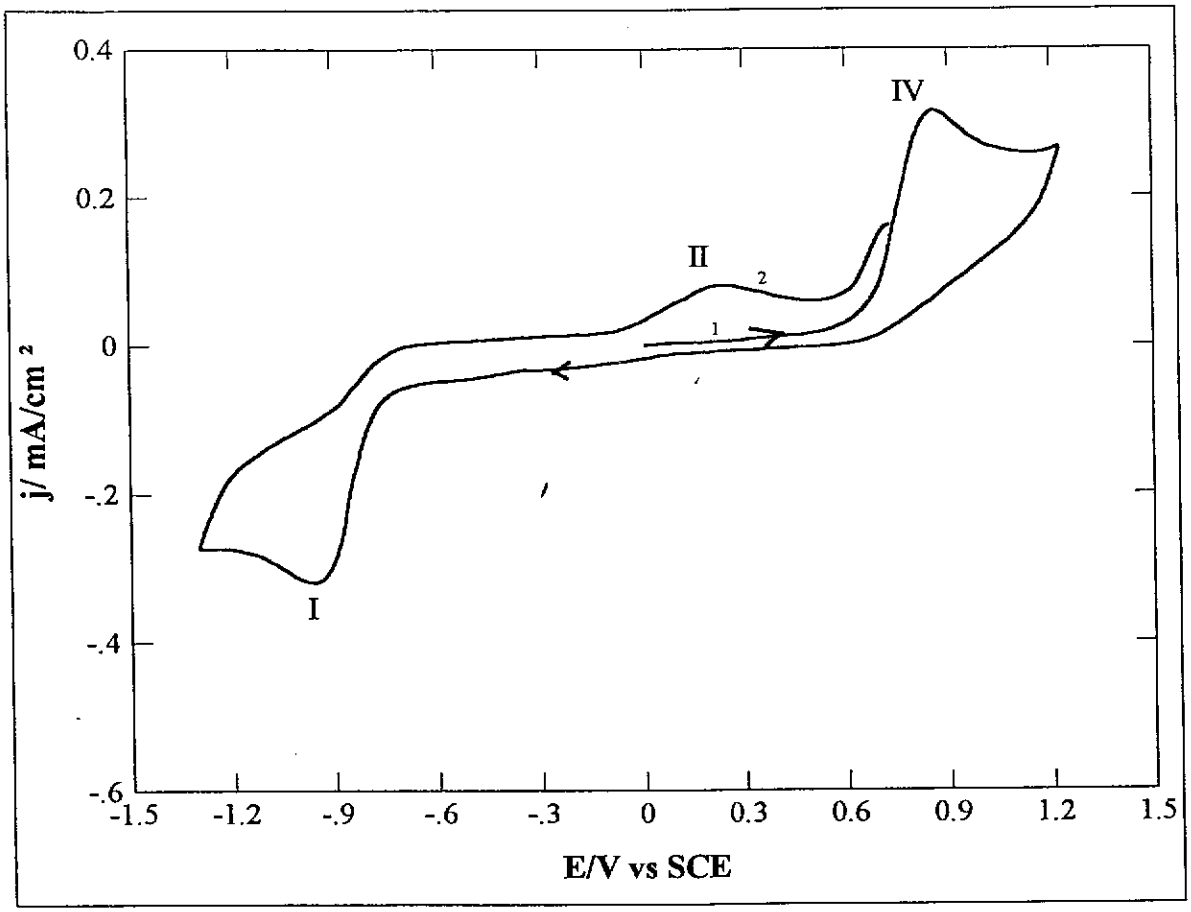

Fig 5.15. A CV of Procion Red MX 5B run in pH 7.06 phosphate buffer solution at the GCE vs SCE.

Concentration of Procion Red MX 5B: 1.0046 mM

Buffer strength: 0.2 M

Initial potential: 0.00 V

Positive limit: 1.25 V

Negative limit: -1.30 V

Scan rate: 150 mV/s

5.2.2.1 Bulk Controlled Potential Electrolysis.

Since at pH 7.06 the dye does not precipitate, further experiments could be performed. It was assumed on the basis of peaks II, III and VI dependence on peak I that the dye was undergoing electroreduction into corresponding aromatic amines at peak I. The fact that peak I is a typical irreversible cathodic peak also consolidated the assumption. The plot of j vs $\nu^{1/2}$ for peak I, gave a straight line, which means reduction is diffusion controlled, i.e. the transfer of electrons is fast compared to the rate of diffusion of the molecule to the surface of the electrode. The plot is shown in fig.5.16.

With this assumption in mind bulk electrolysis of Procion Red MX 5B was performed and monitored by UV-vis spectroscopy since the dye absorbs in the visible region from 511-540 nm. According to Beer-Lambert's law the intensity of the UV-vis peak is directly proportional to the concentration of the absorbing species when the path length of radiation is constant, therefore the absorption at 511-540 nm was expected to decrease as electrolysis progressed. The electrolysing potential was set 100 mV more negative than peak I potential. Fig.5.17 shows the UV-vis spectra of Procion Red MX 5B recorded after 10 and 20 minutes of 110 minutes of controlled potential electrolysis.

Fig.5.17 proves that the dye chromophore (-N=N-) has been broken, since λ_{max} of the dye has decreased systematically. A CV of the completely electrolysed solution was run to see if peak I would appear or not. Fig.5.18 shows the cyclic voltammogram of completely electrolysed solution. The absence of peak I confirms that indeed the dye has been electrodegraded and also supports the UV-vis spectroscopy results.

On the basis of these results a mechanism of electroreduction of the dye was proposed. The proposed Procion Red MX 5B mechanism is shown in fig.5.19. To support the proposed mechanism the corresponding aromatic amines should be produced during bulk controlled potential electrolysis. Controlled potential electrolysis was performed at pH 7.06 phosphate buffer solution. The completely electrolysed solution was extracted with chloroform hoping to extract non-polar aniline since it is one of the proposed corresponding amines.

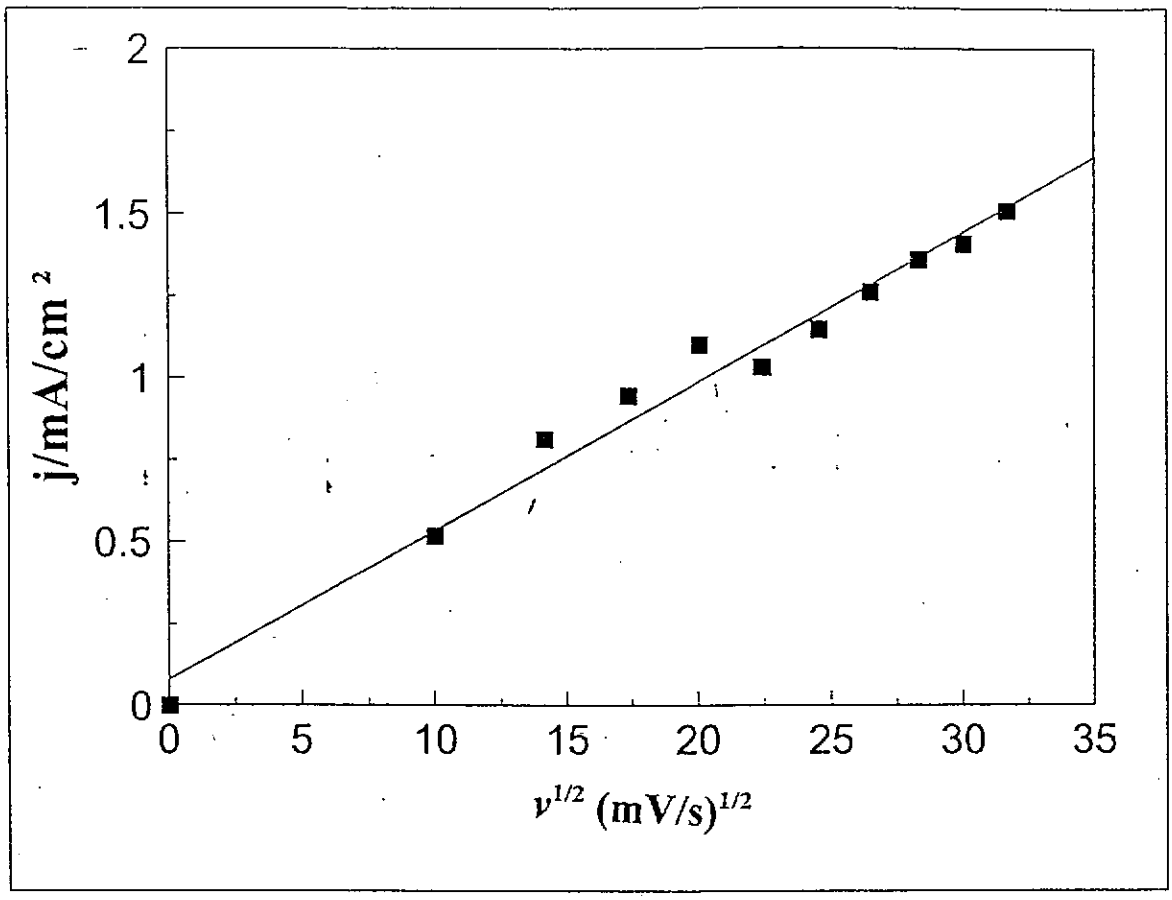

Fig.5.16. A graph of peak I current density (j) vs square root of scan rate ($v^{1/2}$)

Current density (j) (mA/cm^2)	Square root of Scan rate $\nu^{1/2}$ $(mV/s)^{1/2}$
0.52	10.00
0.81	14.14
0.94	17.32
1.10	20.00
1.03	22.36
1.15	24.50
1.26	26.46
1.36	28.28
1.41	30.00
1.51	31.62

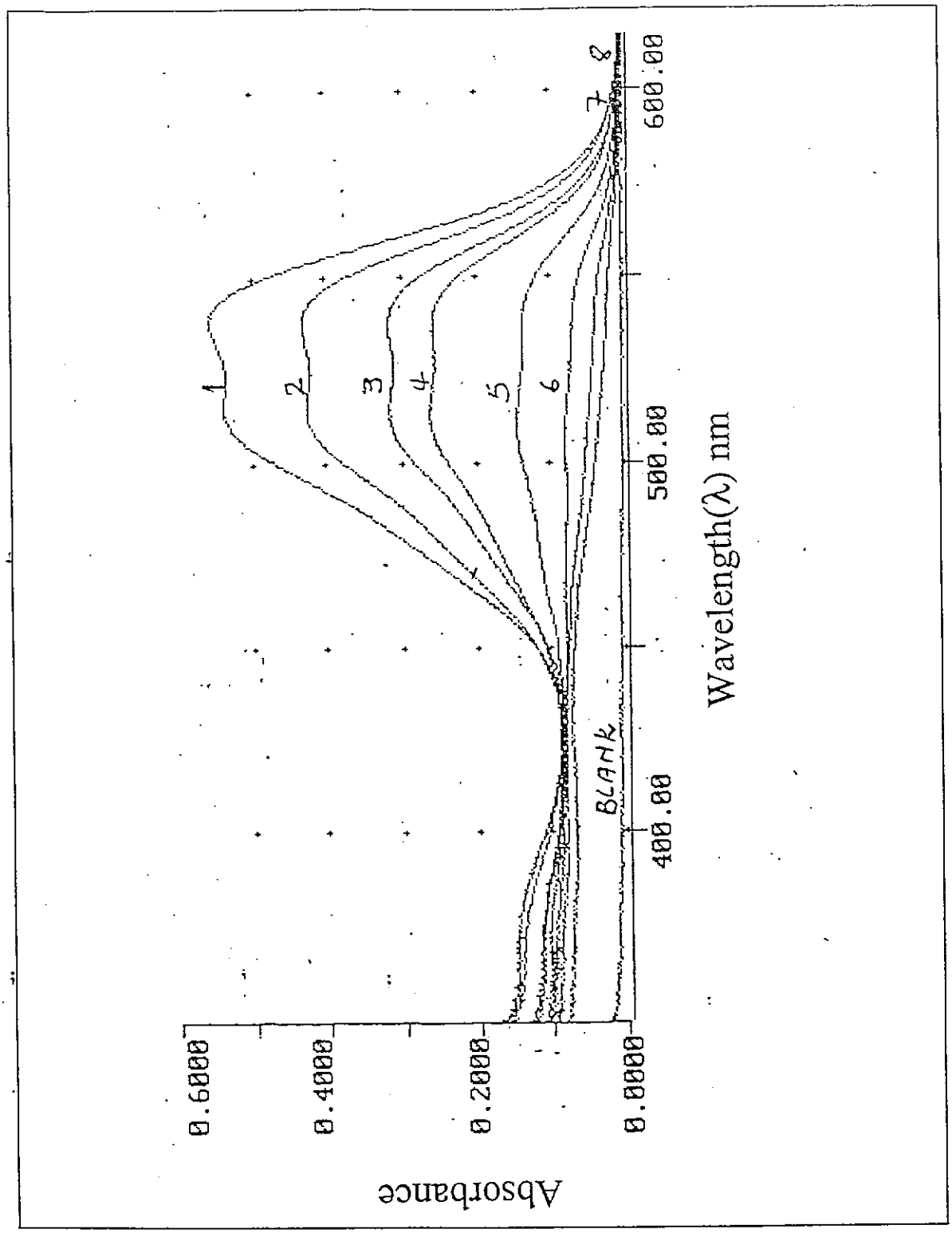

Fig.5.17. Observed spectral changes during electrolysis of 1.0046 mM Procion Red MX 5B at pH 7.06 at the graphite electrode vs SCE.

Applied potential: -0.965 V vs SCE. Curves were recorded at 0 (1), 10 (2), 20 (3), 30 (4), 50 (5), 70 (6), 90 (7), and 110 minutes (8).

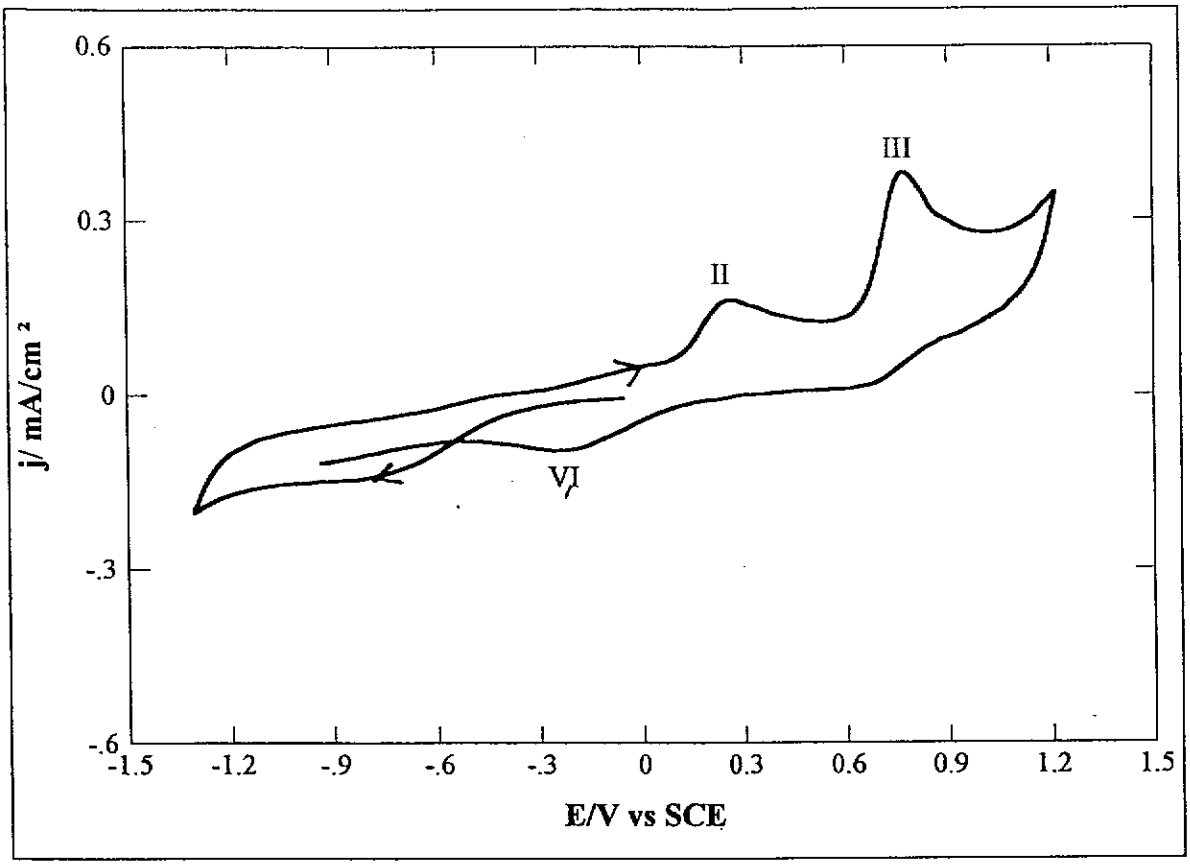

Fig.5.18. The CV of completely electrolysed solution of Procion Red MX 5B run in pH 7.06 phosphate buffer solution at the GCE vs SCE.

Concentration of Procion Red MX 5B before electrolysis:

1.0046 mM

Buffer strength: 0.2 M

Initial potential: 0.00 V

Positive limit: 1.25 V

Negative limit: -1.30 V

Scan rate: 150 mV/s

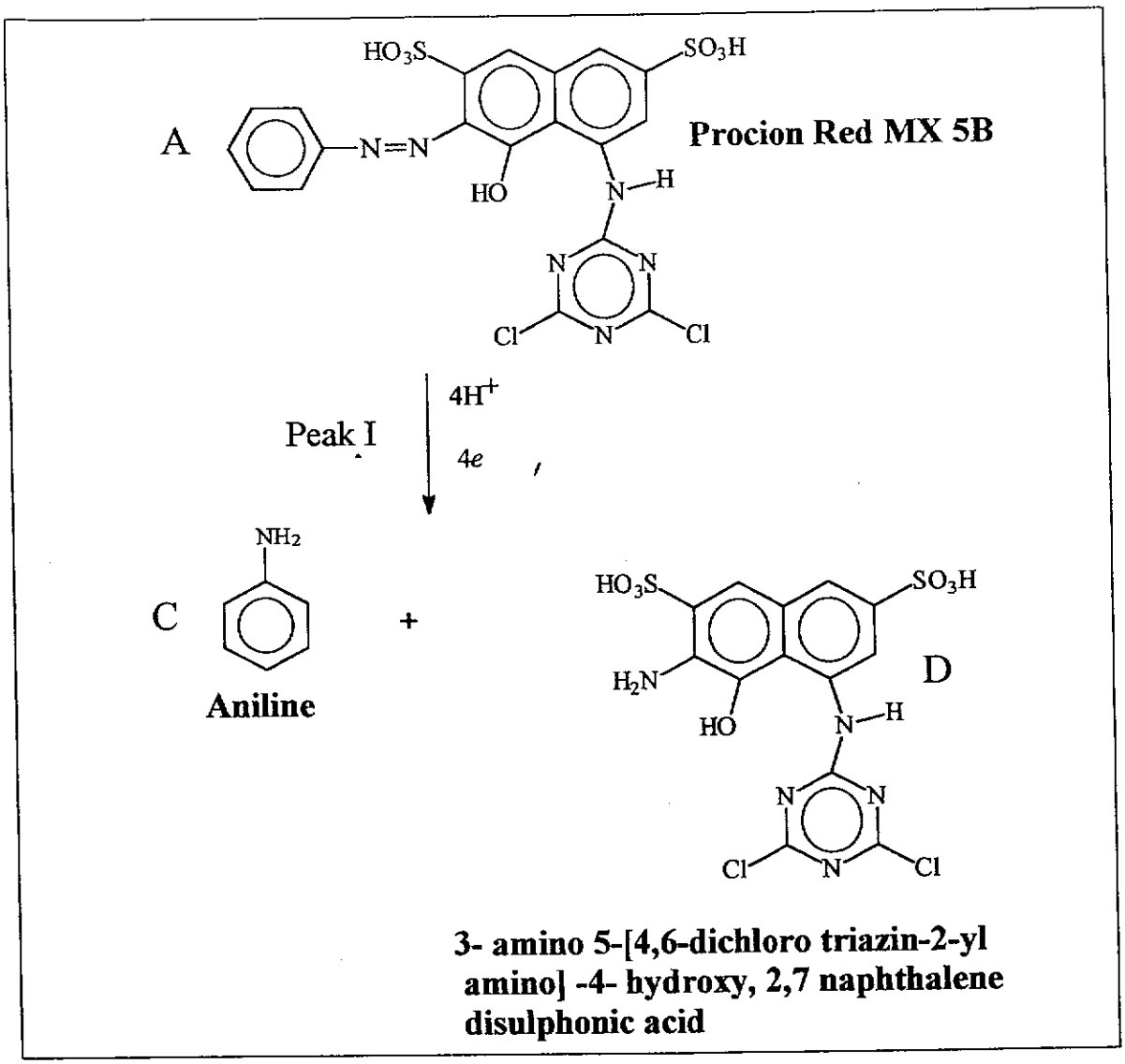

Fig.5.19. The proposed mechanism of Procion Red MX 5B electroreduction

After vacuum evaporation of chloroform extracts an oil residue was left. The ^{1}HNMR analysis proved that the oily residue was aniline. The ^{1}HNMR spectrum of the residue is shown in appendix II (spectrum 7). The identification of aniline unequivocally confirmed that the proposed electroreduction mechanism is feasible. Fig.5.20 shows the CV of authentic aniline run in pH 7.06 phosphate buffer solution. The concentration of the sample was 0.998 mM.

The CV was initiated in the negative direction and cycled between -1.30 V and 1.25 V. It shows three peaks like the voltammogram of the completely electrolysed solution and the peaks are at the same position showing that indeed one of the corresponding amines was aniline. The other peaks displayed by the voltammogram of Procion Red 5B can be interpreted as follows:

Peak IV appears as a result of oxidation of Procion red MX 5B (A) forming an azoxy compound[1] as shown below:

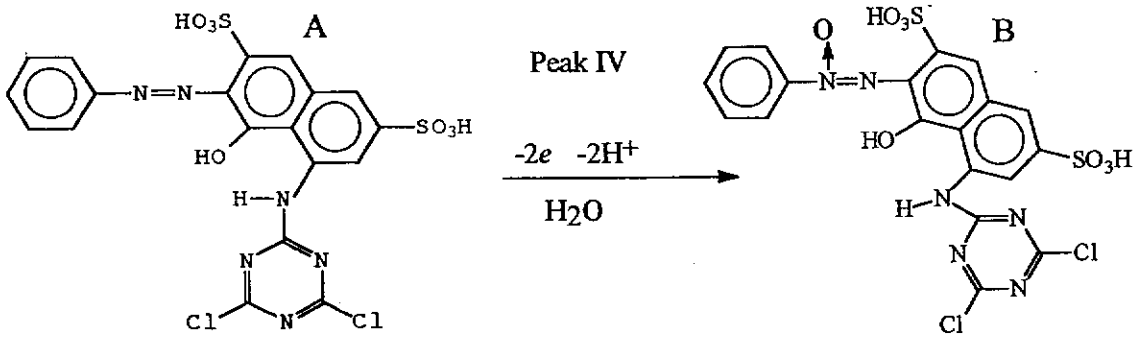

Procion Red MX 5B

Azoxy derivative of Procion Red MX 5B

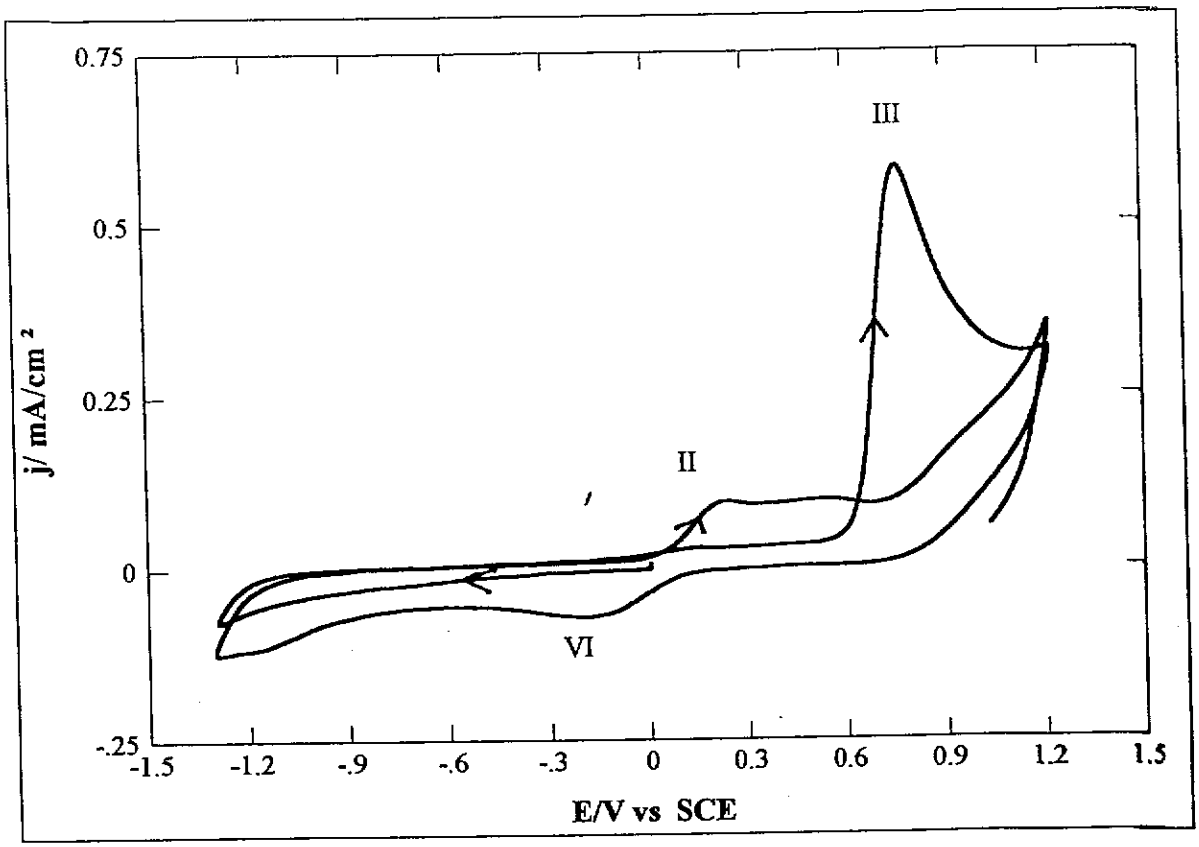

Fig.5.20. A CV aniline run in pH 7.06 phosphate buffers solution at the GCE vs SCE.

Concentration of aniline: 0.998 mM

Buffer strength: 0.2 M

Initial potential: 0.00 V

Positive limit: 1.25 V

Negative limit: -1.30 V

Scan rate: 150 mV/s

Peak III appears as a result of one electron oxidation of aniline[5] (C) which is pH dependent. The mechanism is shown below:

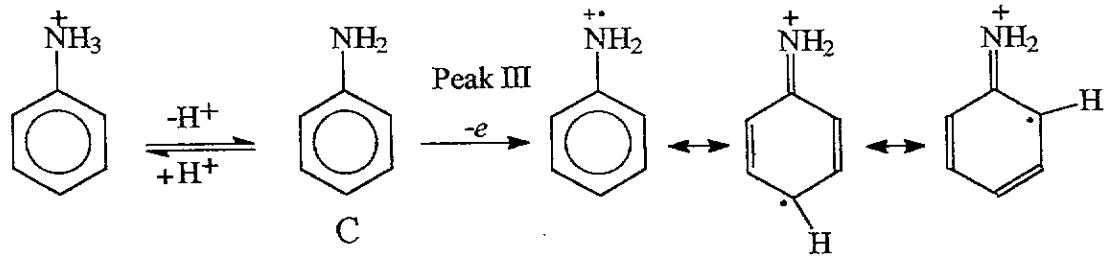

Peak II and VI appear as a result of quasireversible redox reaction of 4-amino diphenyl amine [5] (E) formed from head to tail coupling of aniline radicals as shown below:

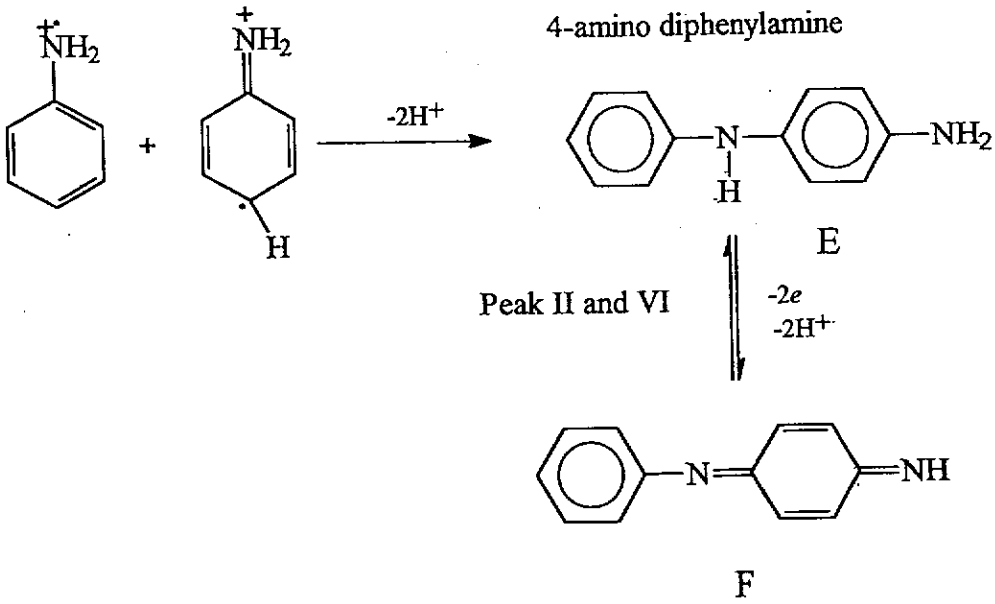

Peak V can be attributed to benzidine which according to Bacon and Adams[5] is formed by tail to tail coupling of the aniline radical as shown below. Bacon and Adams also reported that benzidine formation is pH dependent and at pH 4 in Britton-Robinson buffer it approaches zero concentration. This explains the disappearance of peak V at pH 5.06.

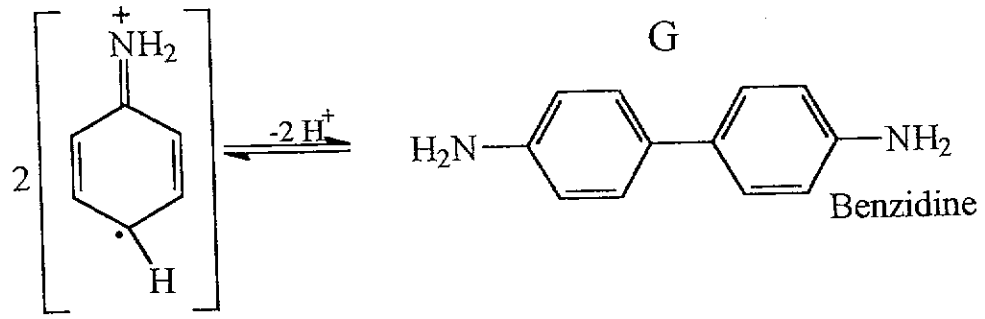

5.2.3 Cyclic Voltammetry of Procion Red MX 5B at pH 9, 10 and 11.

Fig.5.21. shows the CV of Procion Red MX 5B run at pH 9.09 phosphate buffer solution. Peak I has shifted to more negative potential as expected but its height has decreased. The decrease of peak I height continued throughout to pH 10.86. Peak II is still present but has also decreased in height and peaks V and VI are absent. The decrease of peak II height continues through to pH 10.86. Peaks III and IV are still present but their demarcation has faded. Peaks II and III still depend on peak I as in the previous section.

One would expect peak I's height to be the same as in pH 7 and 8, since the precipitation of the dye stopped at pH 6.04, but in fact it started to decrease at pH 9.19. According to Mairanovskii[6] the decrease in limiting current observed for many organic compounds when non-aqueous solvents were added to the supporting electrolyte could be explained on the basis of the decrease in the rate of the pre-protonation reaction which occurs at an electrode surface. This seems to be the case with Procion Red MX 5B since peak I potential varies with the pH.

The higher the pH the more negative the peak potential. At high pH, the concentration of protons in the solution will be small hence the rate of pre-protonation will be low giving rise to small limiting currents. Also at high pH's Procion Red MX 5B will be a negatively charged anion because of the two sulphonate groups hence it will be repelled by a negatively charged electrode. This repulsion will lower the rate of electrode reaction and lead to lower limiting currents.

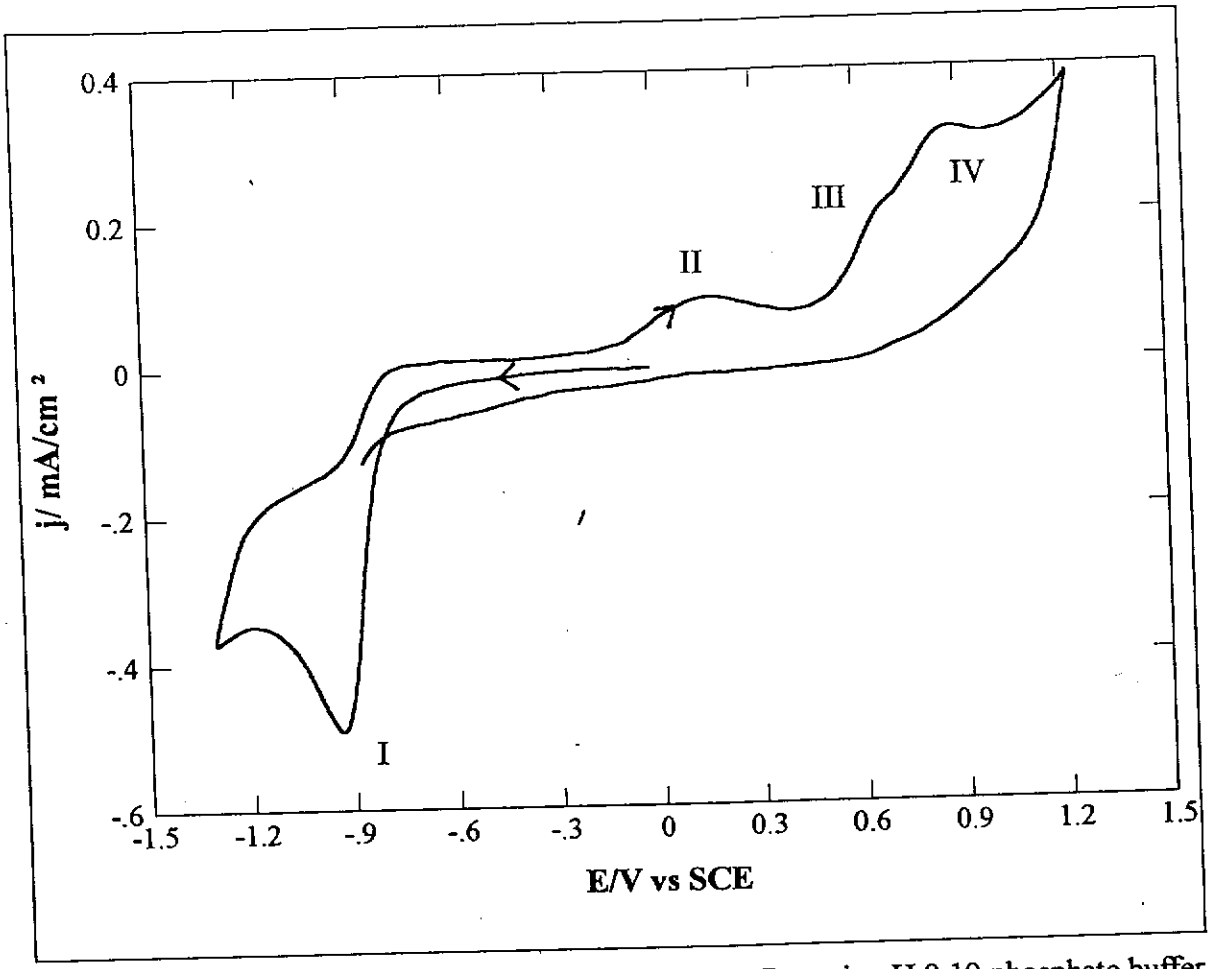

Fig.5.21. A Cyclic voltammogram of Procion Red MX 5B run in pH 9.19 phosphate buffer solution at the GCE vs SCE.

Concentration of Procion Red MX 5B: 1.0046 mM

Buffer strength: 0.2 M

Initial potential: 0.00 V

Positive limit: 1.25 V

Negative limit: -1.30 V

Scan rate: 150 mV/s

This seems to be the case with Procion Red MX 5B since peak I potential varies with the pH. The higher the pH the more negative the peak potential. At high pH, the concentration of protons in the solution will be small hence the rate of pre-protonation will be low giving rise to small limiting currents. Also at high pH's Procion Red MX 5B will be a negatively charged anion because of the two sulphonate groups hence it will be repelled by a negatively charged electrode. This repulsion will lower the rate of electrode reaction and lead to lower limiting currents. The repulsion was observed for multi-negatively charged dye Chrome Blue K shown in fig.5.22 even in aqueous supporting electrolyte by Florence[7].

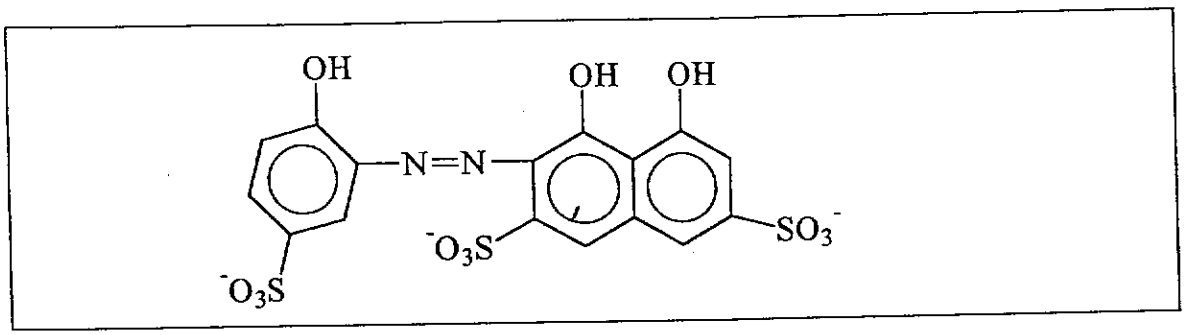

Fig.5.22. The Chemical structure of Chrome Blue K

He also found that in strongly alkaline solution the half wave potentials of the azo dyes studied became constant and independent of the pH. This is what has been observed for Procion Red MX 5B at pH 10.46 and 10.86 (fig.5.23) where peak I potential was found to be the same. Florence attributed the independence of the peak on pH to the direct addition of electrons to the organic molecules without any pre-protonation reaction. The rate of such direct electron addition is usually slow, which accounts for the small limiting currents and their kinetic nature.

Although the peak I height had decreased the presence of peaks II and III means that the dye was still undergoing electroreduction into corresponding amines.

Since it was established that peak I potential depended on pH, a plot of peak I potential vs pH was constructed and an equation was derived from the plot. The equation is shown below and the plot is shown in fig.5.23.

$-E_p = (0.0489\ pH + 0.495)$ V vs SCE

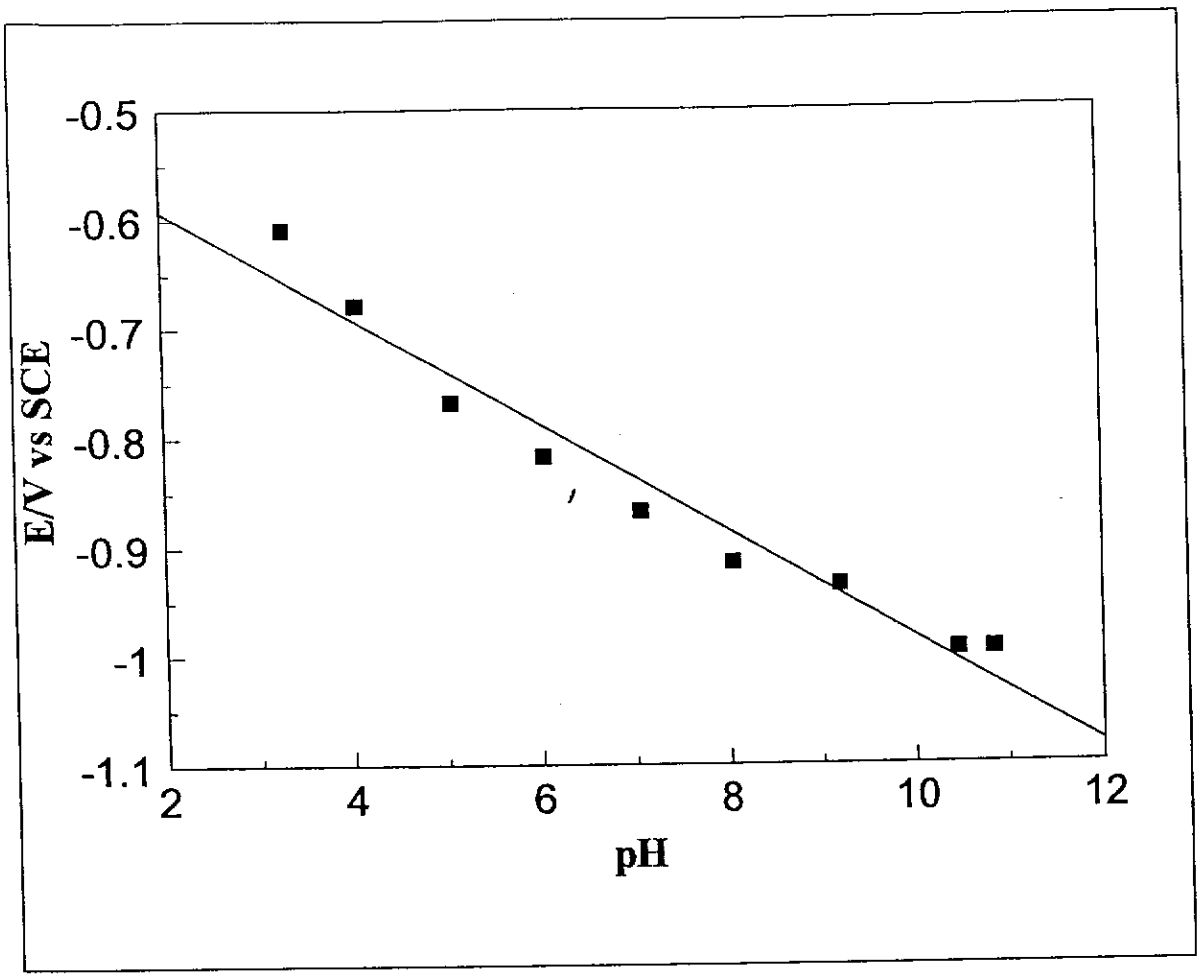

Fig.5.23 A plot of peak I (fig.5.13) potential vs pH of the buffer solutions.

pH	Peak I potential (V)
3.29	-0.61
4.07	-0.68
5.06	-0.77
6.04	-0.82
7.06	-0.87
8.04	-0.92
9.19	-0.94
10.46	-1.00
10.84	-1.00

5.3 Summary

The aim of this study was to investigate the electrochemical degradability of reactive azo dyes via electroreduction. The electrodegradation was aimed at decolourising the dyes by electroreducing them into corresponding aromatic amines. Procion Red MX 5B was the commercial reactive azo dye studied, and it was shown, using this dye, that electrodegradation was possible, and effective.

The UV-vis spectra taken during the bulk electrolysis of Procion Red MX 5B showed the decrease of λ_{max} of the dye as electrolysis progressed, confirming that the dye chromophore (N=N) was broken in the process. The (N=N) chromophore is responsible for the colour displayed by the dye. At the end of the electrolysis the absorbance at λ_{max} was negligibly small and the colour of the solution had changed from red to a tint of yellow. Naidoo[8] found the same results when reducing the same dye chemically using stannous chloride dissolved in concentrated HCl in methanol. Clearly the addition of these chemicals to the water defeats the object of the exercise, however.

Isolation and identification of aniline, one of the corresponding amines expected from the electrodegradation of the dye, from the completely electrolysed solution confirmed that dye was being reduced into the corresponding aromatic amines.

Cyclic voltammograms run on the completely electrolysed solution of the dye showed that reduction peak I was absent, confirming that the dye has been electrodegraded completely since peak I appears as a result of the reduction of the dye.

It can be concluded that commercial Procion Red MX 5B can be electrodegraded into the corresponding aromatic amines thereby decolourising it. The aromatic amines produced could be a cause for concern in the environment in which this process could be applied since they are possibly carcinogenic. However, the research by Carliell[9] showed that the aromatic amines resulting from the dye reduction can be aerobically converted into carbon dioxide, methane and water.

5.4 References

1. T. M. Florence, F. J. Miller and H. E. Zittel, **Voltammetric Determination of Aluminum by its Oxidation of its Solochrome Violet RS Complex at the Rotated Pyrolytic Graphite Electrode,** ***Anal. Chem.,*** 38(8), (1966) p 1065

2. R. N. Goyal, S. K. Srivastava and A. P. Nautiyal, **Electrochemical Behaviour of Naphthol Red-J, an Azo dye,** ***Indian J. Chem.,*** 26(A), (1987) p. 871

3. N. Naidoo, **The Identification of Dyes and Dye Degradation Products,** MSc. Thesis, University of Natal, Durban (1995) p.8-4 & 8-5

4. W. U. Malik, R. N. Goyal, and N. C. Marthur, **Electrochemical Reduction of Fast Sulphone Black-F, a Bisazo Dye,** ***J. Electroanal. Chem.,*** 235, (1987) p.225

5. J. Bacon and R. N. Adams, **Anodic Oxidations of Aromatic Amines. III. Substituted Anilines in Aqueous Media,** ***J. Am. Chem. Soc.,*** 90(24), (1968) p. 6596

6. S. G. Mairanovskii, **Effect of the Double Layer Structure and of the Adsorption of Electrode Reaction Participants upon Polarographic waves in the Reduction of Organic Substances,** ***J. Electroanal. Chem.,*** 4 (1962) p. 166

7. T. M. Florence, **Polarography of Azo Compounds and Their Metal Complexes,** ***J. Electroanal. Chem.,*** 52, (1974) p115

8. N. Naidoo, **The Identification of Dyes and Dye Degradation Products,** MSc. Thesis, University of Natal, Durban, South Africa (1995) p.9-12

9. C. M. Carliell, **Biological Degradation of Azo dyes in an Anaerobic System,** MScEng Thesis, University of Natal, Durban, South Africa (1993) p. 2-21

Appendix I

Spectrum 1

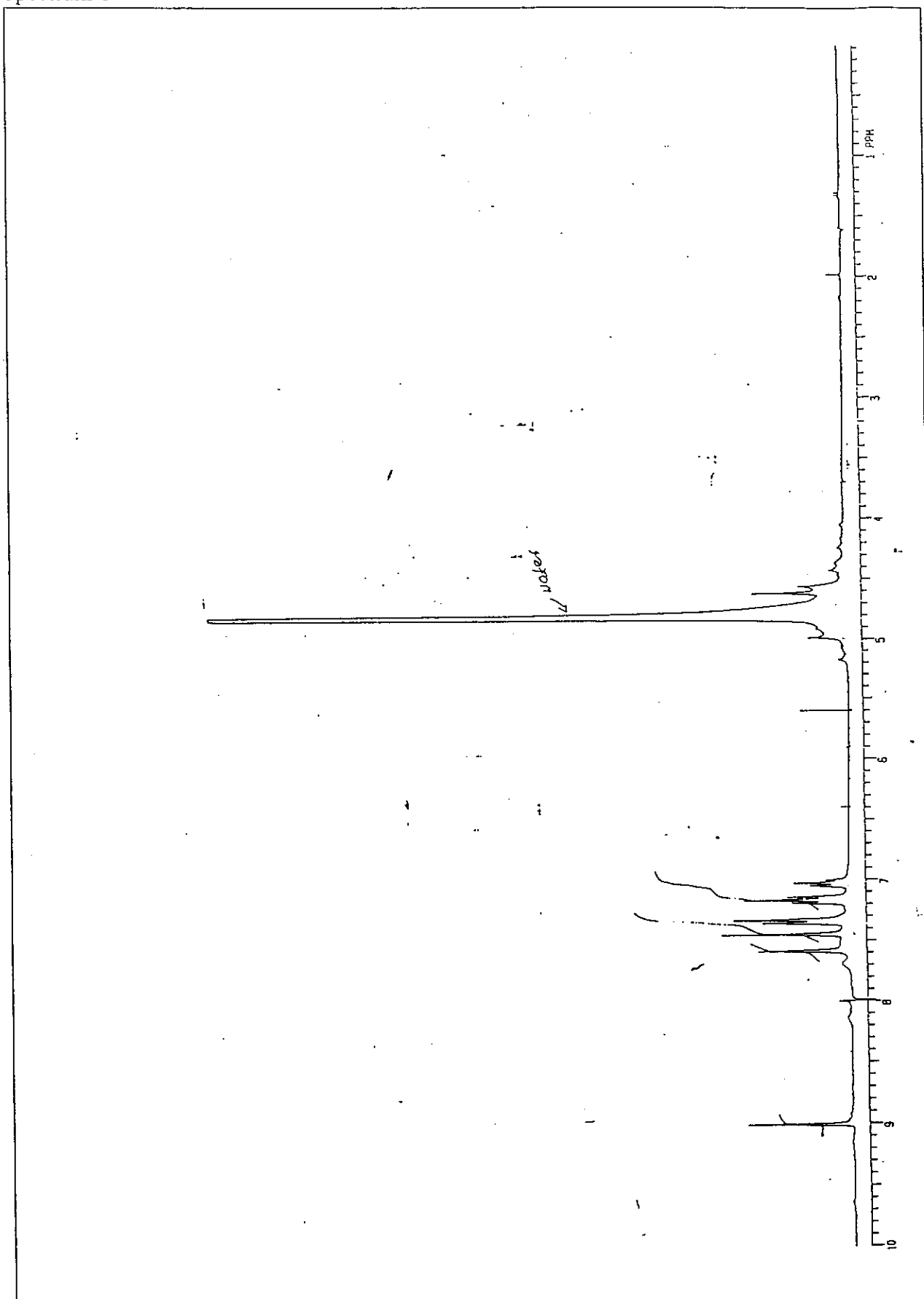

^{1}HNMR spectrum of Procion Red MX 5B

Spectrum 2

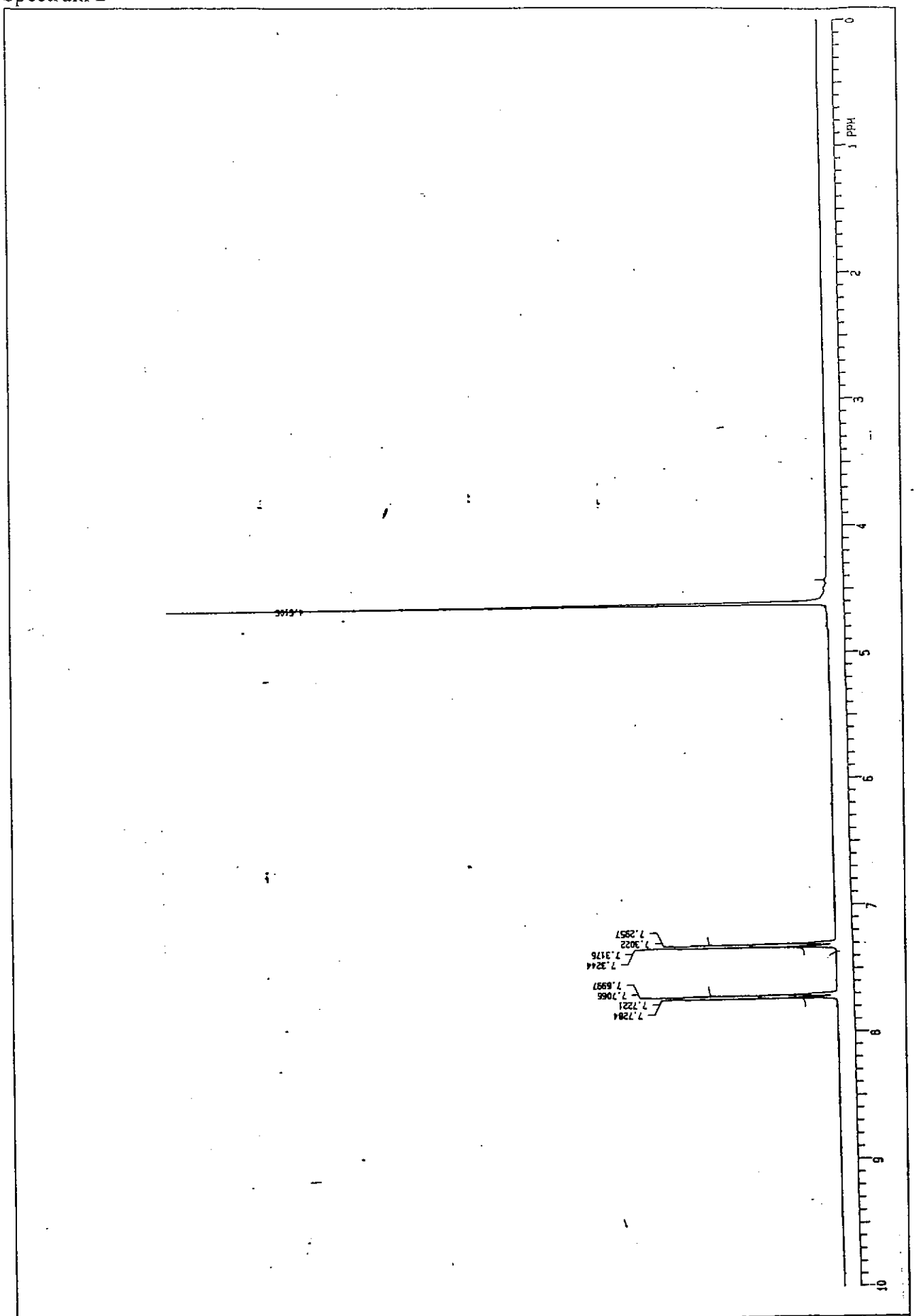

^{1}HNMR spectrum of sulphanilic acid

Spectrum 3

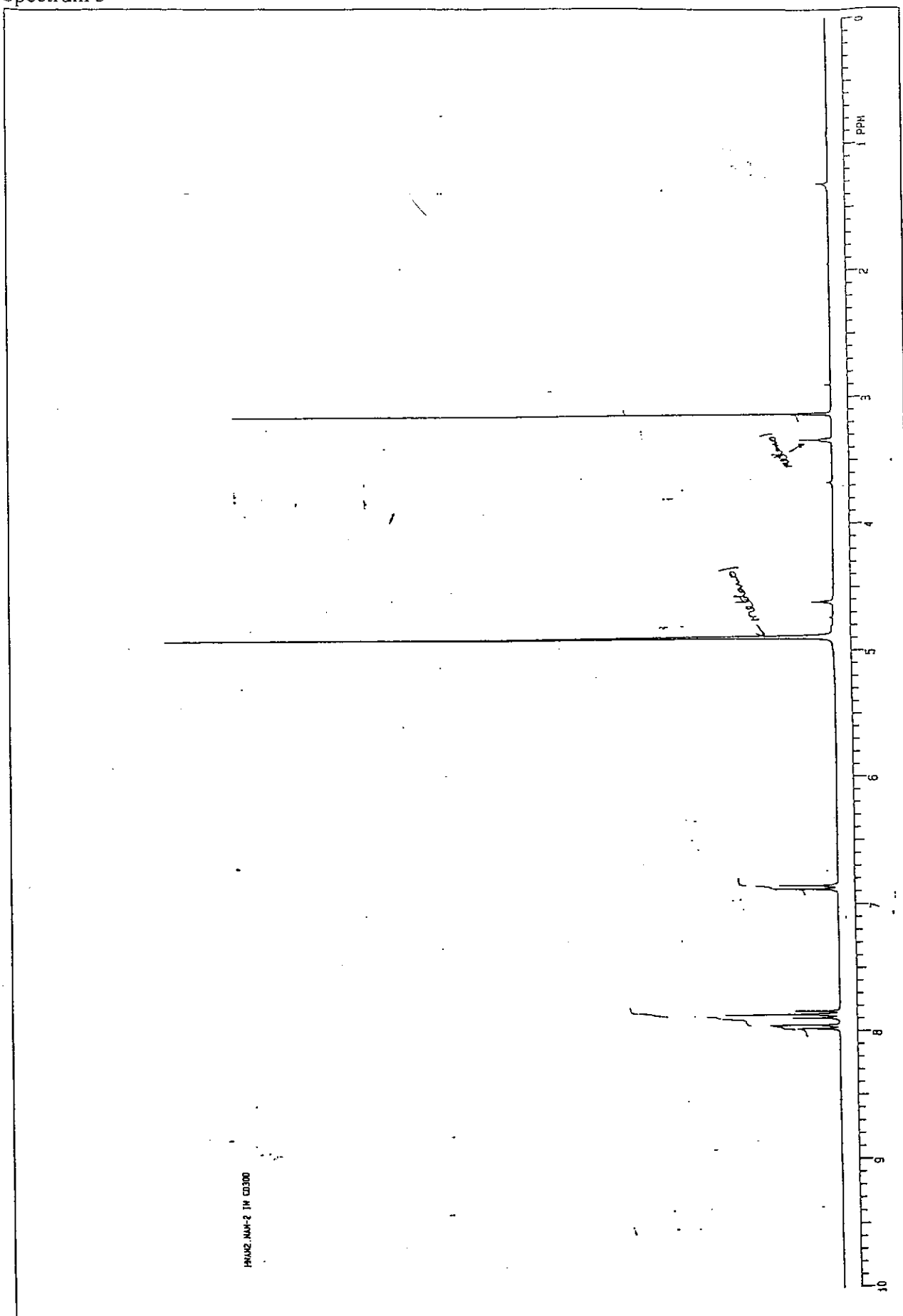

^{1}HNMR spectrum of methyl orange

Spectrum 4

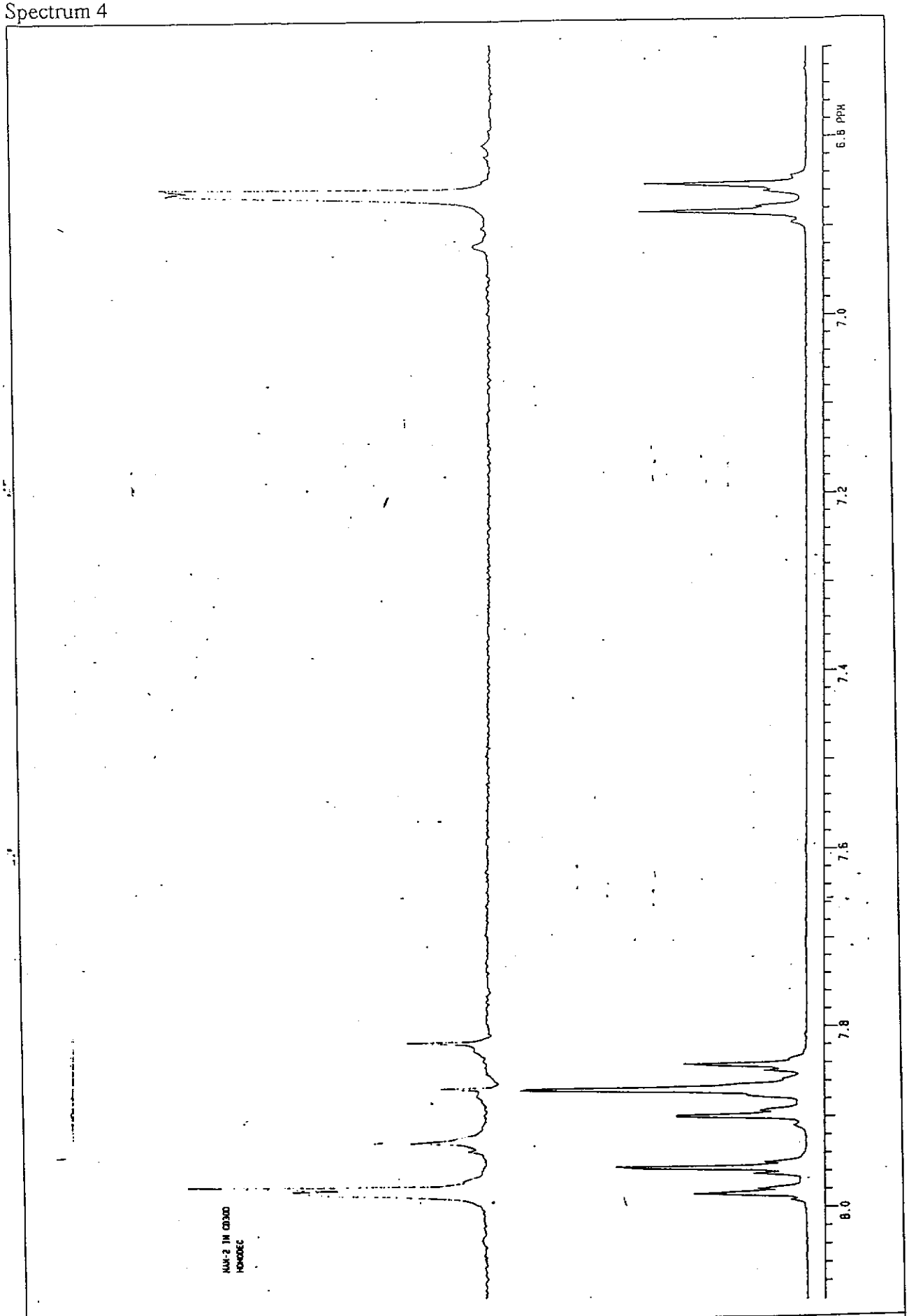

^{1}HNMR spectrum of methyl orange irradiation experiment.

Spectrum 5

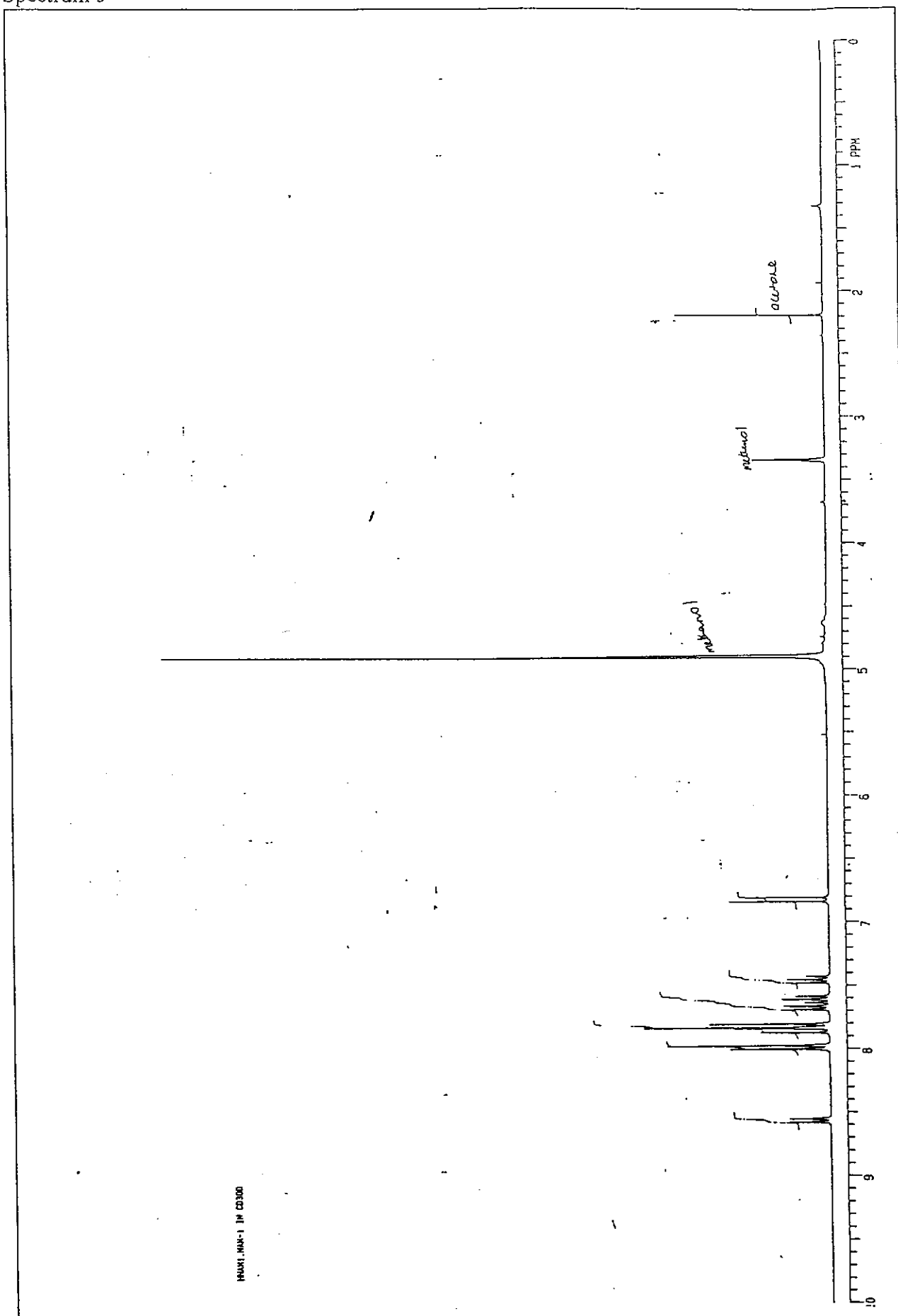

^{1}HNMR spectrum of Orange II

Spectrum 6

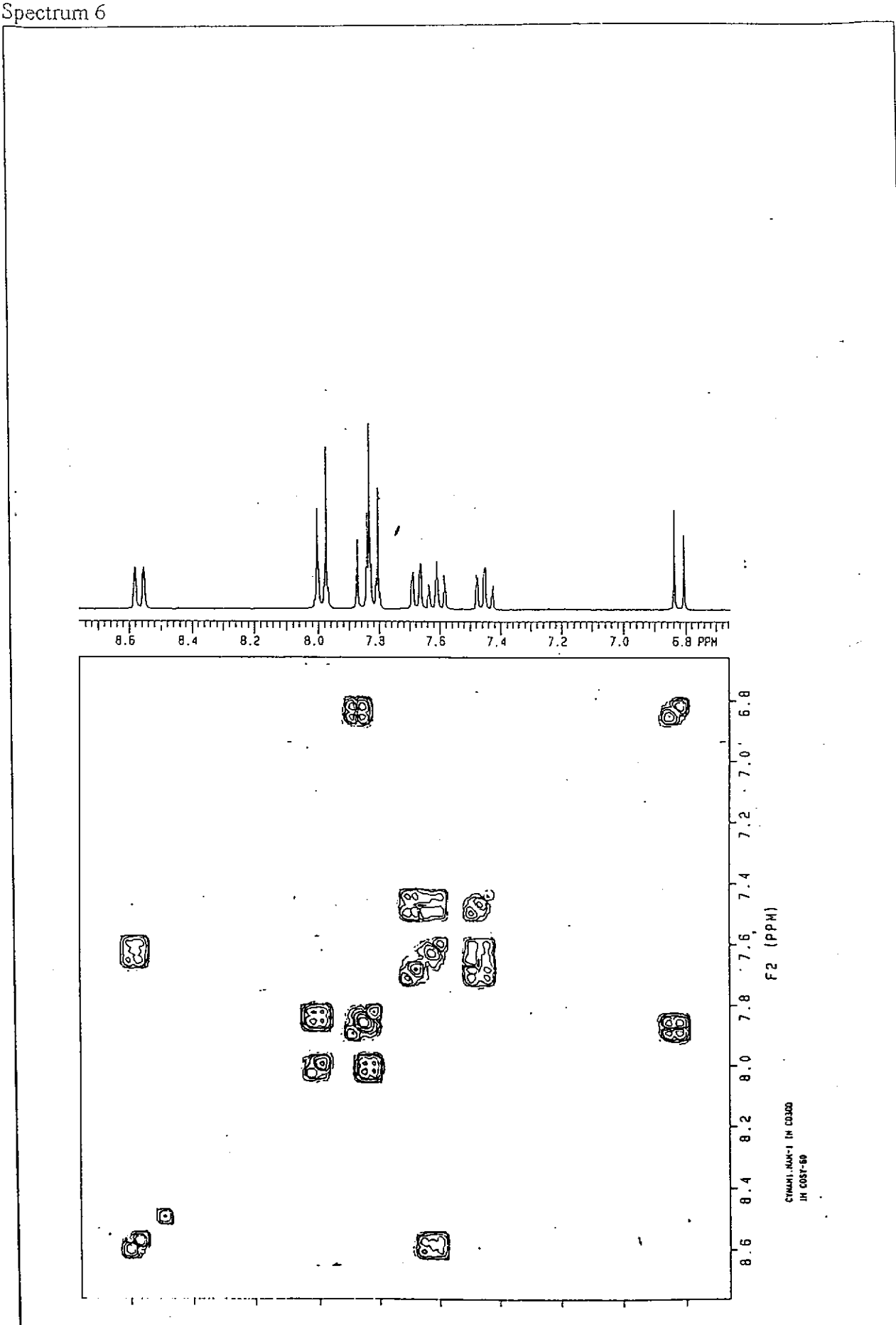

COSY spectrum of Orange II

Spectrum 7

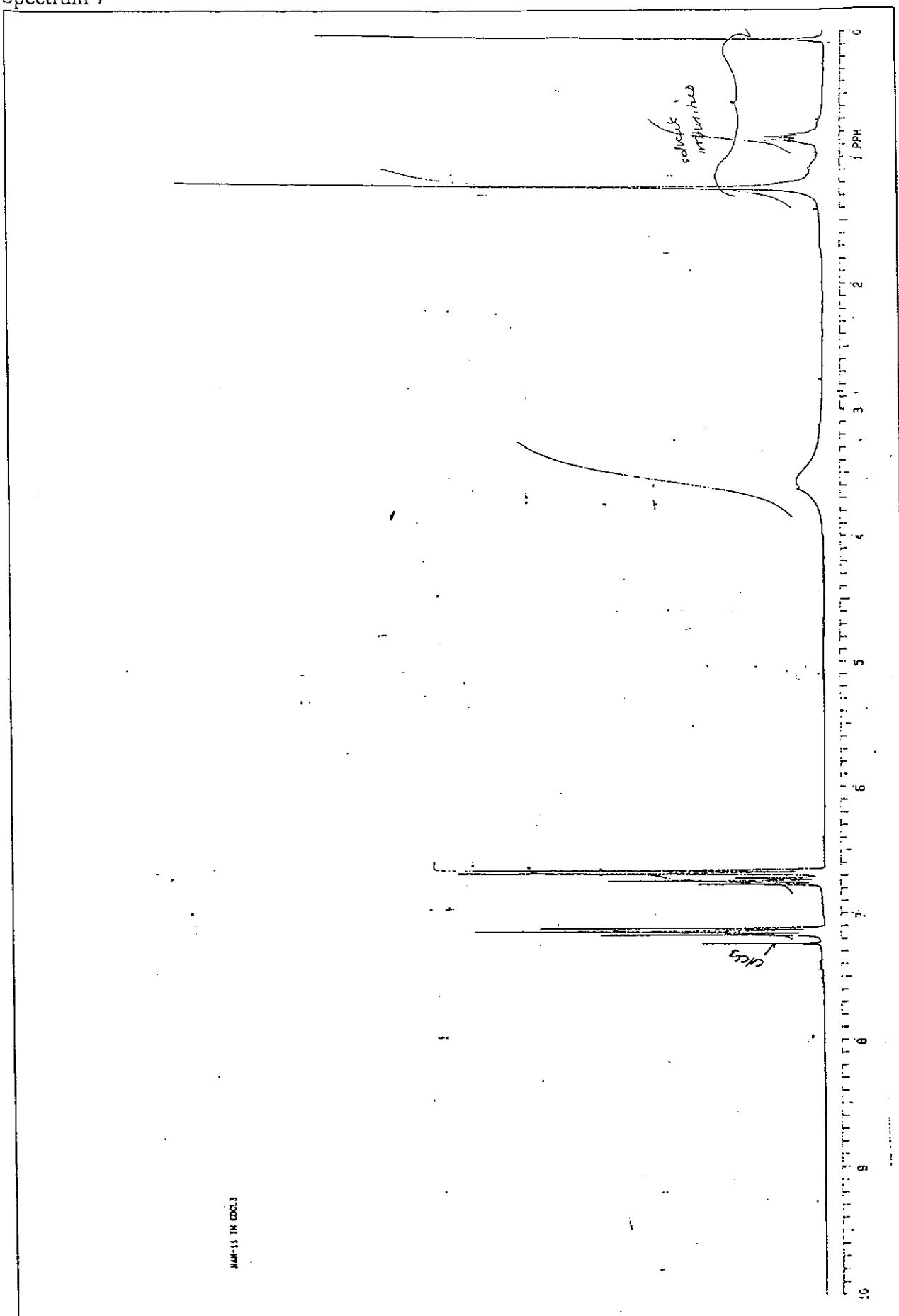

^{1}HNMR spectrum of dried chloroform extracts from the completely electrolysed solution

Spectrum 8

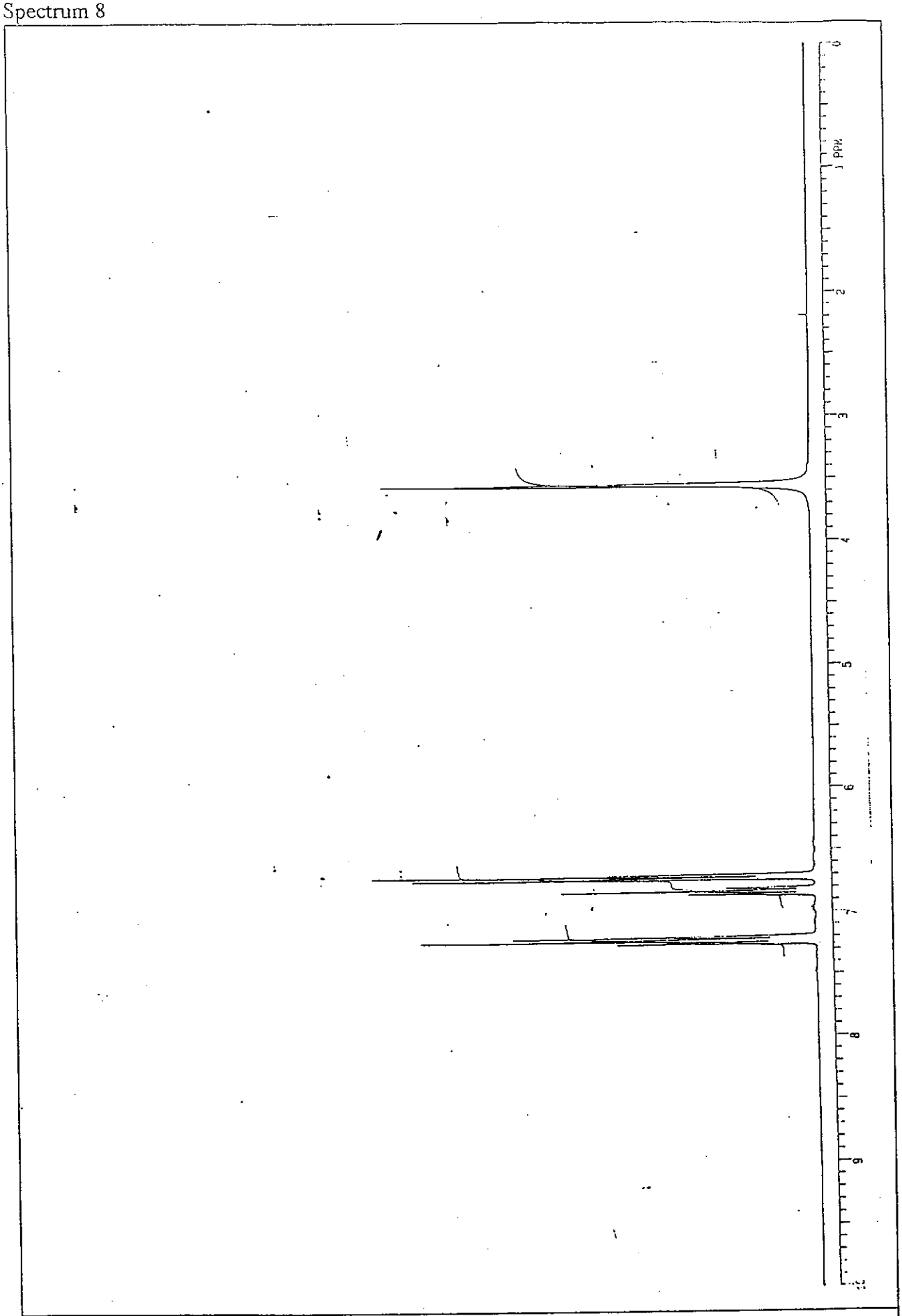

^{1}HNMR spectrum of aniline

Appendix II

Matlab filtering program

A modified matlab filtering program was used to filter the processed data from collver8 to produce the smooth curve.The following is the way how to execute the program in the matlab command screen, where file **Pro00190.cyv** from collver8 was used as an example. The input and output data are in an **ascii** format.

```
load pro00190.cyv
v=pro00190(:,2);
c=pro00190(:,1);
C=fil(c);
V=fil(v);
a=[V C];
save pro00190.cyv a -ascii
```

The following is the description of the execute program:

load pro00190.cyv; : Pro00190.cyv is a processed file from collver8 program which contains two columns. Column number 1 contains current and column number 2 contains potential.

v=pro00190(:,2); : Here the program defines v which is potential

c=pro00190(:,1); : Here the program defines c which is current

C=fil(c); : Here the program assigns the filtered current as column C and fil is the filtering program saved as file **fil.m**.

V=fil(v); : Here the program assigns the filtered potential as column V

a=[V C]; : Here the program put the two columns V and C together to form a 2 by 4000 matrix

save pro00190.cyv a -ascii : Here the program saves the filtered file and replaces the unfiltered one.

The following file was stored as **fil.m** file in matlab

```
%%%%%%%%% start

function y=fil(d)
% parameters
m=10;M=2*m+1;
delta=30;

% filter
x=linspace(-1,1,M);F=exp(-x.^2/delta);F=F/sum(F);

% filtering
N=length(d);
start=flipud(d(2:m+1));
finish=flipud(d((N-m):(N-1)));
D=[start;d;finish];

for ind=1:N
r=ind:(ind+M-1);
y(ind)=F*D(r);
end
y=y';
end
%%%%%%%%%% end
```